NAVAL POSTGRADUATE SCHOOL
Monterey, California

THESIS

W627177

THE SPATIAL AND TEMPORAL VARIABILITY OF THE ARCTIC ATMOSPHERIC BOUNDARY LAYER AND ITS EFFECT ON ELECTROMAGNETIC (EM) PROPAGATION

by

Zdenka S. Willis

December 1987

Thesis Advisor W. J. Shaw

Approved for public release; distribution is unlimited.

T239322

REPORT DOCUMENTATION PAGE

a REPORT SECURITY CLASSIFICATION UNCLASSIFIED	1b RESTRICTIVE MARKINGS
a SECURITY CLASSIFICATION AUTHORITY	3 DISTRIBUTION / AVAILABILITY OF REPORT Approved for public release; distribution is unlimited
b DECLASSIFICATION / DOWNGRADING SCHEDULE	
PERFORMING ORGANIZATION REPORT NUMBER(S)	5. MONITORING ORGANIZATION REPORT NUMBER(S)
a NAME OF PERFORMING ORGANIZATION val Postgraduate School	6b. OFFICE SYMBOL (If applicable) 63
7a. NAME OF MONITORING ORGANIZATION Naval Postgraduate School	
c ADDRESS (City, State, and ZIP Code) Monterey, California 93943-5000	7b. ADDRESS (City, State, and ZIP Code) Monterey, California 93943-5000
a NAME OF FUNDING / SPONSORING ORGANIZATION	8b. OFFICE SYMBOL (If applicable)
9. PROCUREMENT INSTRUMENT IDENTIFICATION NUMBER	
c ADDRESS (City, State, and ZIP Code)	10. SOURCE OF FUNDING NUMBERS

PROGRAM ELEMENT NO.	PROJECT NO.	TASK NO.	WORK UNIT ACCESSION NO

TITLE (Include Security Classification)
HE SPATIAL AND TEMPORAL VARIABILITY OF THE ARCTIC ATMOSPHERIC BOUNDARY LAYER AND ITS FFECT ON ELECTROMAGNETIC (EM) PROPAGATION

. PERSONAL AUTHOR(S)
Willis, Zdenka S.

a. TYPE OF REPORT	13b. TIME COVERED	14. DATE OF REPORT (Year, Month, Day)	15 PAGE COUNT
Master's Thesis	FROM _____ TO _____	1987 December	108

. SUPPLEMENTARY NOTATION

COSATI CODES			18. SUBJECT TERMS (Continue on reverse if necessary and identify by block number)
FIELD	GROUP	SUB-GROUP	Atmospheric Refractivity, IREPS, EM Systems Performance, Horizontally Homogeneous Atmosphere, Refractive Index

. ABSTRACT (Continue on reverse if necessary and identify by block number)

Gradients of temperature, pressure and moisture affect the propagation of electro-gnetic (EM) waves. Navy systems which are dependent on EM propagation can be either nhanced or degraded due to atmospheric conditions which affect atmospheric refractive index rofiles. The Navy's model for predicting the refractive index is the Integrated Refractive ffects Prediction System (IREPS) version 2.2, developed by the Naval Ocean Systems Center NOSC). Atmospheric parameters of temperature, vapor pressure and relative humidity - with elative humidity being the most critical - are used by IREPS to predict the atmospheric efractivity.

Data collected in the Fram Strait during MIZEX-84 (18 June - 15 July) showed that the efractive structure varied over the ice, the MIZ and the water adjacent to the ice edge. patial studies showed that the average values of duct height, thickness and strength were ower over the pack ice and the MIZ than over the water. A large increase in these values ere seen as one travels away from the ice in the adjacent water. Little spatial homogeneit

0. DISTRIBUTION / AVAILABILITY OF ABSTRACT	21. ABSTRACT SECURITY CLASSIFICATION
☒ UNCLASSIFIED/UNLIMITED ☐ SAME AS RPT. ☐ DTIC USERS	UNCLASSIFIED
2a. NAME OF RESPONSIBLE INDIVIDUAL Prof. W.J. Shaw	22b. TELEPHONE (Include Area Code) (804) 646-3430
	22c. OFFICE SYMBOL Code 63Sr

D FORM 1473, 84 MAR 83 APR edition may be used until exhausted. All other editions are obsolete

SECURITY CLASSIFICATION OF THIS PAGE

☆ U.S. Government Printing Office: 1986--606

UNCLASSIFIED

Item 19 continued
was seen in the refractive conditions. Ducting was clearly dependent on the synoptic situation. A majority of the ducts were detected when high pressure dominated. No ducts were recorded when a cyclone moved directly over the ships. Stationarity was present to a limited degree.

A significant number of profiles showed an unusual feature of the dewpoint curve in that, once it became saturated below the inversion, this curve continued to indicate saturation above the inversion. It could not be determined whether this was solely due to a sensor problem or a real meteorological phenomenon. Therefore, the data were analyzed with and without correction for this behavior.

Approved for public release; distribution is unlimited.

The Spatial and Temporal Variability of the Arctic Atmospheric Boundary Layer and its Effect on Electromagnetic (EM) Propagation

by

Zdenka S. Willis
Lieutenant, United States Navy
B.S., University of South Carolina, 1981

Submitted in partial fulfillment of the
requirements for the degree of

MASTER OF SCIENCE IN METEOROLOGY AND OCEANOGRAPHY

from the

NAVAL POSTGRADUATE SCHOOL
December 1987

Thesis
N6797
c.1

ABSTRACT

Gradients of temperature, pressure and moisture affect the propagation of electro-magnetic (EM) waves. Navy systems which are dependent on EM propagation can be either enhanced or degraded due to atmospheric conditions which affect atmospheric refractive index profiles. The Navy's model for predicting the refractive indexes is the Integrated Refractive Effects Prediction System (IREPS) version 2.2, developed by Naval Ocean Systems Center (NOSC). Atmospheric parameters of temperature, vapor pressure and relative humidity - with relative humidity being the most critical - are used by IREPS to predict the atmospheric refractivity.

Data collected in the Fram Strait during MIZEX-84 (18 June - 15 July) showed that the refractive structure varied over the ice, the MIZ and the water adjacent to the ice edge. Spatial studies showed that the average values of duct height, thickness and strength were lower over the pack ice and the MIZ than over the water. A large increase in these values were seen as one travels away from the ice in the adjacent water. Little spatial homogeneity was seen in the refractive conditions. Ducting was clearly dependent on the synoptic situation. A majority of the ducts were detected when high pressure dominated. No ducts were recorded when a cyclone moved directly over the ships. Stationarity was present to a limited degree.

A significant number of profiles showed an unusual feature of the dewpoint curve in that, once it became saturated below the inversion, this curve continued to indicate saturation above the inversion. It could not be determined whether this was solely due to a sensor problem or a real meteorological phenomenon. Therefore, the data were analyzed with and without correction for this behavior.

TABLE OF CONTENTS

LIST OF TABLES

LIST OF FIGURES

ACKNOWLEDGEMENTS

I would like to extend my sincere appreciation to Professors Shaw and Davidson for their knowledge, guidance and support. I also thank John Cook of the Naval Environmental Prediction Research Facility (NEPRF), for his assistance in converting the IREPS program so it could be run on the IBM 3033 mainframe at the Naval Postgraduate School. I would also like to thank Lt. Mike Dotson whose thesis provided the background and much of the software from my work.

I would like to thank my husband, Paul, for his untiring patience, his love, and his expertise in math and physics. Finally, I would like to extend my sincere appreciation to my parents who instilled in me the value of education and, have always been my number one fan.

This research was made possible in part by funding from NEPRF, Monterey, CA. under program element 62435N, project R3581 "System Environmental Sensitivity".

I. INTRODUCTION

A. GENERAL

The environment in which modern naval weapon and communications systems operate is a controlling factor in the effective deployment of these systems. The Navy has begun to realize the importance of the environment to weapon and communication systems. The immediate past Secretary of the Navy, John Lehman, recognized the tactical importance of the environment in stating that in a military balance where the navy of our principal adversary is superior in numbers and near in technology, it is likely that the Navy with the better knowledge of the environment will have the war end on its terms.

The environment is not homogeneous. Atmospheric properties such as moisture and temperature vary considerably from one region to another. This regional variability of the atmospheric properties can have unique and significant effects on many electromagnetic and electro-optical systems, making it necessary to develop localized rules governing the effects of the atmosphere on these systems.

The Navy has recently turned its attention to the Arctic. At a cold weather operations symposium held in 1985, Rear Admiral Mooney, then Chief of Naval Research, stated "The strategic importance of the Arctic is increasing. Soviet capabilities, coupled with the extensive deployment of Soviet surface ships and submarines in the Arctic/Subarctic Oceans near Europe make this region an area of growing importance to both commercial and strategic defense interests of the United States." Accordingly, we must continue to familiarize ourselves with the Arctic area. Fig. 1.1 taken from OP-03, Vice Chief of Naval Operations for Surface Warfare, is the Navy's arctic/cold weather surface ship plan. This shows the Navy's goals for being able to continuously operate in the Arctic. Currently, very few military operations take place north of 70°N. This figure clearly illustrates the Navy's goal to be able to conduct routine surface operations in the Greenland Sea by the year 2010.

The recent interest in the Arctic spawned the Marginal Ice Zone Experiment (MIZEX). The pilot program was conducted in 1983. The second MIZEX was conducted in the Fram Strait area between Greenland and Svalbard during the period 18 May to 30 July 1984. The purpose of MIZEX-84 was to understand the mesoscale

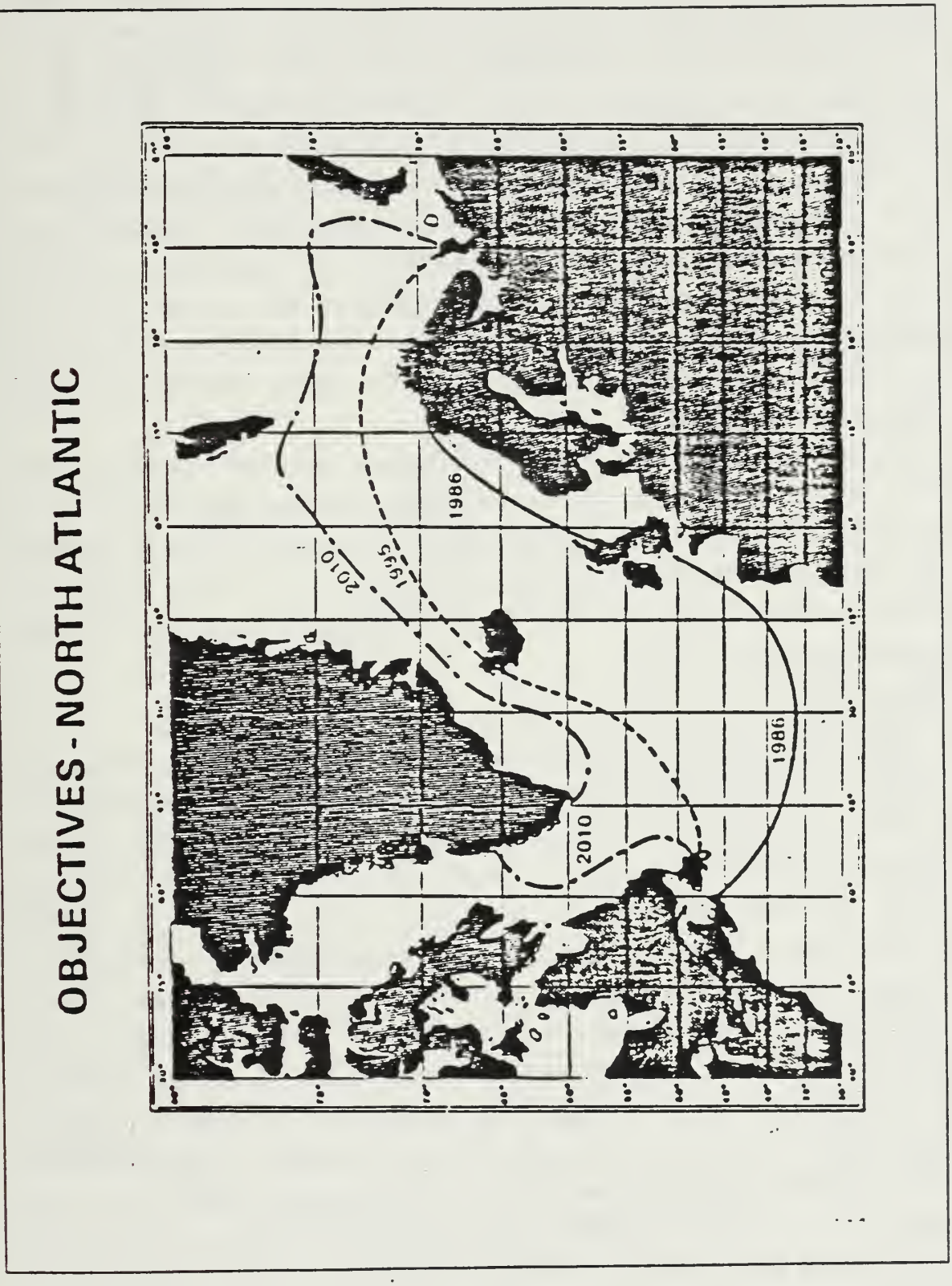

Fig. 1.1 Navy's Goals for Arctic Surface Operations.

processes that dictate the advance and retreat of the ice margin. Data collected during MIZEX were used to study the mesoscale physical processes by which the ice, ocean and atmosphere interact in the Marginal Ice Zone (MIZ) during the summer. Atmospheric and oceanographic data were collected by seven ships, eight remote sensing/meteorological aircraft and four helicopters. Atmospheric data collected during this experiment included temperature, relative humidity measurements and upper-level winds by rawinsondes, hourly weather observations by all ships, extensive passive-active microwave remote sensing data by aircraft and cloud measurements by aircraft. Ice conditions were determined by satellite information and by tracking ARGOS drifting oceanographic-meteorological buoys and by transponders. Daily weather maps were provided by the Weather Forecasting Center for northern Norway (Johannessen and Horn, 1984)

Fig 1.2 shows the area of MIZEX-84. The area's northern boundary is along 82.0°N, its southern boundary 77.0°N, the eastern boundary along 11.0°E and its western boundary along 11.2°W. This area was chosen because most of the heat and water exchange between the Arctic ocean and the rest of the world is through this strait and because it is crucial to study the energy interactions across the ice margin (Johannessen, and Horn, 1984).

B. PURPOSE AND SCOPE OF THESIS

This thesis continues a study of how the spatial variability of the atmospheric boundary layer (ABL) affects the refractive conditions in an area. This thesis follows the work done by Dotson (1987) who compared and contrasted the refractive conditions between data collected over water (sub-tropical) and over land (mid-latitude). This thesis will evaluate the varying ABL and its effect on the refractive conditions in the the Arctic utilizing data collected during MIZEX-84. Specifically the differences in the ABL between the pack ice, the MIZ and the adjacent water and how these differences affected the refractive conditions are presented. McNitt (1984) completed a study on the refractive conditions during MIZEX-83. During MIZEX-83 data were collected from only one ship, so no comparison of the refractive conditions between the pack ice, MIZ or the adjacent waters was possible. During MIZEX-84 however, data from four ships located in the ice, the MIZ and the adjacent waters were available. The final goal is to provide guidance for effectively using or modifying the available models such as the Navy's Integrated Refractive Effects Prediction System (IREPS) to predict the refractive conditions in the Arctic.

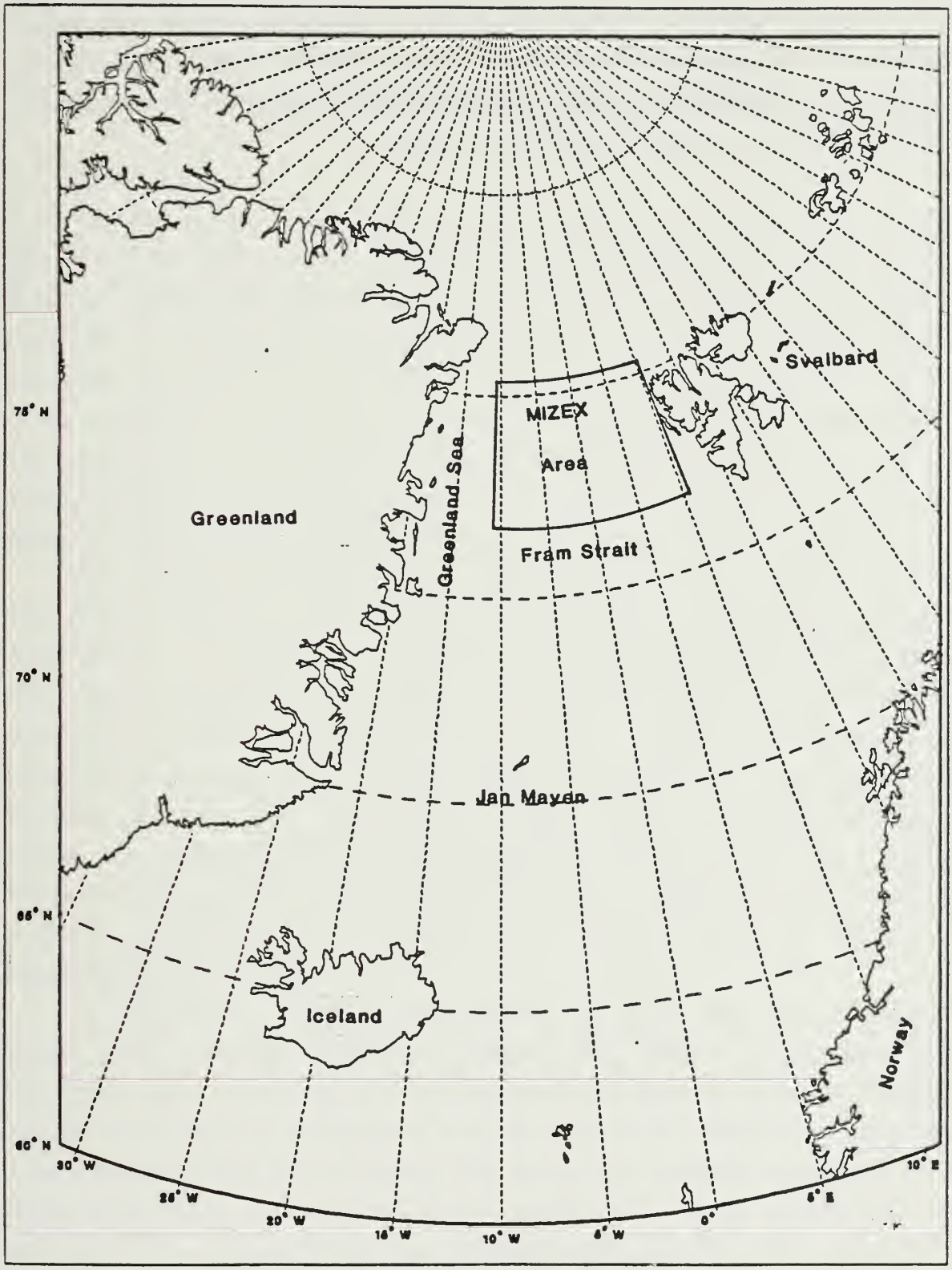

Fig. 1.2 MIZEX-84 area.

The vertical temperature and dewpoint profiles obtained from radiosondes launched during MIZEX-84 were used to describe the mesoscale temporal and spatial variability of the troposphere below 500 mb. These profiles were used to determine the atmospheric refractive index gradients which significantly modify the electromagnetic (EM) radiation as it propagates through the atmosphere.

II. ARCTIC MARINE BOUNDARY LAYER

A. GENERAL

The atmospheric boundary layer (ABL) is defined by Stewart (1979) as the portion of the lower atmosphere which has turbulent flow and is in direct contact with the earth's surface. The ABL extends from the surface to a height of a few meters in conditions of strongly stable stratification and to thousands of meters in highly convective conditions. On the average, the ABL extends through the lowest kilometer of the atmosphere and contains 10% of the mass of the atmosphere (Holton, 1979). The boundary layer is very important to the dynamics and thermodynamics of the atmosphere because it is in this layer that all momentum, water vapor and thermal energy exchanges between the atmosphere and the earth's surface takes place.

The thermodynamic stability of the ABL is a function of its density structure. The density structure in turn is a function of water vapor and temperature distributions. The boundary layer is stable when the potential temperature increases with height and becomes unstable when there is heating from below. Stable and unstable ABLs have some energy for vertical mixing as a result of shear production of turbulent kinetic energy (TKE). This turbulence extends through a shallower layer in the stable case than in the convective case. When there is heating from the earth's surface, the heating produces a density distribution which enhances vertical mixing. When the ABL is unstable, the total level of the TKE is greater and hence the mixing is greater. The majority of the unstable ABL comprises a relatively homogeneous mixed layer (Wyngaard,1973).

Near the surface, the values of stress, heat and moisture fluxes are independent of height. There are strong mean vertical gradients in wind, temperature and moisture in this surface layer. Depending upon the magnitude and direction of the thermal flux, and the overall depth of the boundary layer, the depth of the surface layer ranges from a few meters to several ten's of meters. The surface layer generally extends to a lower height in the stable ABL compared to the unstable ABL. In the unstable ABL the surface layer is conveniently defined as the lowest tenth of the ABL (Wyngaard,1973).

The last 50-100 m of the unstable ABL is an inversion layer. An inversion is defined as temperature increasing with height. The layer through which the

temperature increases with height is called the inversion layer and acts as a physical cap to the boundary layer. Clouds are often present at the base of the inversion and are used to trace the extent of the ABL.

In the marine atmospheric boundary layer (MABL), the oceans and atmosphere exchange energy directly in the form of turbulent heat, moisture and momentum fluxes. Businger (1985) states that over most of the oceans the marine boundary layer is nearly neutral. The air in the marine boundary layer has generally traveled long distances over water and has come close to equilibrium with the underlying surface. He further states that since the fluxes at the interface are most sensitive to variations in stability in near-neutral conditions variations in the sea surface, temperature may have a noticeable effect on the marine boundary layer.

B. SYNOPTIC WEATHER

The changing synoptic conditions of the Arctic will affect the temperature and moisture distributions in the boundary layer and, this in turn will affect the stability and height of the boundary layer. Sater *et al.* (1971) discuss several features unique to the Arctic which have a profound effect on the nature of the flow over the area. These include: the presence of the massive Greenland ice cap; the presence of snow and ice; the low elevation angle of the sun; and the low elevation of the Arctic region. The Greenland land mass, extending upward to an elevation of 2000-3000 m, produces strong katabatic flow over the area. The high surface albedo characteristics of the snow and ice means a high proportion of the incoming solar radiation is reflected and the low temperatures are maintained. Although the elevation of the sun is low, the variation in the elevation is small. Therefore, the Arctic experiences 24 hours of twilight during the summer. The inversion does not undergo the diurnal variations of the lower latitudes, where the variation in the solar elevation can be as great as 79°. The flat Arctic region facilitates the free atmospheric flow between the middle latitudes and the Arctic. This allows the cyclones which are generated in the midlatitudes to move over the Arctic region. Due to the constant low temperatures and lack of available moisture in the snow regions, these cyclones often stagnate and fill over the Arctic basin.

The synoptic conditions and boundary layer structure during MIZEX-84 have been summarized in papers by Lindsay *et al.* (1986), Fairall and Markson (1987) and Johannessen *et al.* (1986). The remainder of this chapter is a summary of the synoptic conditions and boundary layer structure seen during MIZEX-84.

Sater *et al.* (1971) characterize the Arctic summer climatology by a weak and variable surface high in the central Arctic basin and an upper-level low nearly centered on the pole. At the surface the Icelandic low is weak and centered to the west of Iceland. The circumpolar vortex is much weaker and further north than in the winter. Slow-moving midlatitude lows move through the Fram Strait causing brief periods of extraordinarily high winds. The overall pattern during MIZEX was similar to the climatology. Fig. 2.1 shows the 500 mb mean height. Superimposed on this figure is the primary and secondary track of the midlatitude lows which move through this area. Also superimposed on the figure is the average position of the ice edge during MIZEX 1984.

An anomalous ridge in the mean monthly 700 mb charts persisted west of Great Britain in both June and July. The mean 700 mb heights were near normal in the MIZEX area. At 500 mb a weak ridge extended northwest from Great Britain to Eastern Greenland and kept the midlatitude storms out of the region most of time. This ridge was stronger than the climatological ridge and east of its mean position. On the surface in June a very weak low existed just to the east of Iceland and a well formed high pressure cell was centered over western Greenland. The mean geostrophic wind in the Fram Strait was out of the northwest. In June a series of storms passed through the area. Four storms moved into the MIZEX area in June, which affected the refractive conditions. The specific movement of these systems will be discussed in Chapter V. In July the mean Icelandic low was not apparent. A very weak high was centered near Jan Mayen, and a weak ridge pushed in from the east over Svalbard. The mean geostrophic wind in the Fram Strait was from the south but very weak. In July one persistent storm passed just north of the area and retrograded from east to west. These storms brought moderately high winds, less than 15 m/s, as they passed.

The ice edge orientation is important for determining whether the flow is from off-ice, along-ice or on-ice directions. The ice edge typically extended in an almost east-west direction from Svalbard to approximately 80°N, 0.0°E, where it shifts to a northeast to southwest orientation. Due to this orientation an off-ice flow was defined when the wind direction was from the northeast through the southwest. This occurred most of the time. The ice edges were near climatological locations throughout the MIZEX period.

The air temperature measured by the ships during MIZEX-84 was within five degrees centigrade of freezing throughout the experiment. The ships operating in the

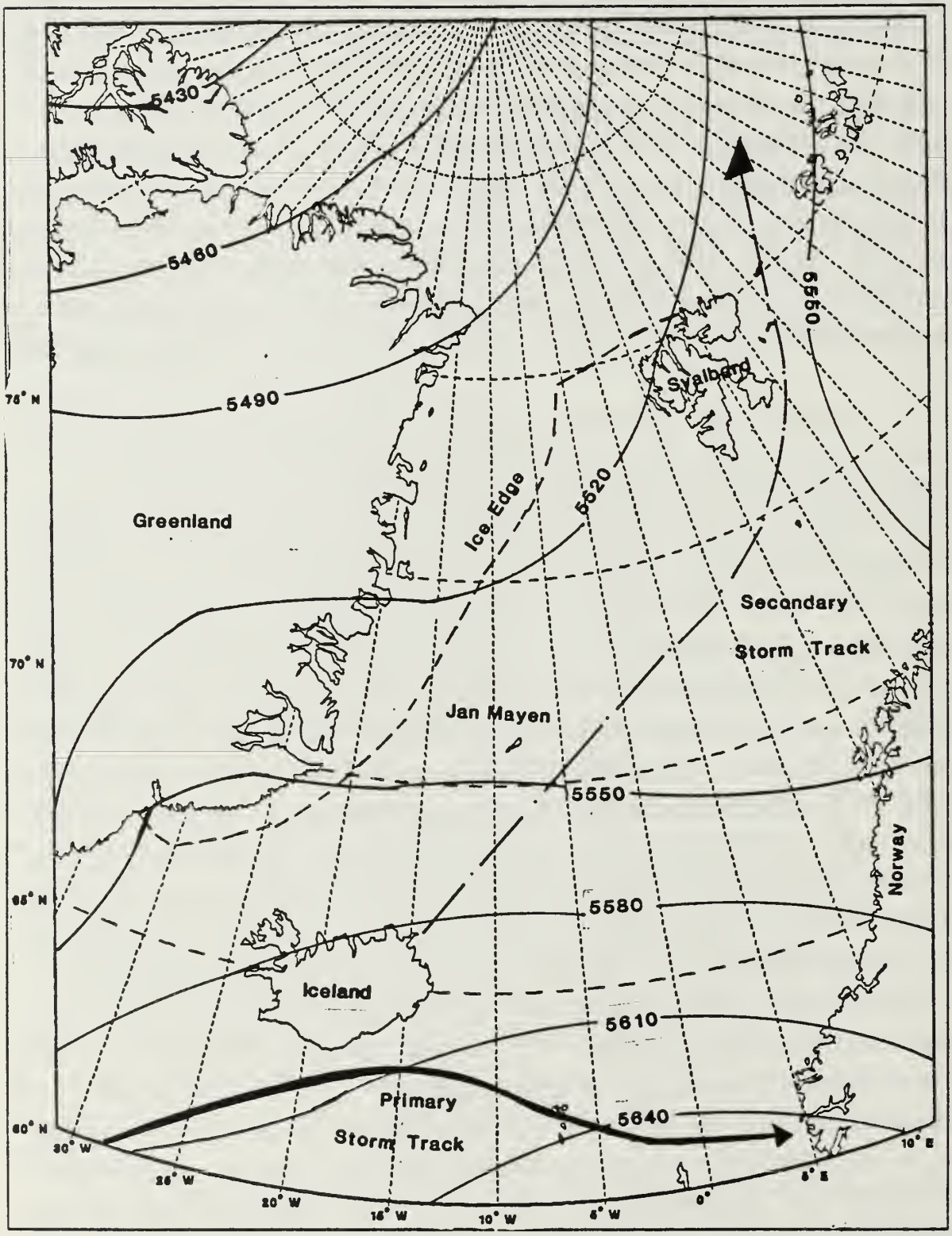

Fig. 2.1 500 mb mean height for June 1984, primary and secondary storm tracks, mean ice edge during MIZEX-84.

open water recorded temperatures slightly warmer than temperatures recorded by the ships operating in the ice. The ships operating in open water recorded a diurnal temperature cycle up to five degrees centigrade. This diurnal cycle was not recorded by the ships operating in the ice (Lindsay *et al.*, 1986).

C. MIZEX-84 BOUNDARY LAYER STRUCTURE

Fairall and Markson (1987) describe the ice/sea interface as forming the lower boundary for an atmospheric turbulent mixed layer which extends upward to a height of 50-500 meters. The mixed layer interacts with the free troposphere at the inversion transition region by means of entrainment.

The presence of the ice is the controlling factor in the exchange of momentum, heat, moisture and radiative energy between the atmosphere, ice, and ocean in the Arctic. The atmosphere "feels" the boundary between the ice and open water as a sharp interface across which discontinuities in physical properties occur. An example of this is the exchange in heat between the atmosphere and the ice versus the atmosphere and the ocean. The exchange of heat between the atmosphere and the ocean may be as much as 100 times greater over the open ocean than over the ice. In off-ice winds the air receives a tremendous increase in the input of heat as it flows from the ice to open water. This results in rapid warming of the lower atmosphere, and changes consequently occur in the wind speed and stress exerted on the water (Muench,1983). Since there is warming of the atmosphere from below, a more unstable and deeper boundary layer is expected over open ocean adjacent the ice edge than over the MIZ or the pack ice.

Overland's (1985) studies have shown a difference in the MIZ boundary layer during the winter compared to the MIZ boundary layer in the summer. In the winter the boundary layer is very shallow with inversion heights less than 100 m. In the summer the inversions are somewhat deeper but inversions are not as sharp. The boundary layer depth ranges from 100 to 1000 m, with a typical value of about 500 m or less.

Analysis of the MIZEX-84 data by Lindsay *et al.* (1986), Fairall and Markson (1987), Guest and Davidson (1987) and Kellner *et al.* (1987) show that there are differences between the boundary layer over the ice and the boundary layer over the ocean. In the absence of direct turbulence measurements, the inversion height is used to describe the upper limit of the boundary layer. Over the ice the inversions were often surface based (30%) or very low (71% less than 300 meters), while over the water

there was only one surface-based inversion. Thirty-seven percent of the time the inversions were greater than 600 meters. The temperature gradient within the inversion was a little stronger over the ice than over the water. The inversions were of similar thickness both over ice and over water. Fig. 2.2 graphically shows the differences in the inversions between the Valdivia, a ship operating in the open water, and the Polarstern, a ship operating in the ice. Profile (a) shows the differences in the height of the inversion base, profile (b) shows the differences in the mean temperature and profile (c) shows the differences in the thickness of the inversions.

Fairall and Markson (1987) showed that the surface heat flux varies considerably from the ocean to the pack ice. The total heat flux was 30 w/m^2 over the ocean and near zero at the ice edge. This larger heat flux over the ocean will cause the inversion to be higher over the water. Due to the increased heat flux, more energy is available for entrainment. This results in a higher inversion over the water adjacent to the ice. The opposite situation, a positive air/surface temperature difference, exists over the pack ice. This results in less available turbulent energy. Mixing is thus damped, accounting for the lower inversion heights observed.

The surface wind stress was also measured during MIZEX. The surface wind stress is a function of the wind speed and the drag coefficient. With all factors being equal Overland (1985), Guest and Davidson (1987) and Fairall and Markson (1987) found the wind stress to be two times greater over the ice than over the water adjacent to the ice. This was due to the higher drag coefficient over the relatively rough ice compared with the drag coefficient over the water. A higher value of wind stress should lead to a higher inversion due to the increased mixing. However, this was not found in the Arctic. In fact the opposite was found. This is partially because the wind over the ice was often less than the wind over the adjacent water, so the difference in the wind stress was not actually as great as a two to one ratio. Also, strong subsidence and colder denser air over the ice counteracted the influence of the wind stress variable on the inversion.

Lindsay *et al.* (1986) showed that the inversion would rise and fall in response to the warming and cooling of the atmosphere in response to the synoptic conditions discussed above. Warming conditions resulted in stronger surface based inversions and occurred when the area had high pressure gradients or very weak gradients over the area.

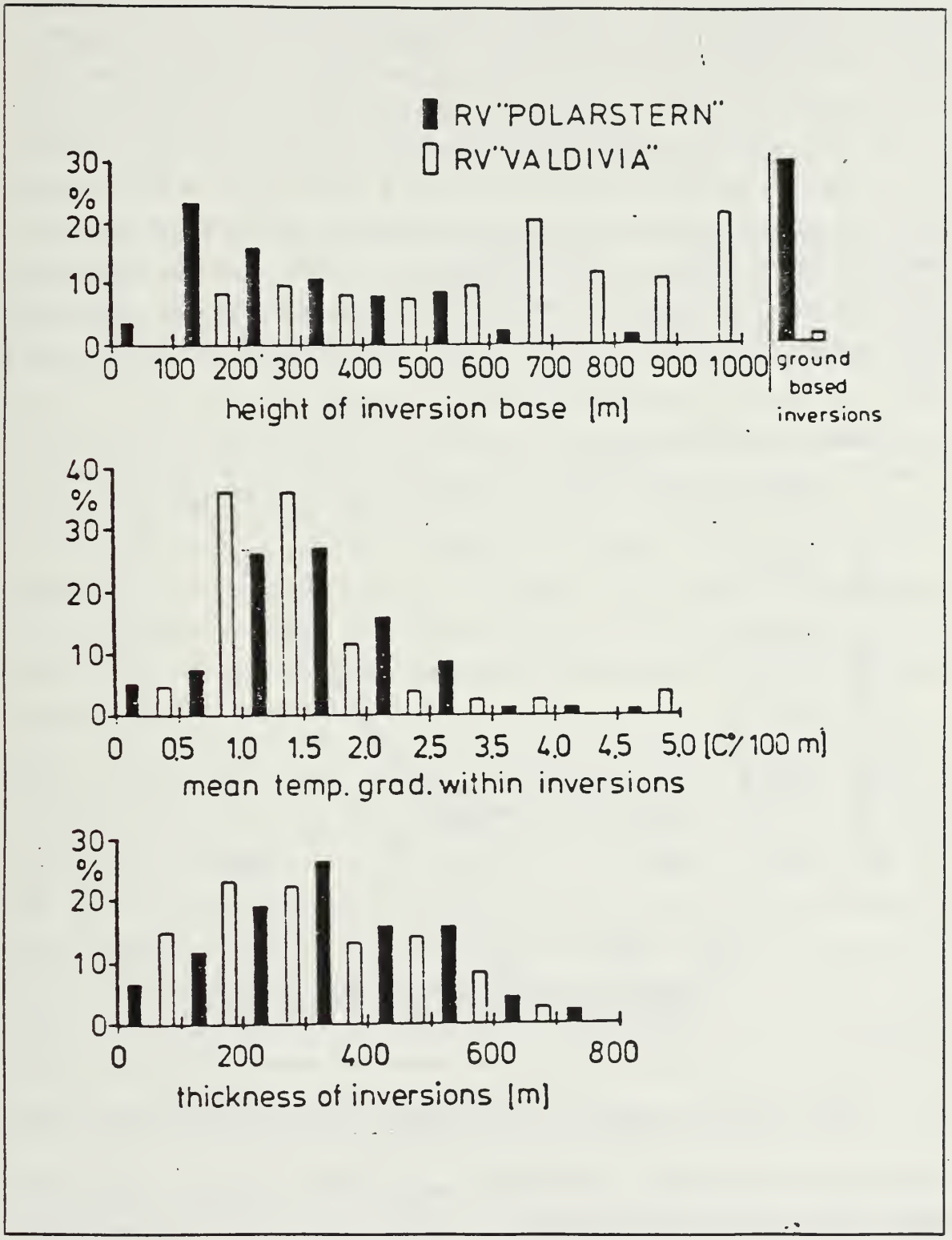

Fig. 2.2 Differences in the inversion between the Polarstern, operating in the ice, and Valdivia, operating in the adjacent water.

Guest and Davidson (1987), and Kellner *et al.* (1987) showed that the height of the inversion depended upon the distance of the ship from the ice edge. Both showed that the inversion height increased with respect to the distance from the ice edge if the ship was operating in the water. The inversion was lower over the pack ice than at the MIZ. Fig. 2.3 taken from Guest's work shows this relationship with the inversion lower over the pack ice than the MIZ followed by a rapid increase of the inversion height as one moves away from the ice edge in the adjacent water. Fig. 2.3 shows that the median inversion height at the ice edge was 250 meters and that the height increased at a rate of 45.3 meters for each 10 km traveled perpendicularly away from the solid ice edge. Kellner's *et al.* (1987) indicated the inversion increased with a slope of 1/200.

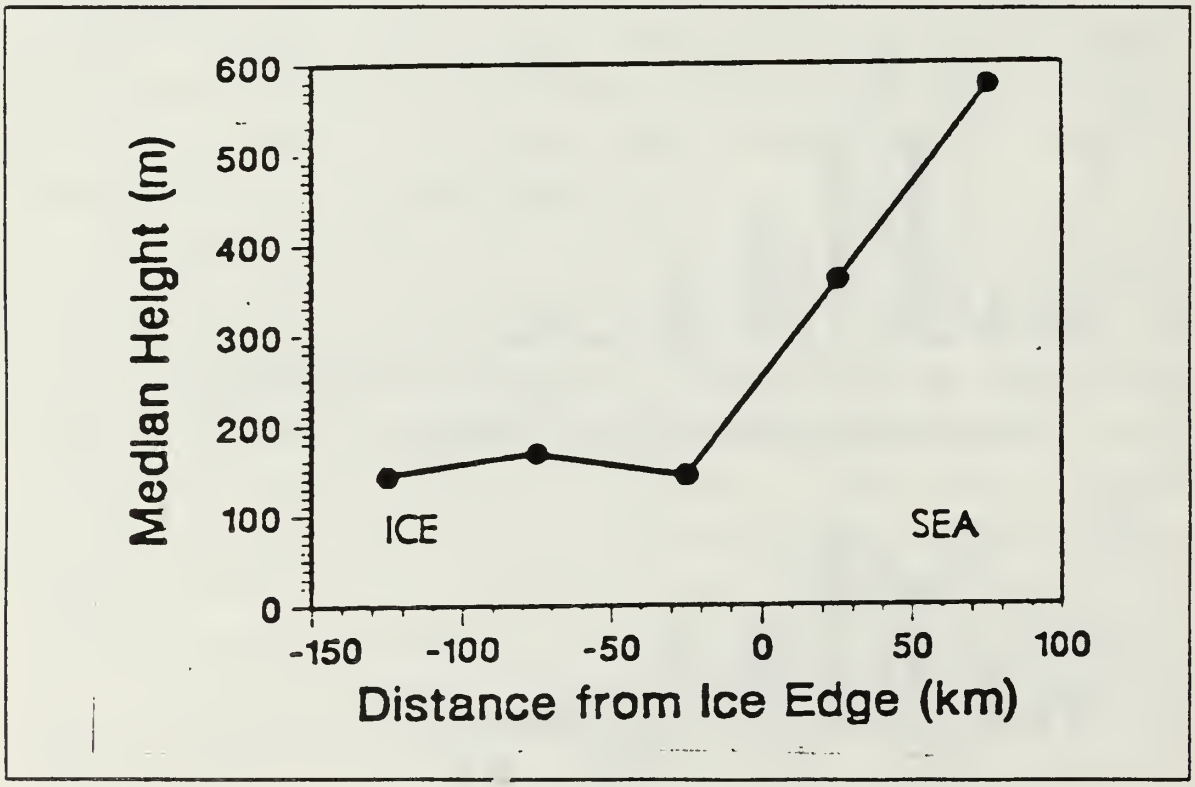

Fig. 2.3 Inversion height in response to distance from the ice (Guest and Davidson,1987).

Guest and Davidson (1987) examined the height of the inversion in relation to the height and layers of clouds present in the MIZEX area. Fig. 2.4 shows these differences. With no clouds and wind speeds less than four m/s, the inversion was surface based and increased with wind speed. With a single cloud layer the inversion

was not surface based and showed a slight increase with response to an increase in wind speed. The average inversion height with winds less than four m/s was 275 m and increased to 325 m as the wind increased to 12 m/s. With a thick layer of clouds the inversion height was approximately 200 m higher than in the thin cloud case. The inversion height, with a thick cloud layer, showed no response to an increase in wind speed.

The difference between the inversion height without the clouds present and with clouds present is due to the effect of radiational cooling by the cloud. The base of the inversion corresponds to the height of the cloud. The difference in the inversion when a thin cloud was present and versus a thick cloud was not due to a difference in the cloud itself, but due to the mechanism by which these clouds were generated. Thick clouds were present when there was less divergence, making entrainment more effective. This resulted in a deeper boundary layer. The deeper boundary layer also tended to produce a higher lifting condensation level in the thick cloud than in the thin cloud. The response of the inversion to a change in the surface wind speed is directly a function of the height of the inversion. The closer to the surface the inversion was located, the greater the impact of the increase in the surface wind. This was due to the fact that the shallower the ABL the less the wind is dissipated through mixing and thus the greater the effect on the inversion.

A common feature of the summer MIZ boundary layer was fog. The occurrence of fog is also expected to influence the height and features of the inversion. Lindsay *et al.* (1986) defined fog to exist when the horizontal visibility was less than 1 km. Wind direction was a good indicator of the existence of fog. Fog occurred 80% of the time when the surface wind direction was directly from the water to the ice edge within 15 degrees and when the surface wind speed was greater than 5 m/s. Fog was observed only 10% of the time when the surface wind direction was in an off-ice direction. Even during this situation the fog only occurred when a tight pressure gradient brought air from the water to the ice and then the air was quickly forced back to the ice edge. Fog rarely occurred when the winds were either less than 2 m/s or greater then 8 m/s.

Lindsay *et al.* (1986) described two mechanisms for the generation of fog in the Arctic: frontal fog and stratus lowering. Frontal fog is not associated with synoptic fronts but is used to describe fog when it approached the ship rapidly with a distinct edge. The winds were usually parallel to the ice edge when this type of fog was seen.

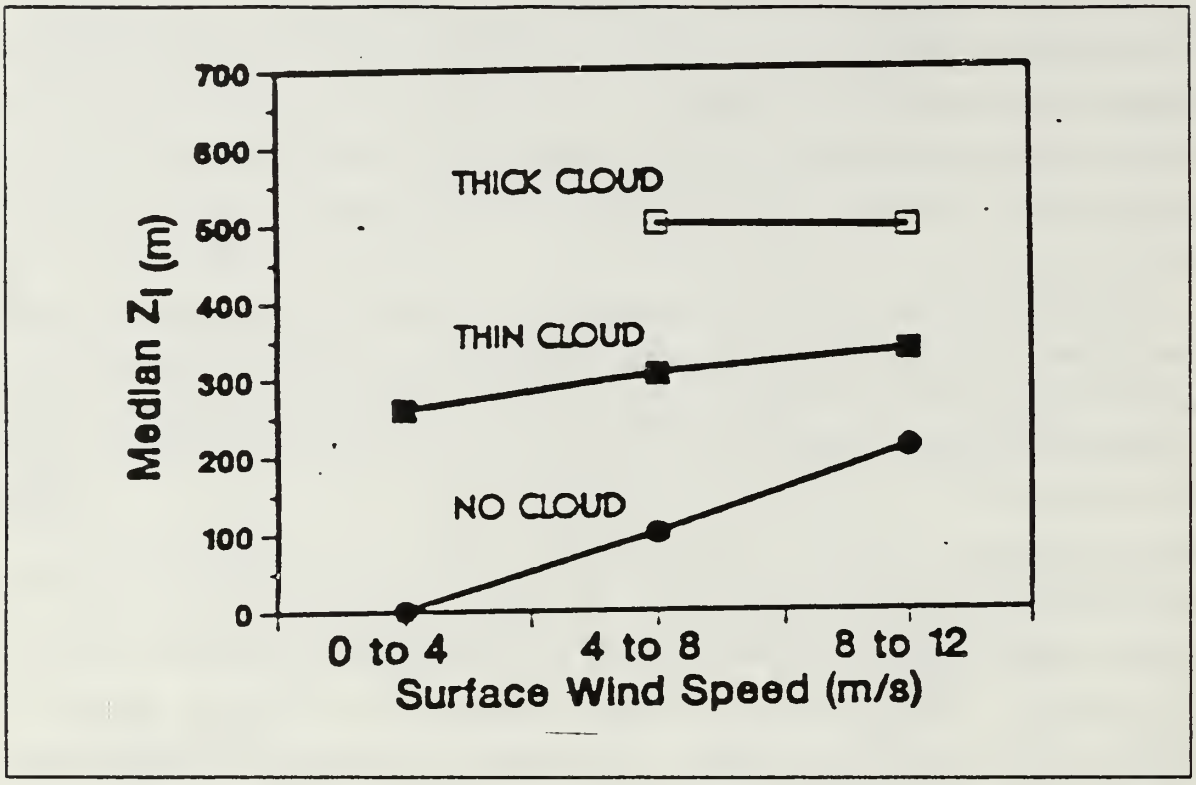

Fig. 2.4 Inversion height in response to different cloud conditions,(Guest and Davidson,1987).

The second type of fog experienced was due to stratus lowering. This occurred when the surface wind direction was from the sea to the ice, causing a stratus layer to be present. The stratus layer was caused by the warm moist air over the ocean being advected over the ice. When this air came in contact with the cold air over the ice, the water vapor in the warm air condensed and stratus cloud formed. The vertical extent of the stratus layer varied in response to wind speed, wind direction and the tightness of the pressure gradient. When the stratus layer lowered to the surface it was described as fog. Whether the stratus layer would lower sufficiently to reach the surface could not be predicted by specific wind speed, wind direction or pressure gradient values (Lindsay *et al.*, 1986)

Lindsay *et al.* (1986) found that frontal fog was more common than stratus fog in a ratio of two to one. There was one period of exception to this during 10-20 July when the winds were persistently on-ice and fog lifted to stratus and then quickly lowered again several times. The dissipation of this fog was also categorized as two types, frontal and stratus rising, and was related to wind directions opposite to those which caused the fog. Frontal dissipation was the term used when the fog was rapidly

advected out of the area resulting in complete clearing. With stratus rising the horizontal visibility increased to greater than 1 km but a stratus layer of clouds was still present over the area (Lindsay *et al.*, 1986).

III. ATMOSPHERIC REFRACTIVITY

Electromagnetic (EM) radiation is energy which travels as waves. The EM spectrum comprises radiation of all wavelengths, and in a vacuum these waves travel with a constant speed (the speed of light). This discussion is limited to refraction of EM radiation having wavelengths from one centimeter to 10 meters. This includes microwave, ultra high frequency (UHF) and very high frequency (VHF). Wave velocity is reduced when EM radiation interacts with air molecules. The atmosphere, vertically nonhomogeneous in temperature, pressure and humidity will cause the bending or refraction of electromagnetic waves.

The interaction of EM waves with the medium is described by the dielectric constant ϵ, which is dependent upon the characteristic of the medium and upon the frequency of radiation. The index of refraction n is defined by (3.1) where ϵ is the dielectric constant, c is the velocity of an EM wave in free space, and v is the velocity of the same EM wave in the medium.

$$n = \epsilon^{1/2} = c/v \tag{3.1}$$

Thus the index of refraction, n, is the ratio of the velocity of propagation of electromagnetic wave in a vacuum to its velocity in air. EM waves travel only slightly slower in air than in a vacuum, so the value of n is near unity. Bean and Dutton (1966) showed that the value of n is equal to 1.0003 for a Standard Atmosphere. For convenience, the refractivity N is defined by Eqn. 3.2:

$$N = (n-1) * 10^6 \tag{3.2}$$

The index of refraction for air does not significantly depend on frequency over the entire EM range. When expressed in terms of the atmospheric variables pressure P (mb), temperature T (K), and water vapor pressure e (mb), N is expressed by (3.3) (Battan, 1973).

$$N = 77.6\ P/T - 5.6\ e/T + 3.75 * 10^5\ e/T^2 \tag{3.3}$$

More important than the value of N is the vertical gradient of refractivity (dN/dZ) because the EM refraction is dependent upon the gradients of N. Since gradients of pressure, temperature and humidity naturally occur throughout the atmosphere, it follows that gradients of N must also exist. This relationship as a function of temperature (T), pressure (P) and specific humidity (q) is given by Eqn. 3.4

$$dN/dZ = .3\ dP/dZ + 7.2\ dq/dZ - 1.3\ dT/dZ \qquad (3.4)$$

Battan (1973) showed that when $dN/dZ = -157\ km^{-1}$, a propagating EM wave would bend with a curvature exactly equal to that of the earth's. This would cause a horizontally propagating EM wave to remain parallel to the earth's surface. If N decreases at a faster rate than $-157\ km^{-1}$, this wave is refracted downward with a curvature exceeding the Earth's curvature, and a duct is formed. IF N decreases at a slower rate than this, the wave is bent down towards the earth but at a curvature less than that of the earth. In this case no duct is possible. Thus $dN/dZ = -157\ km^{-1}$ is the threshold for whether the EM propagation will be trapped.

It is sometimes convenient to think of the earth's surface as flat and to represent the EM wave refraction in this frame of reference. This can be done simply by subtracting the earth's curvature from the EM wave and from the Earth. A modified refractivity M has been developed to take into account the earth's curvature and to allow for easy identification of ducting. Eqn 3.5 shows the relationship of M to N (Battan,1973).

$$M = N + 157Z \quad Z \text{ in km} \qquad (3.5)$$

IREPS, version 2.2, is the Navy's current software for predicting the atmospheric refractive conditions. This system is a shipboard environmental data processing and display system which is used to predict the effects of refraction on electromagnetic signals for naval surveillance, communications, electronic warfare and weapons' guidance systems. IREPS has been incorporated in the Tactical Environmental Support System (TESS) presently being evaluated in the fleet (Naval Ocean Systems Center, 1981).

IREPS uses the N and M gradients to classify refractive conditions. Table 1 shows IREPS classifications of refraction conditions and the relationship of N units to M units (Naval Ocean Systems Center, 1981).

TABLE 1
IREPS CLASSIFICATION OF REFRACTION CONDITIONS

IREPS CLASSIFICATION	dN/dZ km^{-1}	dM/dZ km^{-1}	RANGE
SUBREFRACTION	>0	>157	REDUCED
NORMAL	0 to -79	79 to 157	NORMAL
SUPER-REFRACTION	-79 to -157	0 to 79	INCREASED
TRAPPING	<-157	<0	GREATLY INCREASED

Ducting is of primary concern to Navy operations and is caused by trapping layers. A trapping layer is defined as the area where M decreases with height. In this region the ray is bent downward relative to the earth's surface. A duct is defined as the region in which the energy is confined. A surface-based duct occurs when an EM wave is refracted downward at a curvature greater than the earth's curvature and is then subsequently reflected up from the earth's surface. It is the continuous refracting down and the reflecting up that forms the duct and makes it a concern to the Navy by allowing detection by surface radars far beyond the normal horizon. The type of duct depends on the height, strength and extent of the trapping layer.

The top of the duct is defined as the height where M reaches a minimum value. It also corresponds with the top of the trapping layer. In practice, thickness of the duct may be found by dropping a vertical line from the top of the duct down towards the surface until it intersects the M profile. Duct strength is defined as the maximum range of M values within the limits of the duct. The optimum coupling height (OCH) is the height where the dM/dZ profile changes from a positive to a negative value.

Three types of ducts have been defined: (1) the surface-based duct (2) the elevated duct and (3) the evaporative duct. Profile (a) of Fig. 3.1 depicts an elevated duct which is the type often found when an inversion layer is present. Large temperature and humidity gradients are usually present within the inversion. The boundary layer is cool and moist relative to the overlying air, and over the ocean it is often referred to as the marine layer. These jumps of the gradients in temperature and humidity are associated with warming and drying due to subsidence (sinking air) above the inversion and turbulent mixing in the boundary layer. In the Arctic this type of ducting is most likely when the Greenland high is well established over the area, causing strong subsidence. Profile (b) of Fig. 3.1 is an example of a surface based duct. These ducts are formed by a relatively warm, dry air being advected over a cool body of water, or by strong subsidence modifying the elevated duct. Fig. 3.1 (c) shows an evaporative duct. The evaporative duct can be created by two different mechanisms. First, an evaporative duct may be created by the very rapid decrease of moisture immediately above the ocean surface. The air adjacent to the ocean is saturated with water vapor and the relative humidity is 100 %. This high relative humidity decreases rapidly in the first few meters to an ambient value which depends on varying meteorological conditions. This initial rapid decrease in humidity will cause M to decrease with height to a minimum and then M will increase with height. The second way in which an evaporative duct can be formed is independent of the decrease in humidity. This "evaporative duct" is caused by strong cooling at the surface. This cooling could cause a sufficient positive temperature gradient between the air near the surface and the air just above this to create a duct. Radiational fog is often associated with this condition because the overlying air is cooled sufficiently by radiational transfer for the relative humidity to increase to the point of condensation. Evaporative ducts almost always exist but it is the strength and upper boundary which are critical in determining the importance of this duct to tactical operation. The evaporative duct, although present, is generally shallow in the Arctic.

Two other important refractive effects are subrefraction and super-refraction. Subrefraction is defined as N increasing with height as shown in Table 1. In this situation the rays actually bend away from the earth's surface. The radar range in this situation is reduced. Super-refraction is defined in Table 1 as N gradients having values between -79 to -157 per km. The EM wave is bent towards the earth's surface, but not strongly enough to form a trapping layer. In this situation the radar range is increased somewhat.

The IREPS revision 2.2 user's manual (Naval Ocean Systems Center, 1981) states that the assumption of horizontal homogeneity of the atmosphere is valid 85% of the time for the purpose of making refractive assessments. Dotson (1987) found this to be a poor assumption and his results showed that 50% of the time horizontal homogeneity could not be assumed. The refractive conditions varied from one location to another. This variation was a function of the existing atmospheric conditions at the specific location at the time of that launch. We will show that in the Arctic, as well, this assumption made by IREPS is not valid.

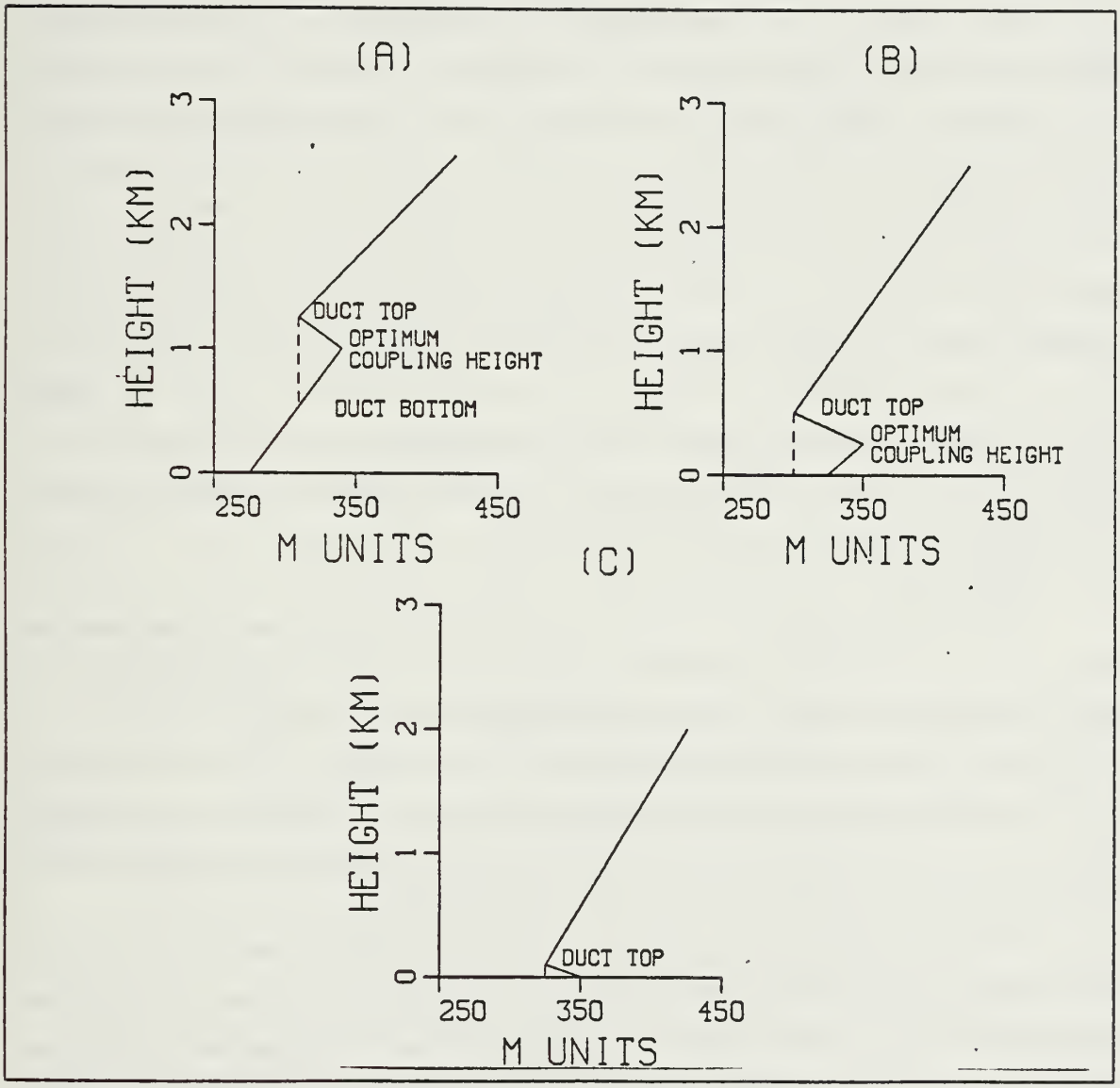

Fig. 3.1 Ducting occurrences for typical M profiles from Dotson (1987).

IV. DATA ACQUISITION AND PROCESSING

A. DATA ACQUISITION

Radiosondes launched from four ships, Polarstern, Polar Queen, Hakon Mosby and Valdivia were used to evaluate the refractive conditions during MIZEX-84. Radiosonde observations were made with the Vaisala Micro-Cora Upper Air Sounding system using the RS-80 radiosondes. Surface weather observations were measured hourly on three of the ships and every three hours on the fourth ship. The surface weather observations were made aboard three of the ships. The exception was the Polar Queen, whose observations were recorded a majority of the time from a profile tower located on the ice floe next to the ship. Generally the Polar Queen and the Polarstern operated in the ice while, the Valdivia and Hakon Mosby operated in the open water within 140 km of the MIZ. A concerted effort was exerted by all the scientists aboard each of the ships to launch the radiosondes within a half-hour of designated launch time. An intense period of launching radiosondes every three hours began midnight 8 July and continued until 15 July.

1. Polarstern

The ship was equipped with two anemometers, wind vanes and temperature sensors. A set of sensors was located on each side of the ship at 25 meters above the deck. The set of sensors used to record measurements was dictated by the direction of the wind flow. Sensors on the windward side was used. Wind data were corrected for the ship's motion to give true wind speed and direction. The winds were ten-minute vector averages. The dewpoint was calculated by a Li-CL sensor and the sea surface temperature was read from the port intake (Augstein, 1984).

The Polarstern operated in a box bounded by 78.2°N, 80.7°N, 6.0°W and 8.0°E. From 17-22 June, the Polarstern operated on the ice side of the zonally oriented ice edge along 80.3°N. This operation included detailed oceanographic surveying as well as recovering and redeployment of two meteorological-oceanographic buoy stations. From 22-25 June, the Polarstern continued the oceanographic survey, including tracking of transponders distributed on nearby ice floes. From 25 June to 8 July, the Polarstern was involved in a large oceanographic survey across the Fram Strait. She operated along three transects, the first transect along 80.3°N, the second

transect along 79.3°N, and the third transect along 78.3°N. For the large-scale meteorological network, 9-15 July, the Polarstern operated near the position of 79.8°N and 6.5°W. The Polarstern was located the furthest into the ice at approximately 140 km from the ice edge (Augstein,1984).

2. **Polar Queen**

Surface observations were recorded by a tower on an adjacent ice floe a majority of the time. Wind velocities from the profile tower were measured at a height of 6.7 meters. These values were corrected to a 10 meter height. When the tower was not operational or the ship sheltered the tower from the true wind, wind speeds were recorded by the ship's anemometer mounted on the ship's mast at a height of 15 m. These winds were also corrected to a 10 meter height. The winds were ten-minute vector averages. The dewpoint was measured on the ship with a cooled mirror dewpoint hygometer. Sea-surface temperature was not recorded, and the sea-surface temperature was assumed to be -1.7°C in any exposed areas (Guest and Davidson, 1984).

The Polar Queen was designated as the primary drift-station vessel and drifted passively with the surrounding ice, while moored securely to a floe. Her mean position was 80.5°N and 3°E, and she never varied more than 100 km from this position. The Polar Queen was located in the ice closest to the MIZ during the intensive meteorology program (Lindsay *et al.*, 1984).

3. **Hakon Mosby**

The Hakon Mosby's instruments were located on the forward mast at a height of 14 m. The wind, temperature and humidity were measured. The winds were thirty-minute vector averages. The sea-surface temperature was measured with a towed thermistor (Davidson and Geernaert, 1984).

The Hakon Mosby operated in the open water along the MIZ. The ship remain in an area bounded by 77.8°N, 80.6°N, 3.0°W, and 11.5°E. The ship participated in the oceanographic survey of the Fram Strait from 22 June to 8 July. During the meteorological intensive program, the Hakon Mosby stayed on the water side of the MIZ but was located closer to the ice edge than the Valdivia, which also operated in the open water (Johannessen and Horn, 1984).

4. **Valdivia**

The weather observations were recorded manually onboard the Valdivia. The observations were recorded in accordance with the World Meteorological Organization

format. Observations were recorded every three hours. Winds were either measured with a standard ships's anemometer with no electronic averaging or estimated according to the sea state. Sea-surface temperatures were recorded at the ship's intake (Quadfasel *et al.*, 1984).

The Valdivia operated in the eastern portion of the Fram Strait during the entire period. Her stations were between the ice edge and and the coast of Svalbard. From 25 June to 8 July she was involved in an oceanographic survey across the Fram Strait. The Valdivia also took hydrographic measurements during this period. From 9 July to 15 July the Valdivia was the furthest away from the ice edge in the open water. The ship operated between 100-140 km from the ice edge (Johannessen and Horn, 1984).

5. **Radiosondes**

The Vaisala balloon-borne radiosondes provided pressure, temperature and relative humidity measurements. This system uses the Omega navigational network to track the balloons and determine the winds aloft. Ascent rates were 120-150 m/min (WMO standard is 300 m/min) with pressure, temperature and relative humidity reported every 10 seconds. The radiosondes were tracked to 200 mb (11-12 km). The Polarstern launched radiosondes every three hours between 19 June and 16 July. A total of 249 successful launches were recorded. The Hakon Mosby launched radiosondes every six hours from 20 June to 8 July and every three hours from 9-15 July. A total of 136 successful launches were recorded. The Polar Queen and the Valdivia launched radiosondes ever 12 hours until 8 July. Both ships launched radiosondes every three hours between 9-15 July. The Polar Queen recorded 120 successful launches while the Valdivia recorded 105 successful launches. A total of 610 successful radiosonde launches were recorded by the four ships. The MIZEX data were put on tape and stored at the MIZEX data bank at the National Snow and Ice Data Center.

B. PROCESSING OF THE DATA

1. **Form of data**

Of the 610 available radiosonde launches, 474 sondes launched between 18 June and 15 July were originally chosen to compose the data set for this thesis. This data set was determined in two steps. The first step was to evaluate each launch time to find at least two ships which had launched the radiosonde within one half hour of the designated launch time. These profiles were grouped according the launch time and

were used in the spatial variability study. A total of 434 profiles were identified for this study. The second screening was done to determine if additional profiles would be needed to complete the temporal study. This was decided by plotting each ship's track to see how long the ship remained in a 30 n mi square. The only ship track which met this criterion was the Polarstern, and an additional 40 profiles were incorporated into the data set. These brought the number of radiosonde profiles in the data set to 474. Approximately 10% of the profiles were unusable due to missing data, so the data set was reduced to a final count of 427 profiles. Although the radiosondes were tracked to 200 mb, this thesis is only concerned with the boundary layer and the radiosondes were evaluated only to 500 mb.

Each profile had to be prepared for input into the IREPS portion of TESS. The IREPS program will accept a maximum of 29 pressure, temperature and dewpoint levels. The profiles were reduced to 29 pressure levels by using an interactive graphing package, Grafstat, available on the IBM 3033 mainframe at the Naval Postgraduate School. Profiles were individually plotted with pressure along the y-axis, and temperature and dewpoint along the x-axis. A cursor was used to choose interactively a maximum of 29 significant levels, and the profiles were edited to reflect these levels.

After the profiles had been plotted and edited, suspicious dewpoint curves were noted in 157 of the profiles. In these profile the dewpoint curve continued along the temperature curve above the inversion layer to a height where the curve rapidly shifted to cooler dewpoint values. Figs. 4.1, 4.3, 4.5 and 4.7 are examples of these peculiar dewpoint curves. This behavior is a substantial concern because proper analysis of refractive conditions depends heavily on having good humidity measurements.

2. Evaluation of the dewpoint effect

The suspicious dewpoint curves were evaluated as to whether there was a problem with the humidity sensor or whether it was a real meteorological phenomenon in the Arctic. A thorough study was conducted on the basis of other results from the Arctic region and reports on basic on sensor performance (Gathman, 1986). The evidence in this study and in the literature was not conclusive regarding either argument. Suitable airplane data were not available for comparison with the data obtained by the radiosonde.

Fairall and Markson's (1987) final report on MIZEX-83 data included temperature and specific humidity profiles which indicated a saturation of the air above

the temperature inversion similar to profiles from the radiosondes launched in 1984. The report states that the airplane made both low-level horizonal passes as well as ascents and descents through the clouds, but the specific flight paths could not be correlated to the profiles provided. A study done by Ohtake *et al.* (1982) at Barrow Alaska on the observations of ice crystal formation in the lower Arctic atmosphere described a calculated relative humidity showing saturation above the inversion. Ohtake *et al.* (1982) stated that the humidities are nearly at saturation levels with respect to water below the inversion. The high humidity continues to an elevation of approximately 100 m above the inversion base, and this is common in association with the summer Arctic stratus clouds. The differences between Ohtake's *et al.* (1982) studies and the dewpoint curves recorded in MIZEX-84 are: (1) theirs were nearly saturated while the ones in MIZEX 84 were completely saturated and (2) theirs was only a calculated profile, not an observed profile as in MIZEX-84. A second study was done by Tsay and Jayaweera (1984) with data taken by an aircraft in the Beaufort Sea in 1980. The airplane runs started from above the stratus deck and descended through the cloud to either an altitude of 100 m if the cloud base extended to below this or to 30 m above the sea-ice surface. Temperature and dewpoint curves were provided for five days and three of the profiles showed similar trends as the data obtained by the radiosondes used in MIZEX 84. Again, none of the dewpoint curves showed complete saturation as did the radiosondes collected in MIZEX 84.

Dynamical or synoptic cases could be conceived for this type of profile, but they are rather unlikely. One way to explain this curve is through advection of warm moist air which could have been brought into the Arctic from a source far away. The direction of the flow would have to be from the south or southwest. A possibility would be relatively warmer and moist air in the vicinity of the Gulf Stream near Iceland which could have been lifted and advected unmodified to the Arctic region. Ohtake *et al.* (1982) suggested another explanation. The unusually high humidities above the inversion layer occur because the water vapor flux from an open lead in the ice increases considerably as the air temperature decreases below freezing. For example, when air at a temperature of -2°C with 70% relative humidity blows over the -2°C sea surface, the vapor pressures over the water surface and in the air differ by a factor of six, which is effectively nearly 500 % supersaturation over the water. The peculiar dewpoint curves were due to the fact that the layer could be supersaturated with respect to the ice even though the air was not saturated with respect to the water.

The above discussion gives some possible explanation to the data collected during MIZEX-84 but is not convincing enough to discard the second possibility of a humidity sensor problem. Basic cloud physics favors an inversion at the top of the cloud. Because inversions are produced in part by subsidence, which is a warming and drying process, one would expect to see a decrease in the moisture above the inversion this layer. Studies done by Brost *et al.* (1982) on marine stratiform clouds off the coast of California showed a distinct dry layer above the inversion. This phenomenon was actually seen as a clear layer by personnel in the aircraft. This behavior is opposite to that suggested by the rawinsonde data of this study. The fact that the values for the temperature and the dewpoint are identical has also led to the suspicion that the dewpoint curves are in error. On the Vaisala radiosonde, a cap is placed over the humidity sensor when being launched through the clouds. Several factors could cause a lag in the reading by the humidity sensor. The faulty reading could have been caused by either moisture as a result of condensation inside the cap or a thin layer of frost or ice which accrued on the sensor as the balloon ascended through the cloud. This problem seemed to occur when the temperature at the inversion was less than 0°C and seemed to correct itself after the temperature was above 0°C for in indefinite period of time. This might indicate that frost formed on the humidity sensor when the temperature was below freezing and melted (evaporating) as the temperatures rose above freezing. As soon as the ice melted and the water evaporated, the sensor would have been able to measure the correct relative humidity. This might account for the sudden large change in the dewpoint curve. The length of saturation was not consistent, sometimes as little as a few meters and sometimes as much as 700 meters.

Two papers have been published documenting problems with the humidity sensors on radiosondes. Helvey (1982) first reported a suspicion regarding the radiosonde data when examining a strong bias toward false analysis of surface based ducts. The error is blamed on sensor characteristics, sonde design and materials, handling prior to release and reduction procedures. Andreas and Richter (1982) evaluated the Vaisala Micro-Cora Upper Air Automatic Sounding system and found similar problems with the accuracy of the relative humidity measurement. To test the radiosondes, 60 launches were made. An airsonde was attached to the balloon and recorded measurements separately. Data received from the two different sensors were received at independent ground stations. The results of this experiment showed excellent comparisons in wind, temperature and pressure readings. However, there

were a large number of failures of the humidity sensor, and there was a tendency for this sensor to drift.

The importance of humidity to the analysis of Arctic ducts was tested by setting $dq/dZ = 0$ and processing the modified data through IREPS. When the profiles were processed through the IREPS program, 100% of the ducts were eliminated. The conclusion drawn from this was that the changes in the humidity gradient are fundamentally important in determining the refractive conditions in the Arctic. The cold temperatures in this area accentuate the problem since they may be responsible for frost and may inhibit melting (evaporating) of the frost which may have accumulated on the sensor.

3. **Correction of the dewpoint curves**

Despite the fact that sensor wetting (or frosting) is a plausible explanation for the suspicious dewpoint behavior, there were no data to confirm this hypothesis. Thus, the data will be presented in an uncorrected and a corrected format. There is no precedent for how to correct the dewpoint curves to compensate for a humidity sensor error due sensor wetting. An attempt was made to establish an objective correction scheme for these radiosondes. The remainder of this chapter discusses this correction method and the effect the correction had on the refractive conditions.

The dewpoint curves were corrected one of two ways. The factor which determined how the dewpoint curve was corrected was whether the dewpoint curve above the suspicious area was colder, equal to, or warmer than the dewpoint at the inversion. Fig. 4.1 is an example of a dewpoint curve above the saturated area which is warmer than the dewpoint at the inversion. The correction in this case was to connect the dewpoint at the inversion with the first good value above the saturated area as indicated by the solid line from point A to point B on Fig. 4.1 The points outlined on Fig. 4.1 are deleted from the data of this radiosonde. Fig. 4.2 shows the temperature and dewpoint curve after the correction has been applied. Fig. 4.3 shows a case in which the dewpoint curve above the suspicious area is nearly equal to the dewpoint at the inversion. The profile was again corrected by connecting the dewpoint value at the inversion with the first good value of the dewpoint above the saturated area. This is indicated by the solid line from point A to point B on Fig. 4.3. The points outlined on Fig. 4.3 are deleted from the data of this radiosonde. Fig. 4.4 shows the temperature, and dewpoint profiles after the radiosonde data have been corrected. Fig. 4.5 shows a case in which the dewpoint curve above the suspicious area is cooler

than the dewpoint at the inversion. A line is drawn through the points above the saturated area to estimate the true dewpoint curve. This curve is extrapolated down to the inversion height at point A on Fig. 4.5. The dewpoint of the datum point just above the inversion is changed to intersect the extrapolated dewpoint curve at point A. Again the points outlined on Fig. 4.5 are deleted from the data obtained by this radiosonde. Fig. 4.6 shows the dewpoint and temperature curve after the correction was made. Fig. 4.7 is a second case in which the dewpoint curve above the saturated area is cooler than the dewpoint at the inversion. This case is included to illustrate the variablity encountered when deciding how to correct the dewpoint curves. Again a line is drawn through the points above the saturated area to estimate the true dewpoint curve. This curve is extrapolated down to the inversion at point A of Fig. 4.7. The datum point just above is the inversion is changed so the new dewpoint value intersects the extrapolated curve at point A. The The points outlined in Fig. 4.7 are deleted from the data set. Fig. 4.8 shows the temperature and dewpoint profiles after the correction was made.

Two problems were identified with the correction scheme discussed above. First, it was not always easy to determine how to extrapolate the dewpoint curve to the inversion as illustrated by the variablity seen in cases three and four. The second and most important problem was the inability to re-create the dry layer seen by the studies done by Brost *et al.* (1982) and seen in many of the other rawinsondes both in which there was saturation below the inversion and in cases where there was not saturation below the inversion.

After processing both the uncorrected and corrected data sets through IREPS, it was found that 50% of the anyalized ducts in the uncorrected data were not present after the corrections were applied to the profiles. In one percent of the cases, when the the duct still existed after the correction was made, the height of this duct was significantly lower in the corrected profiles versus the uncorrected profiles. Fig. 4.9 shows the effect of correcting the profile as discussed in the first case above. The uncorrected profile is on the left and the corrected profile is on the right. In the corrected profile the duct is located at 681 m and in the corrected profile the duct is not present. Fig. 4.10 shows the effect of correcting the profile in case four discussed above. The duct in the uncorrected profile is located at 567 m and lowered to 275 m in the corrected profile. For better representation only the area affected by the correction was plotted.

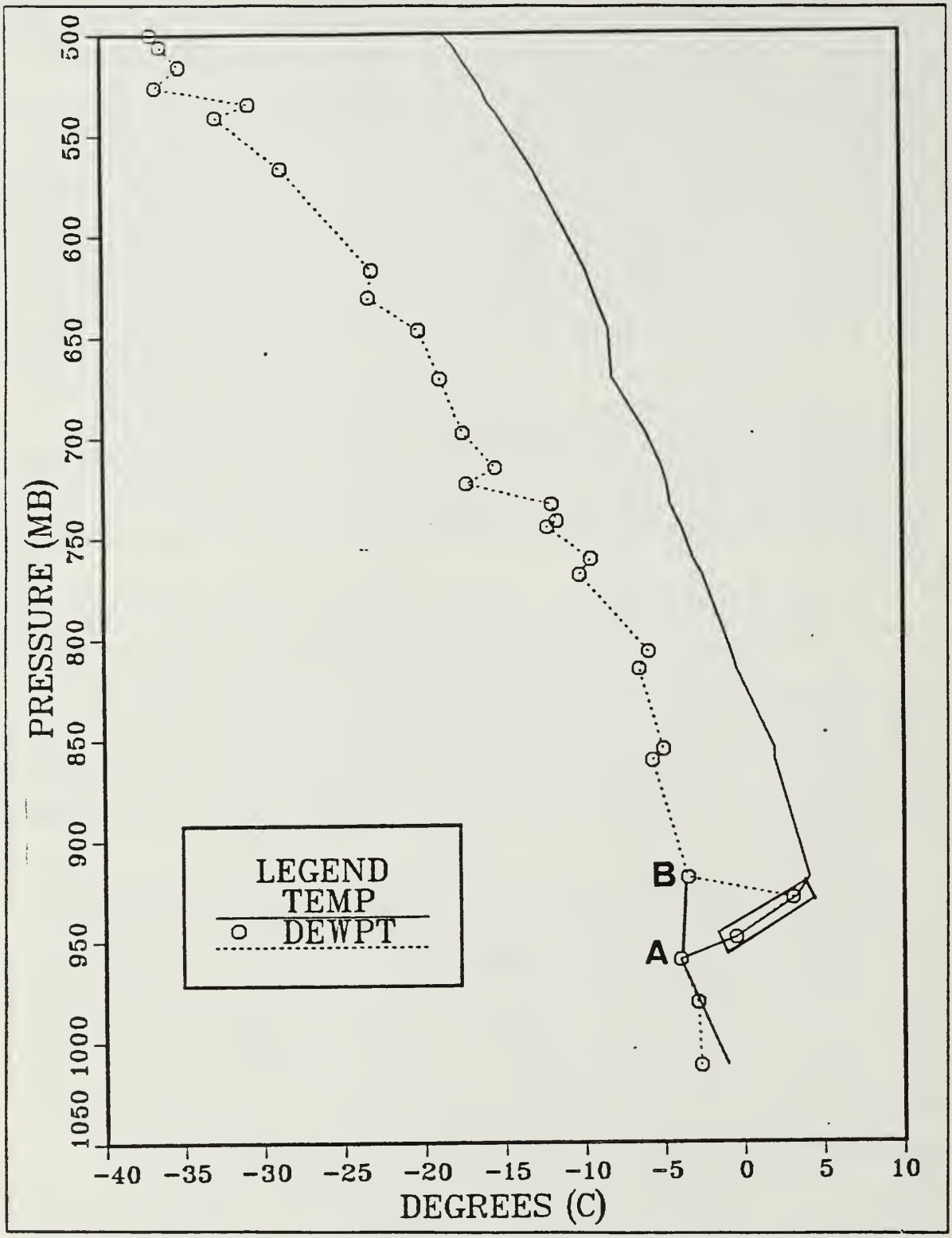

Fig. 4.1 Case One, dewpoint above saturated portion warmer than the dewpoint at the inversion.

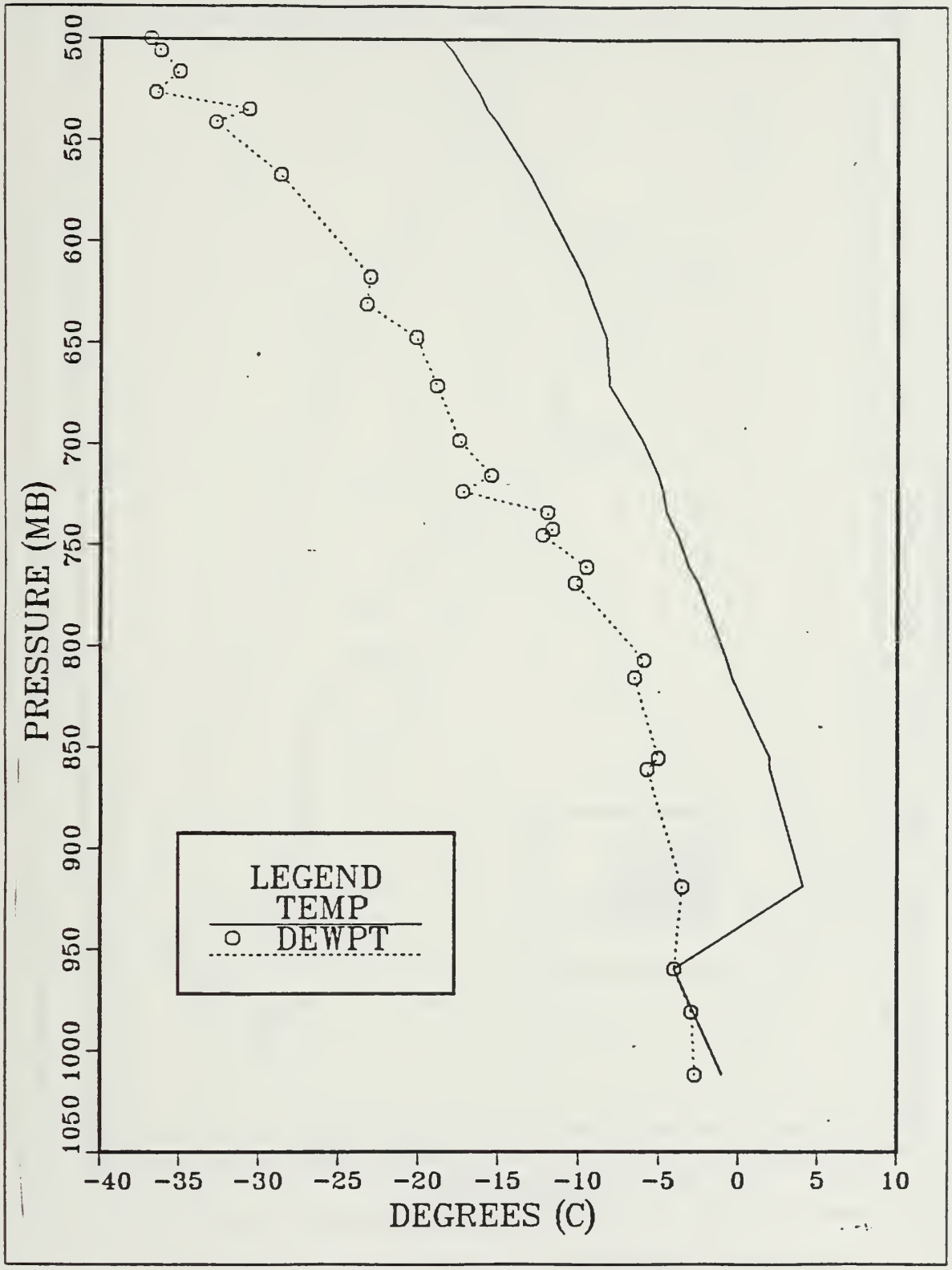

Fig. 4.2 Corrected profile in Case One.

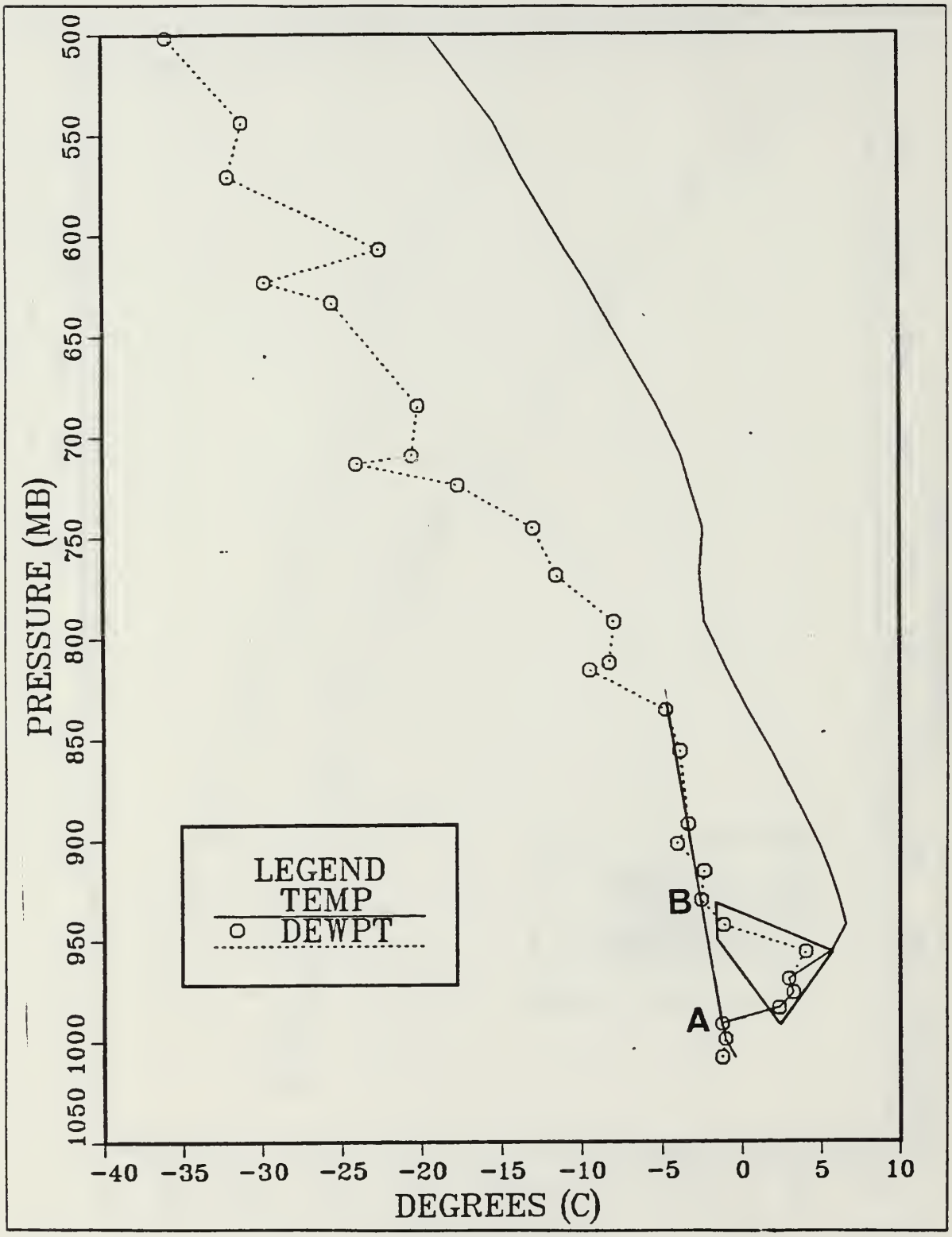

Fig. 4.3 Case Two, dewpoint above saturated portion equal to the dewpoint at the inversion.

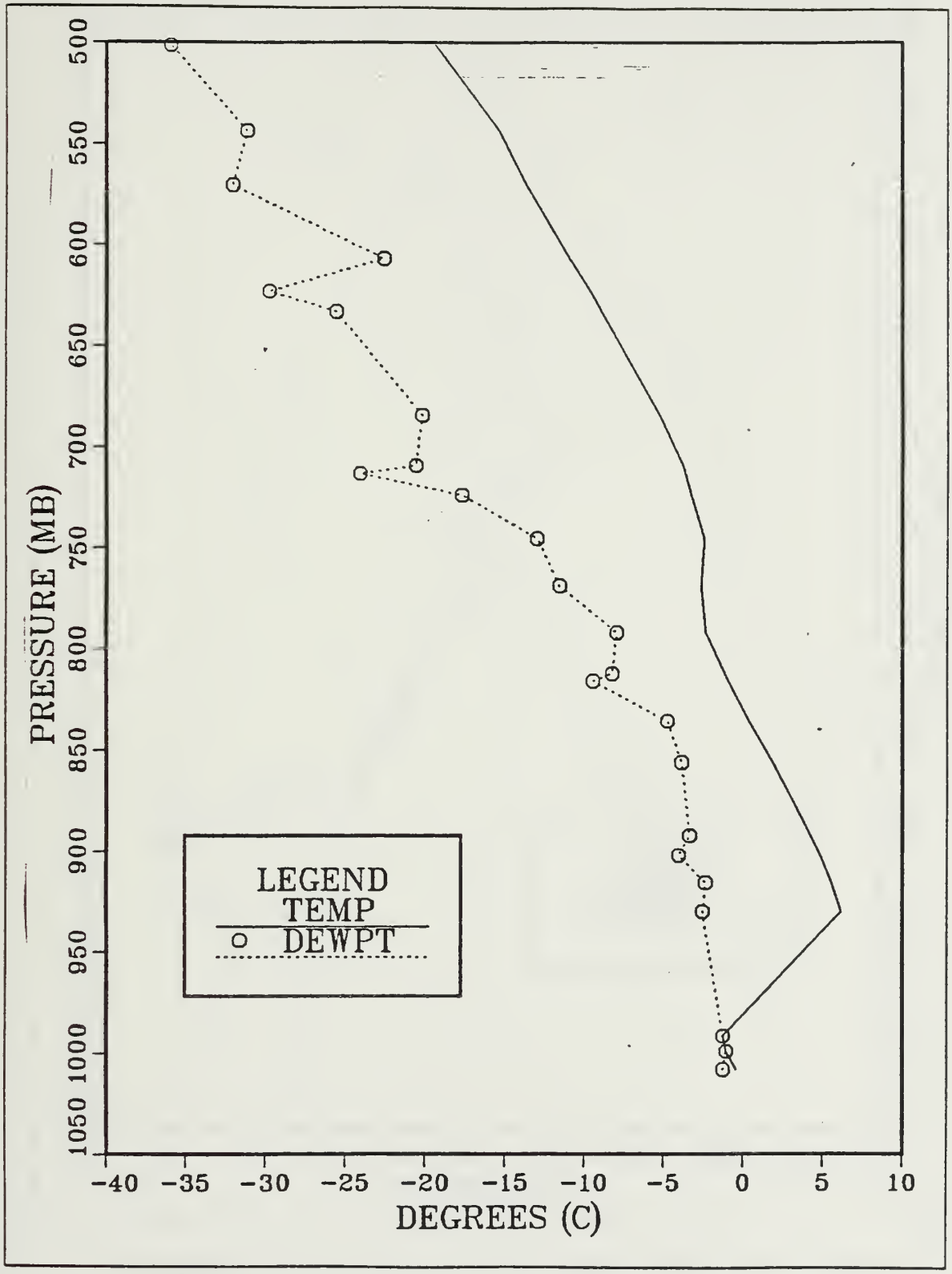

Fig. 4.4 Corrected profile of Case Two.

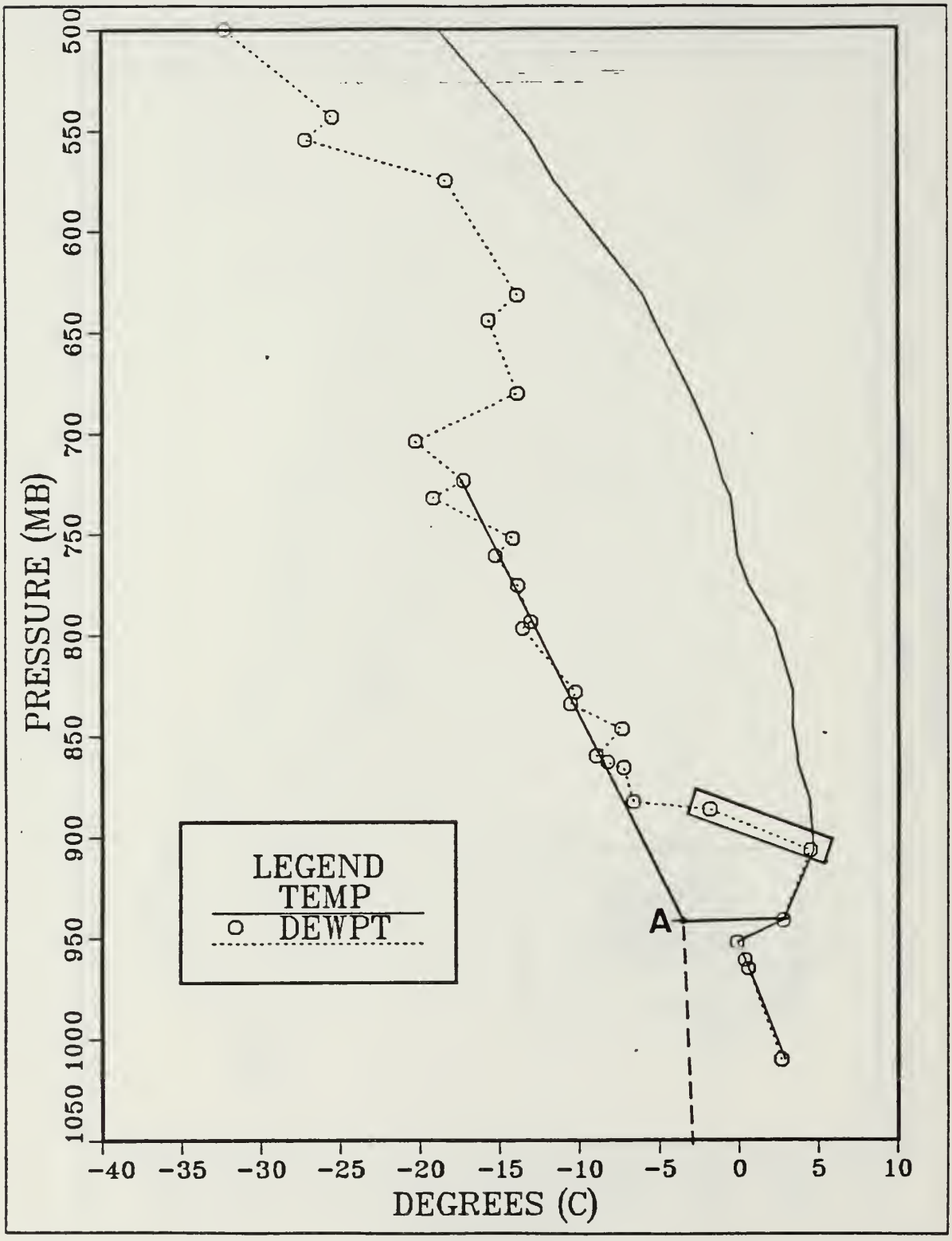

Fig. 4.5 Case Three, dewpoint above saturated portion colder than dewpoint at the inversion.

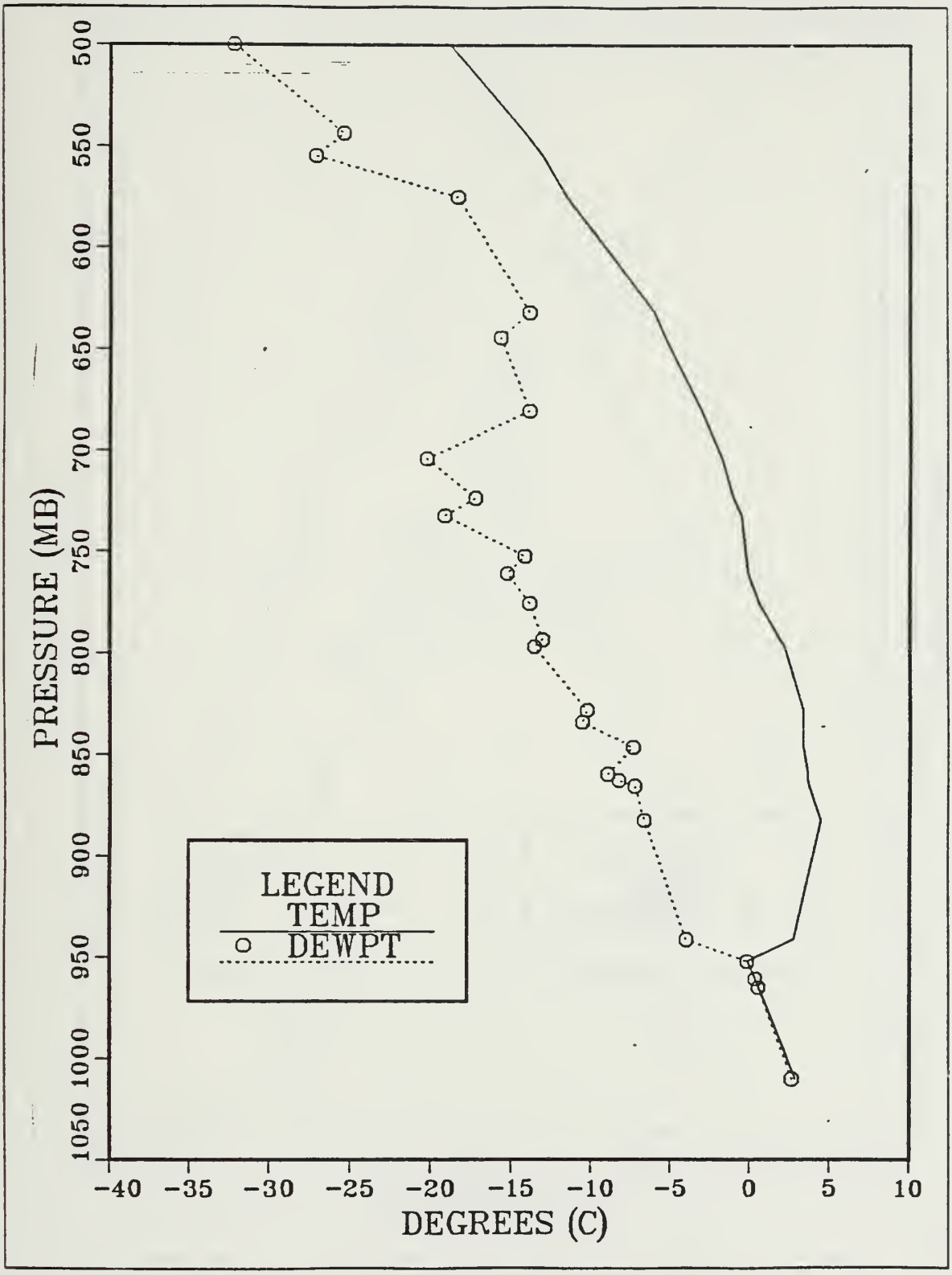

Fig. 4.6 Corrected profile for Case Three.

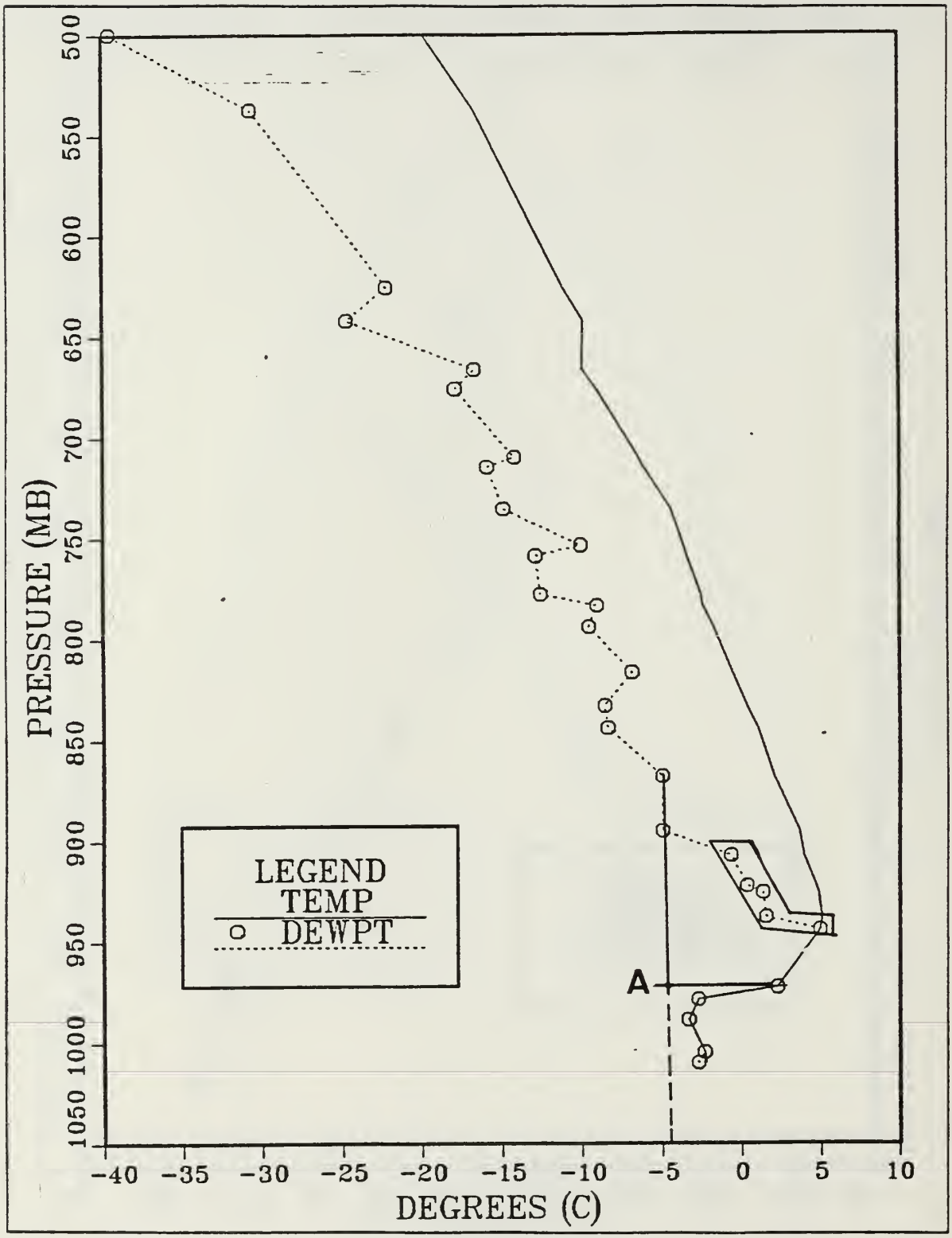

Fig. 4.7 Case Four, dewpoint above saturated portion colder than the dewpoint at the inversion.

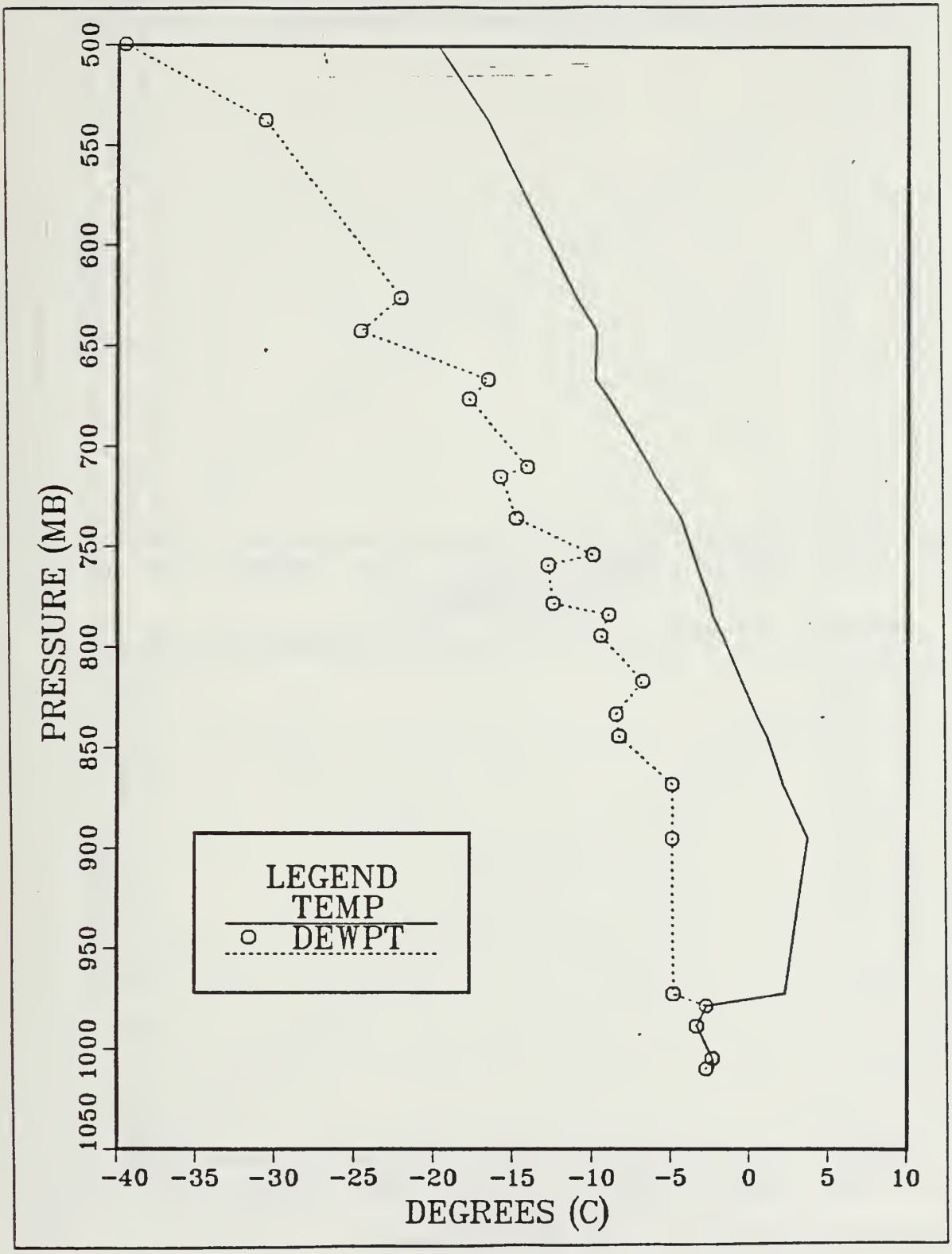

Fig. 4.8 Corrected value for case four.

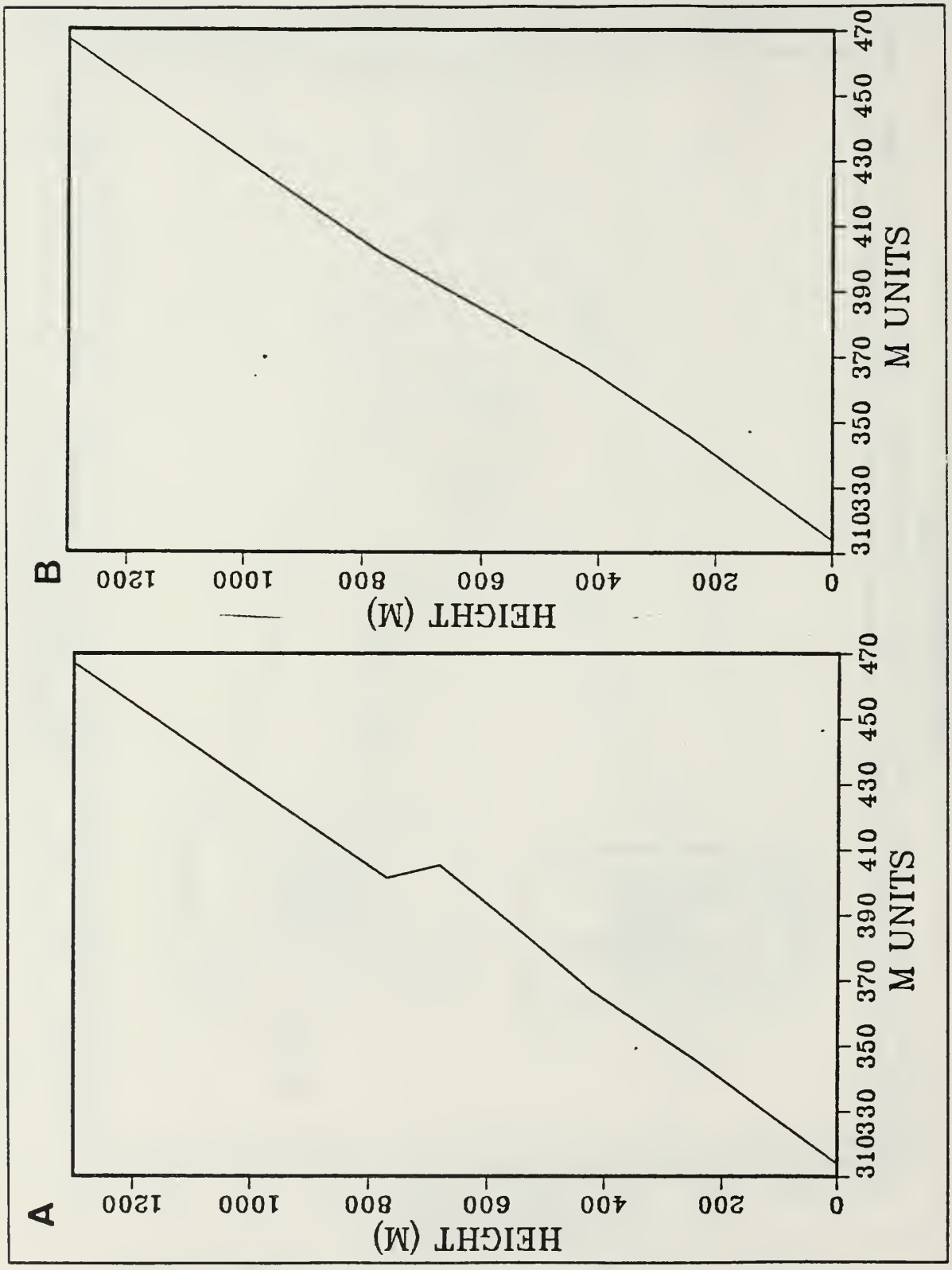

Fig. 4.9 M profiles of case 1, (a) uncorrected, (b) corrected.

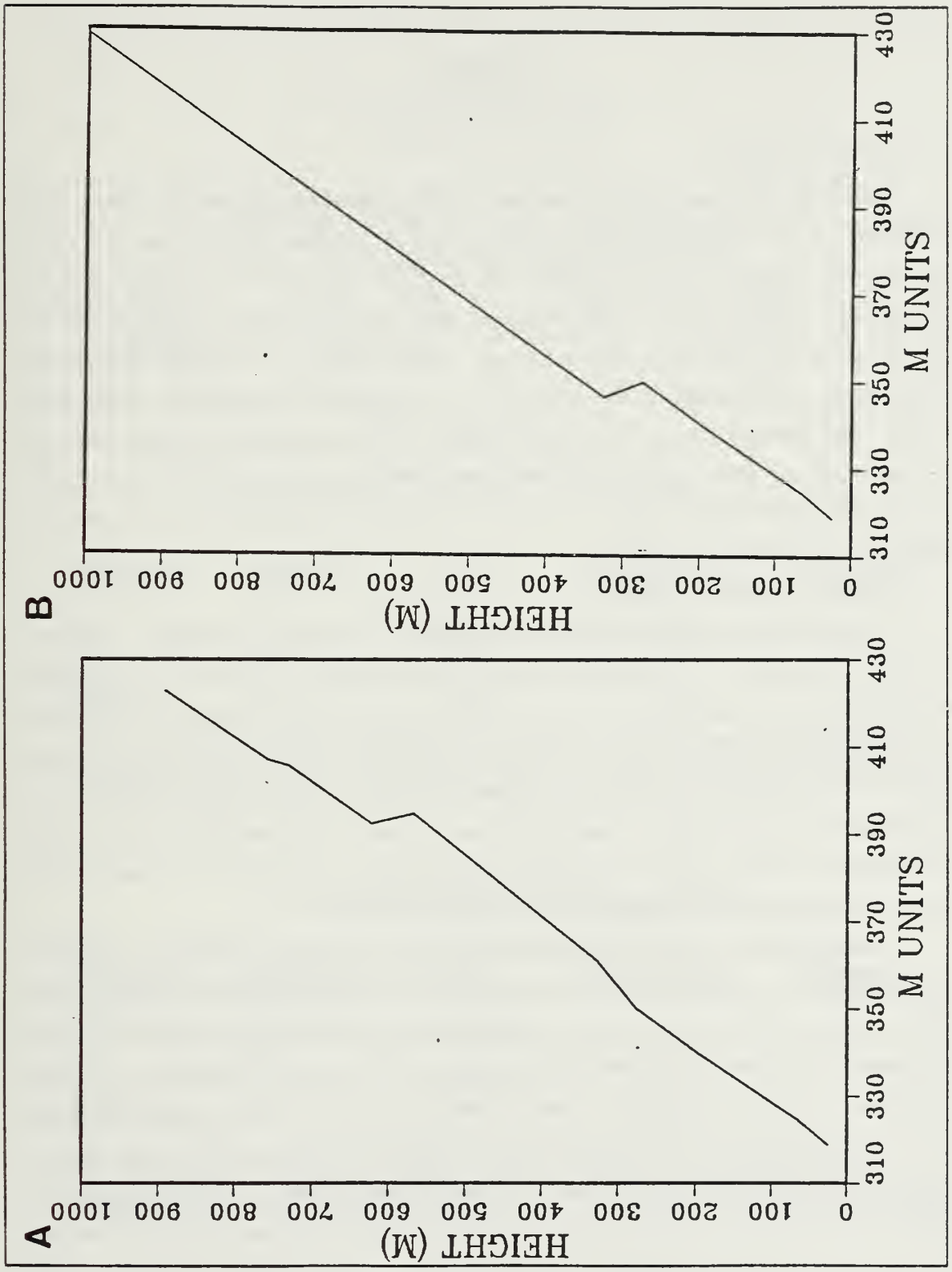

Fig. 4.10 M profiles of case 2, (a) uncorrected, (b) corrected.

V. RESULTS

A. SPATIAL STUDY

There were 126 cases when at least two of the ships launched radiosondes within a half-hour of the designated launch time. Table 2 summarizes the data from this study. Overall, ducting episodes decreased by 36% and the number of individual ducts decreased 50% when the data were corrected. An episode is defined as the occurrence of one or more ducts during a launch period. There seemed to be considerable spatial inhomogeneity, as indicated by the relatively low percentage of episodes in which more than one ship detected a duct on the same launch. The percentages calculated after the data have been corrected probably underestimate the ducting occurrences in the Arctic, since the probable sharp humidity decreases at the inversion could not be accurately recreated by the correction scheme.

1. Vertical refractive structure

Multiple ducts in the vertical were recorded on only six launches. In all six cases, the ships were located within 10 km of the ice edge on the water side, and the flow was parallel to the ice edge or off-ice. In four of the six cases the optimum coupling heights (OCH) of the ducts were within 200 m of each other. In the other two cases there was a large difference between the heights of the ducts, which may be an indication of the presence of more than one air mass in the vertical. The strength and thickness of the duct did not appear to be functions of height, i.e. the lowest duct was not necessarily the stronger or thicker of the two ducts.

Geernaert *et al.* (1987), studying the acoustic sounding (sodar) data collected during MIZEX-84, found that multiple (vertical) inversions periodically existed at the ice edge. They concluded that these inversions were interleaving and were due to mass convergence of different air masses at the ice edge. Their studies focused on two time periods, 1-6 July and 10-15 July. Three of the six cases in which multiple (vertical) ducts were recorded occurred during the first period. On 1 July, sodar traces showed strong returns, which are characteristic of stably stratified layers, at the ice edge at 120 m, 190 m and 220 m. On 1 July the rawinsonde launched by the Polarstern showed two ducts, one at 108 m and the second at 313 m. On the 2nd of July the winds increased and the ABL was observed to increase in depth. Profiles collected at the

TABLE 2

SPATIAL STUDY DATA
(18 JUNE - 15 JULY)

Of launch periods producing ducts, percentage of distribution of duct multiplicity

	Uncorrected / Corrected		
1 ship	61% / 87%	3 ships	6% / 3%
2 ships	33% / 10%	4 ships	0% / 0%

AVERAGE VALUES

Uncorrected data
(based on a total of 88 ducts)

location of ship	percent of ducts	OCH (meters)	Thickness (meters)	Strength (Δ M)
ICE	45	502	95	3.0
MIZ	15	495	76	2.0
WATER	40	848	163	3.8

In 61 out of 126 launches (48.4%) a duct was detected

Multiple (vertical) ducts 6/61 = 9.8% of launch periods

Corrected data *
(based on a total of 45 ducts)

location of ship	percent of ducts	OCH (meters)	Thickness (meters)	Strength (Δ M)
ICE	22	370	62	1.7
MIZ	27	377	71	2.1
Water	51	560	88	3.1

In 39 out of 126 launches (30%) a duct was detected

Multiple (vertical) ducts 7/39 = 17.8% of launch periods

* In 86 of 126 cases at least 1 profile was corrected

MIZ showed multiple ducts at 518 m and 1702 m. Early on the third the wind shifted from an off-ice to an on-ice flow. A profile of a radiosonde launched at 0500UTC showed three ducts at 227 m, 479 m and 576 m. As the winds continued to blow in an on-ice direction, advecting warm air over the ice edge, the duct heights increased to 368 m and 958 m. Sodar traces showed no strong returns. Sodar traces were not available on the 15th of July, but traces from the 13th of July indicated two inversions. The flow remained the same through the 15th of July, which could explain the two ducts recorded at the ice edge by Hakon Mosby.

When the data were corrected, one additional instance of multiple ducting was recorded. A second launch on 2 July detected multiple ducts. The ship was at the ice edge. The flow over the ship was parallel to the ice edge. The ducts were very similar to the multiple ducts already recorded on the 2nd of July.

Dotson (1987) showed that high resolution of the data was critical for determining multiple ducts, and that in an operational mode using lower resolution data these multiple ducts would likely have been combined or not detected. Dotson concluded that the high resolution data revealed almost five times as many ducts than the low resolution data, since the top and bottom of the duct could be better defined. In three of six cases the lowest duct was the strongest duct and in the other three the converse was true. In all cases the strongest duct was the thickest duct. In four of six cases the ducts were within 200 m of each other and we believe that detecting these ducts would have been adversely affected with lower resolution of data. We believe that in this situation the multiple ducts represents a real phenomenon and that higher resolution was critical to detect these ducts.

2. **Horizontal variablity relative to the ice edge**

Guest and Davidson (1987) and Kellner *et al.* (1987) have shown that the inversion was a function of the distance from the ice edge. We expected a similar trend in the height of the duct. Table 2 indicates that the ducts did exhibit different characteristics in height, thickness and strength over the ice, the MIZ and over the water adjacent the ice edge. The percentages of ducts detected by ships operating in the ice, using uncorrected data, nearly equaled that of the ducts detected by the ships operating in the water adjacent the ice edge. When the data were corrected the percentage of ducts recorded by the ships operating in the ice was drastically reduced. This implies that over the ice profiles were affected more by the correction. The average values of height, thickness and strength were much lower over the pack ice than over the water in both the uncorrected and the corrected data.

The data were plotted in scatter diagrams to investigate the specific relationships between the distance from the ice edge and height, thickness and strength. Fig. 5.1 is a scatter diagram of the height of the ducts versus distance from the ice edge. The ice edge is denoted by zero; positive numbers indicate distance from the ice edge in the adjacent water, and negative numbers represent the distance from the ice edge into the pack ice. A linear least squares fit was applied to the data and is indicated by the solid line on the figure. The fit was done in two segments. The first segment was from -140 km to 0 km, where (-) implies interior to the ice edge. The second segment was from 0 km to +210 km. This figure shows that the ducts were lower over the pack ice than over the MIZ. A rapid increase was seen in the height of the ducts as one moved away from the ice edge. This was due to the heating of the lower atmosphere as the cold air flowed off-ice over the warmer water. Fig. 5.4, for the corrected data, shows an almost linearly increasing relationship of the OCH from the pack ice through the MIZ to the adjacent water. Figs. 5.2, 5.3 show that with respect to thickness and strength, the value over the pack ice was slightly higher than the value at MIZ. Figs. 5.5, 5.6 show the relationship of the thickness and strength with respect to the ice edge for the corrected data exhibited the same trends as seen in the uncorrected data. Again the values rapidly increased over the water as one moved away from the ice edge. Comparing Figs. 5.1 and 5.4 with Figs. 5.2, 5.3, 5.5 and 5.6 shows that the relationship of the thickness and the strength with respect to distance from the ice edge is not as strong as it is with the height. Comparing the values at -90 km to values at 90 km, the percent of change of the height was greater (77%) than the change in the thickness (16%) and the change in the strength (10%). Also, when comparing individual cases, it was found that the height versus distance relationship always held, whereas for the thickness and and strength data these relationships were valid approximately 60% of the time.

When comparing the uncorrected and corrected data, several differences were noted. Although there were fewer points in the corrected data, the trends were similar. The overall average values of height, thickness and strength were lower. This may have been due simply to fewer data points. More likely it was related to the correction applied to the data. In the uncorrected data the height, thickness and strength reflected the values above the saturated portion of the profiles. The ducts reflected sharper humidity changes at greater heights, which could give erroneously high heights and thickness values. The decrease in the strength may be explained by the fact that

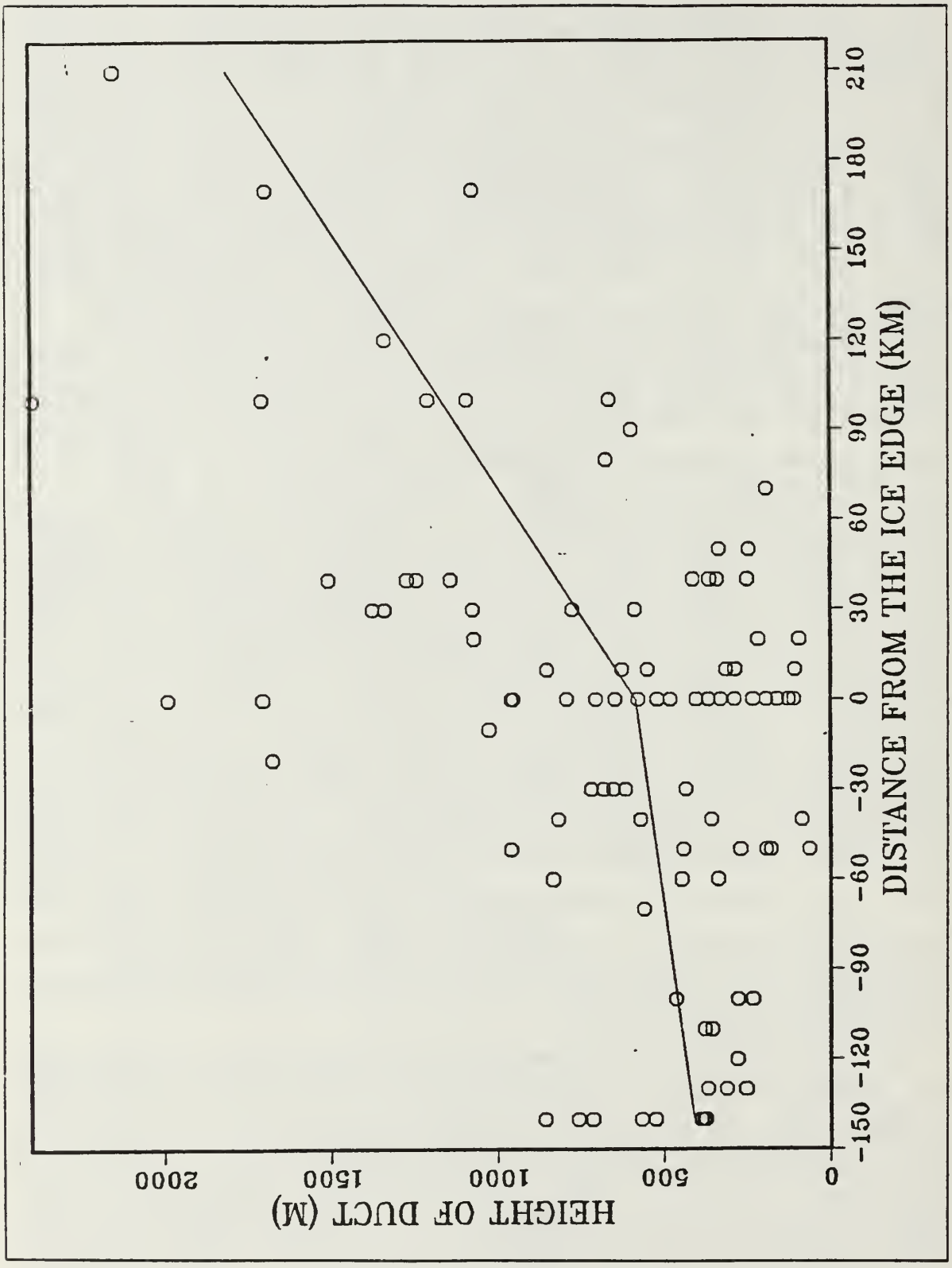

Fig. 5.1 Duct height with respect to distance from the ice edge, uncorrected data.

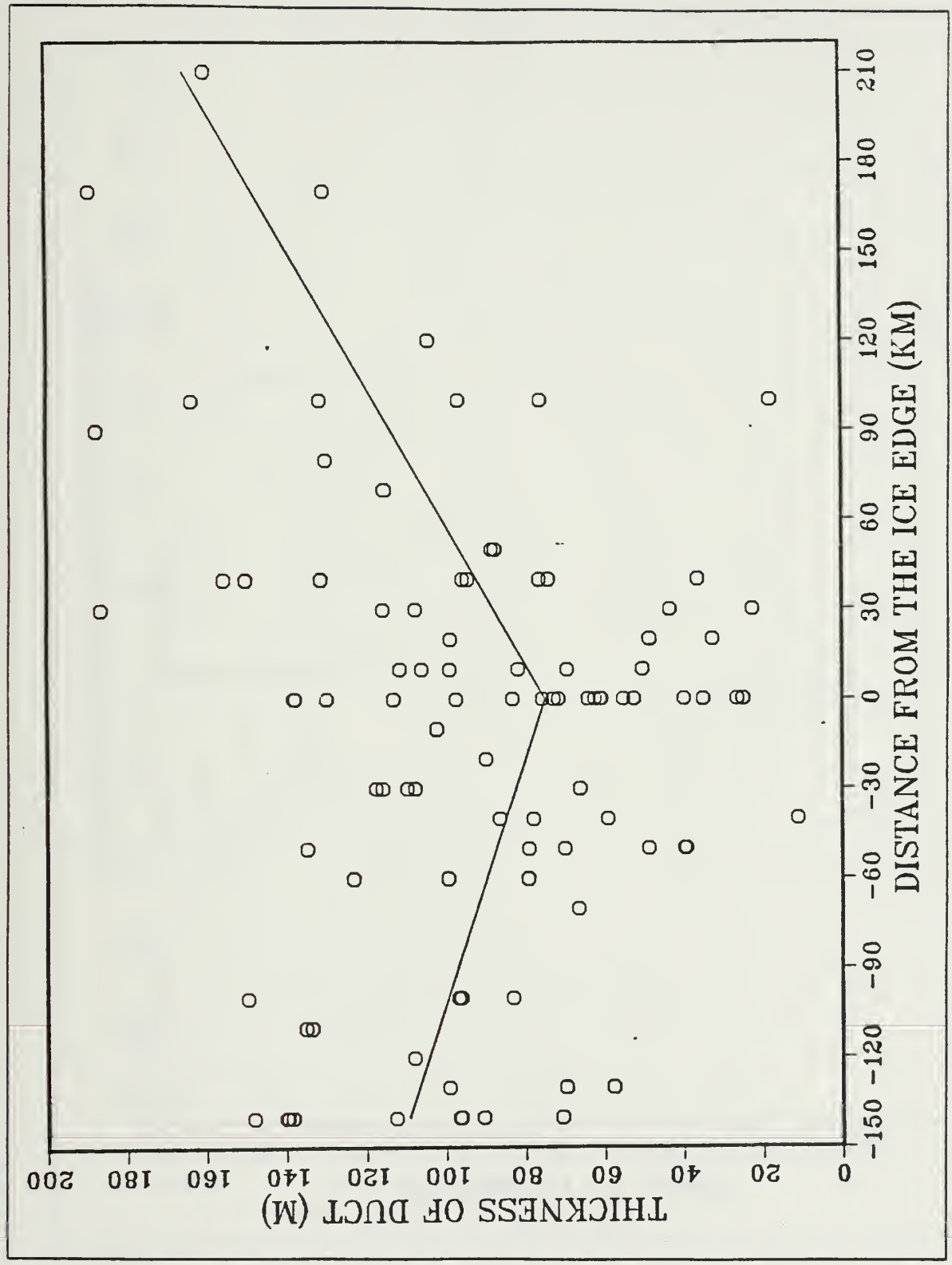

Fig. 5.2 Duct thickness with respect to distance from the ice edge, uncorrected data.

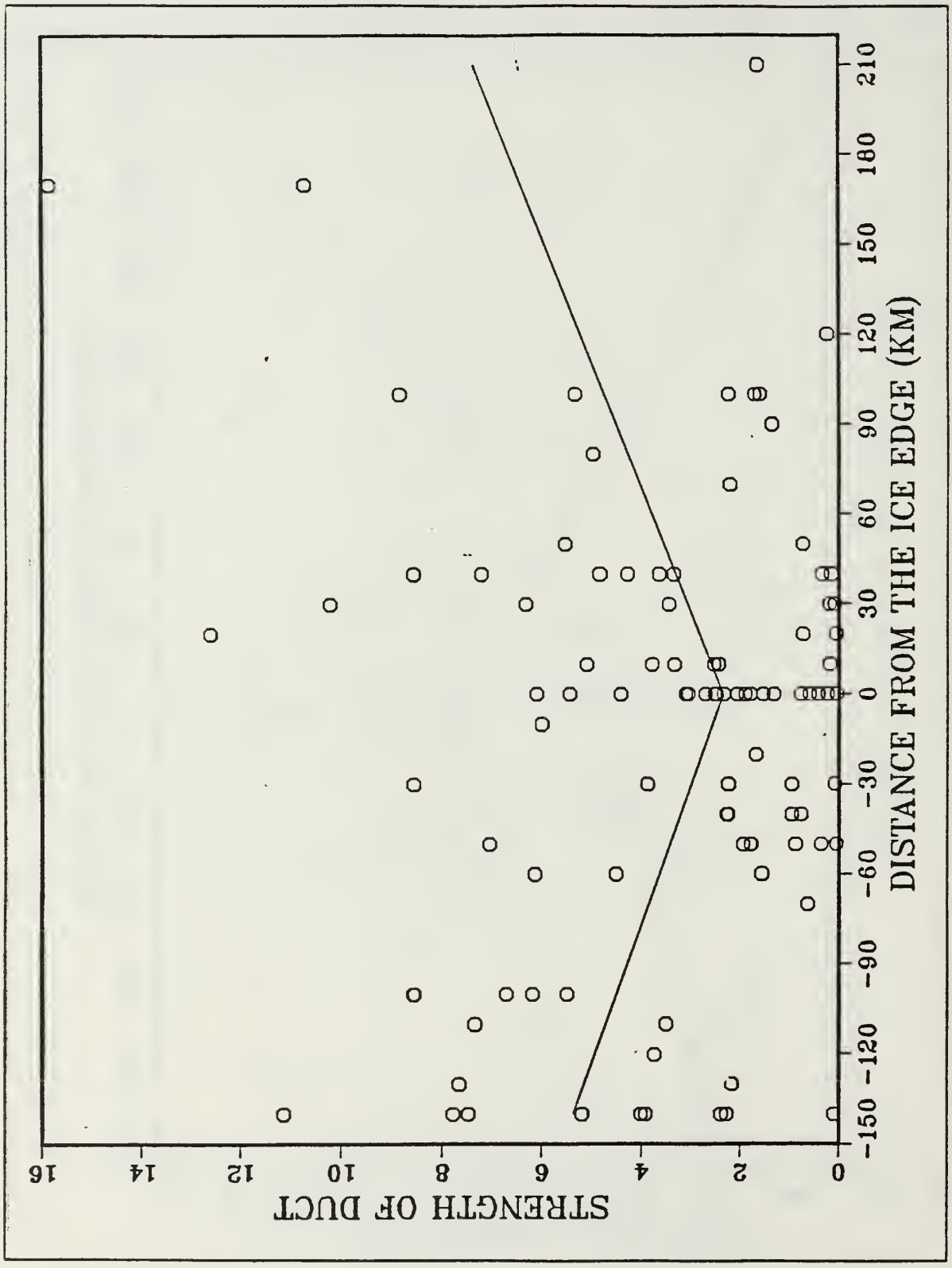

Fig. 5.3 Duct strength with respect to distance from the ice edge, uncorrected data.

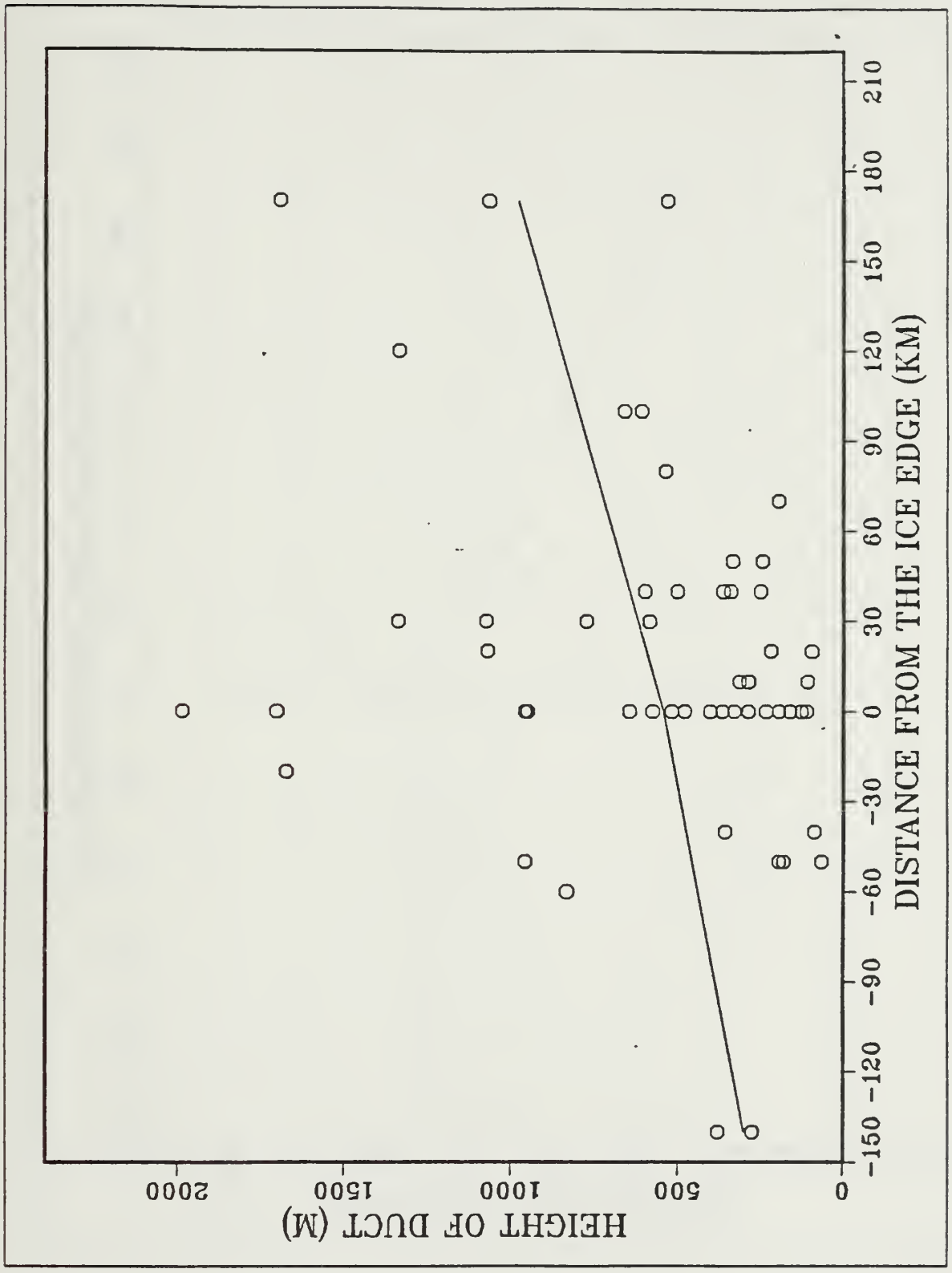

Fig. 5.4 Duct height with respect to distance from the ice edge, corrected data.

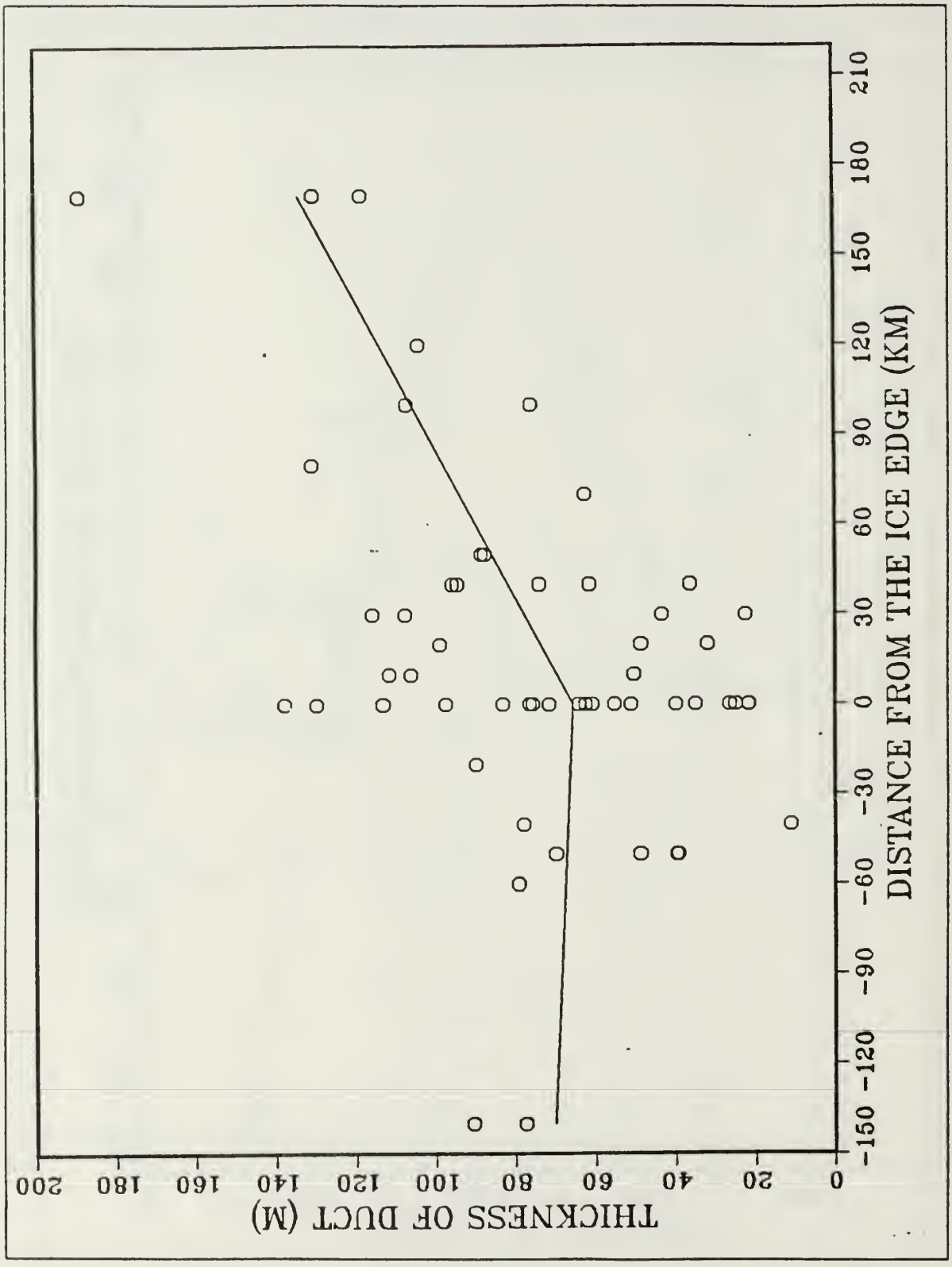

Fig. 5.5 Duct thickness with respect to distance from ice edge, corrected data.

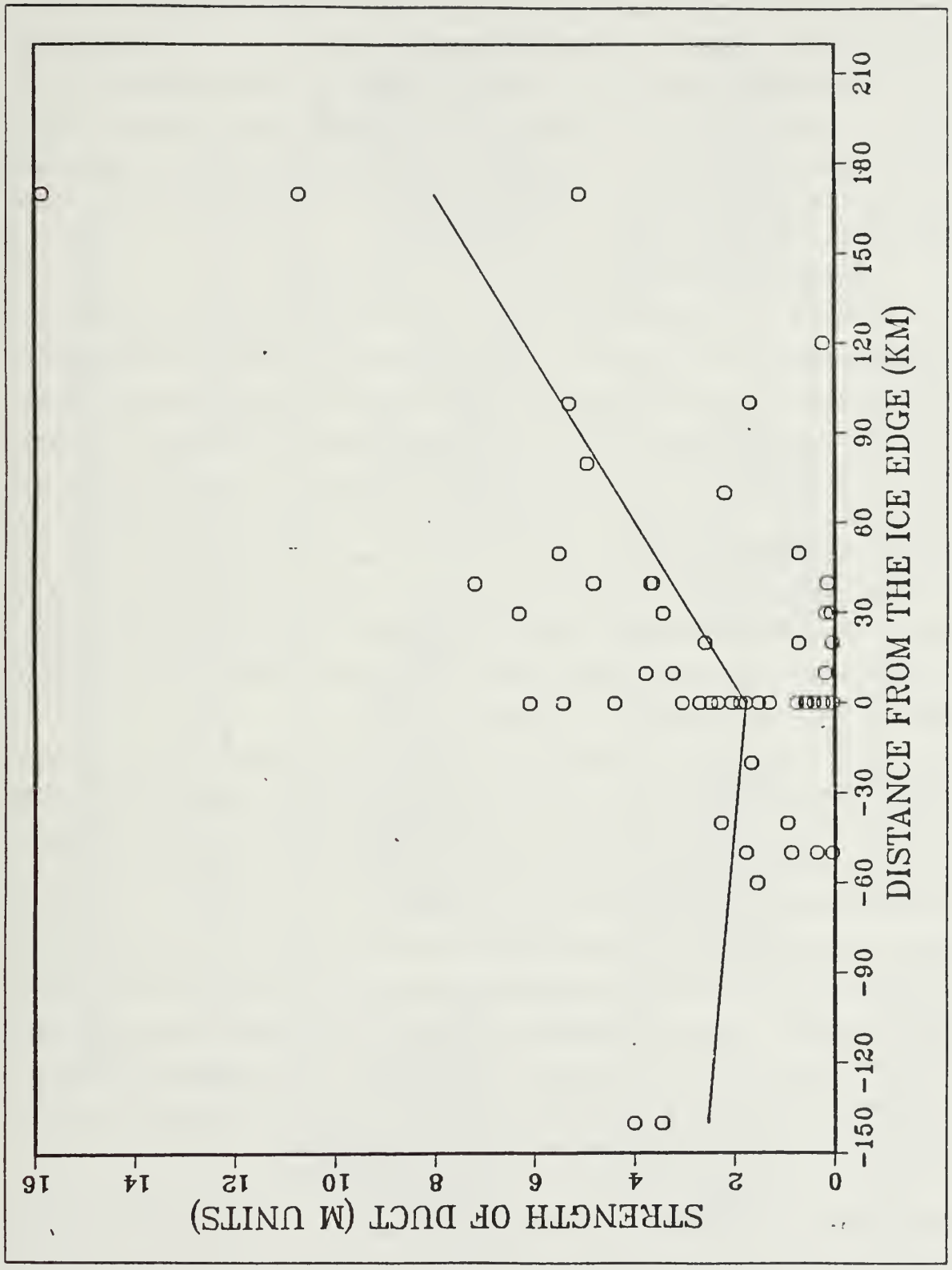

Fig. 5.6 Duct strength with respect to distance from ice edge, corrected data.

the strength in the uncorrected data reflected the abrupt jump of the dewpoint curve. This gradient may be greater due to this jump than actually existed at the inversion. More of the profiles collected over the ice were affected than those collected over the water. This may have been due to the fact that the clouds were colder over the ice. With the colder temperatures (sub freezing), saturation below the inversion could form ice or frost on the launch sensor. The air temperature over the water was not below freezing at the inversion as much as it was over the ice.

3. **Variability in the refractive structure from ship to ship**

Table 3 is a summary of the numbers of cases when two ships recorded a duct at the same launch time. From Table 3 one can see that the refractive structure varied from launch time to launch time and from the ice to the MIZ, and to the water. When the data were corrected the number of cases when two ships detected ducts at the same launch time dropped to four. These cases were the same as those recorded in the uncorrected data. These cases included: (1) one case when the two ships in the adjacent water recorded ducts, but the two ships in the ice did not detect a duct; (2) two cases when one ship in the adjacent water and one ship in the ice recorded a duct while the other two ships between them did not detect a duct and; (3) one case when two ships at the MIZ recorded ducts while the other two ships, one in the adjacent water and one in the ice, did not record ducts.

Table 3 includes two cases when the ducts were recorded by the two ships operating in the water adjacent the MIZ, while the other ship, operating in the ice, did not record a duct. In the first case the two ships recording ducts were within 40 km of each other. The height of the ducts recorded at each ship was similar; however, the duct recorded by the ship to the south was weaker and not as thick. A low pressure system was approaching from the southwest and may explain these differences. The flow at the ship to the south may have been influenced by the approaching low and the smaller subsidence value associated with proximity to this system could explain the weaker and thinner duct seen at that ship. In the second case, one ship was located at 10 km and the other is 170 km from the ice edge. The duct of the ship which was closer to the MIZ was lower, thinner and substantially weaker.

Table 3 indicates that there were 13 cases in which a duct was detected by one ship operating in the ice and by a second ship operating in water adjacent to the ice edge. In five of these cases the other two ships did not have successful launches. The height of the ducts followed the same trend seen in Fig. 5.1. The thickness of the duct

TABLE 3

CASES WHEN 2 SHIPS RECORDED A DUCT ON THE SAME LAUNCH

There were 20 out of 61 cases *

The following indicates the distribution of ducts on each launch

- 4 Cases: 2 ships in the ice reported ducts and the other 2 ships in the adjacent water reported no ducts
- 2 Cases: 2 ships in the adjacent water reported a duct and the 3rd ship in the ice reported no duct
- 13 cases: 1 ship in the adjacent water and 1 ship in the ice reported ducts
  - 5 cases: no other ships launched radiosondes
  - 2 cases: the 3rd ship in the adjacent water did not detected a duct
  - 2 cases: the 3rd ship further in ice, and the 4th ship further in the adjacent water did not detect ducts
  - 4 cases: 2 ships between those which detecting ducts did not detect ducts
- 1 Case: 2 ships at the MIZ reported a duct while the 3rd ship in the ice and the 4th ship in the adjacent water reported no ducts

* Uncorrected data

followed the trend seen in Fig. 5.2, and the strength of the duct followed the trend seen in Fig. 5.3, a majority of the time. Although it could not be determined it there had been a continuous duct from the ice to the water, if the duct had been continuous, the data indicates that the height, thickness and strength would increase from the ice to the water.

The table also indicates that in two cases a third ship was located in the water near the ship recording the duct but did not record a duct. The flow was parallel to the ice and both ships were near the ice edge. The difference in the refractive conditions may be explained by the difference in the interaction of the air masses along the ice edge. The duct recorded at the ship operating in the ice was lower, thicker and stronger in both cases.

In all cases the duct detected by the ship operating furthest into the ice was closest to the surface. Statistics on the the strength and thickness were not as consistent. Also there was no apparent relation between strength and thickness, i.e. the thickest duct was not always the strongest duct.

The difference in the refractive structure when ships operating in the ice detected ducts while those operating in the water did not could be explained by the location of the high pressure. The high was centered over Greenland causing more subsidence over the ice than over the water.

There were four cases when ducts were detected by three ships on the same launch. In one of the cases only three ships had a successful launch. The Polarstern was located 100 km into the ice, the Hakon Mosby was at the MIZ and the Valdivia was located 100 km into the adjacent water. The duct recorded at the ship in the ice was significantly lower than the duct at the MIZ or over the water. This duct was also the thinnest. The strength of the ducts decreased from the ice to the water. In the fourth case, the Polar Queen was located 50 km into the ice, the Hakon Mosby at the MIZ and, the Valdivia was 20 km into the ice. The Polarstern located 140 km into the ice did not record a duct. The duct recorded by the ship in the ice was the lowest, increasing in height to the MIZ and then decreasing again over the water. The thickness and strength of the ducts did not follow any pattern. This case was the only one which remained after the data was corrected, and remained unchanged.

4. **Case Studies**

Four cases were selected and developed into individual case studies to try to explain the lack of homogeneity in the refractive structure. Two cases were chosen

when two ships detected ducts and the two ships did not detect ducts on the same launch. The first of these case studies was chosen because two ships, operating between the two ships who recorded ducts, did not detect ducts. The flow was off-ice. The second case was chosen because two ships operating at the MIZ recorded ducts but the other two ships one in the water and one in the ice did not record ducts. Off-ice flow dominated all four ships. The last two cases studies were chosen when three ships recorded ducts at the same launch. These two were chosen because there was on-ice flow and the two launch times were consecutive.

a. Case One

In this case the sondes were launched at 2000UTC on 10 July by all four ships. The Polarstern was located 140 km into the ice, the Polar Queen was located at the ice edge, the Hakon Mosby was located 40 km into the water. The Valdivia was located 90 km into the water. Fig. 5.7 shows the ships' positions relative to the ice edge. The surface analysis is also given in Fig. 5.7. A 992 mb low was located north of Greenland and the trough associated with this low extended southwest over the Greenland sea. A weak high was centered centered over northern Norway.

Fig. 5.8 shows the temperature and dewpoint curves of each ship. The temperature profile increased from the ice to the water. The inversion monotonically increased from a height of 990 mb at the Polarstern to 940 mb at the Valdivia. The dewpoint curves above the inversion from the Polarstern, Polar Queen and the Hakon Mosby radiosondes were nearly the same. The Valdivia showed a significantly higher dewpoint than the other three. This may be explained by the difference of the flow over this ship. The flow over the Valdivia was from the back side of the high located over Norway. This flow had not interacted with the ice edge and was considerably more moist.

Fig. 5.9 show the M profiles for each of the ships. We expected to see a duct which would increase in height from the Polarstern to the Valdivia. Fig. 5.9 shows that the Polarstern recorded a duct at 376 m and, the Hakon Mosby recorded a duct at 339 m, while the Valdivia and Polar Queen did not detect ducts. The Hakon Mosby's profile was a plausible representation of the atmosphere, with the dry layer just above the inversion. The Polarstern showed saturation below the inversion and, with the temperature below zero at the inversion, the dewpoint curve remained saturated above the inversion. The height of the duct reflected the saturation of the profile. The true height of the duct at the the Polarstern should probably have been

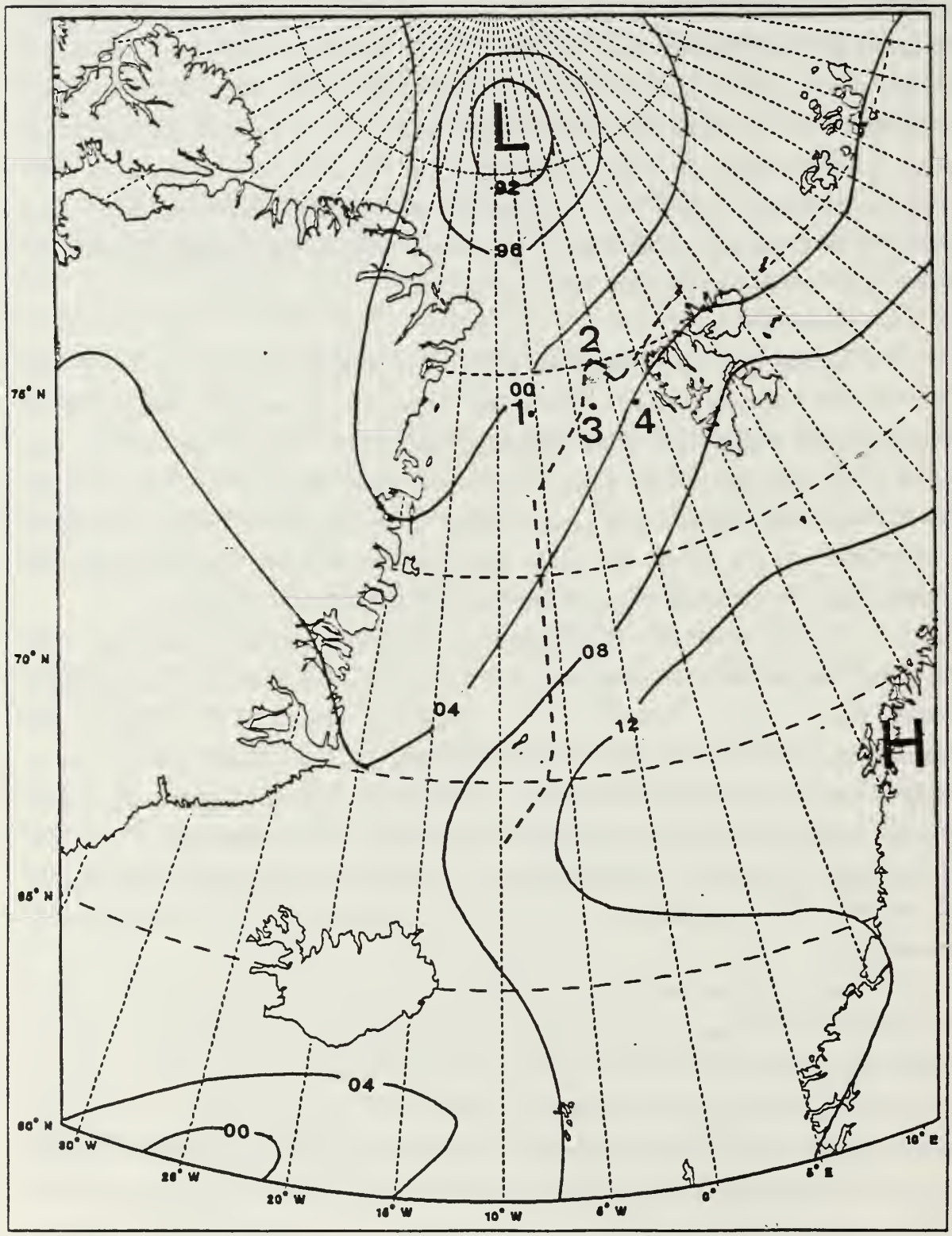

Fig. 5.7 Case 1, Sfc isobars, 10 Jul,1200UTC, and ship's locations at launch,2000UTC, (1) PS, 140 km into ice (2) PQ, MIZ (3) HM, 40 km in water (4) VL, 90 km in water.

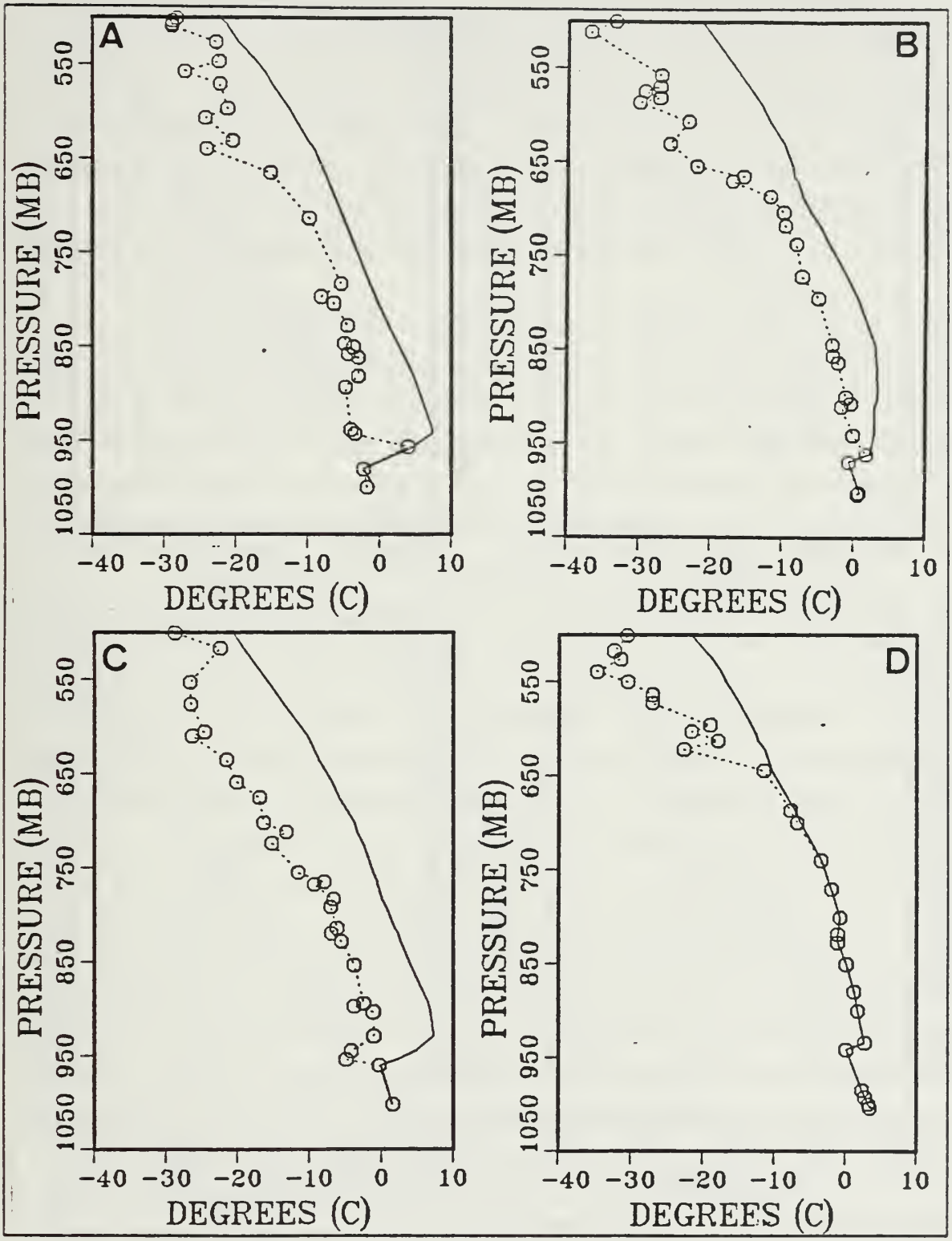

Fig. 5.8 Case 1 radiosonde plots: (a) PS (b) PQ (c) HM (d) VL, temperature is indicated by a solid line, dewpoint is indicated by a dashed line.

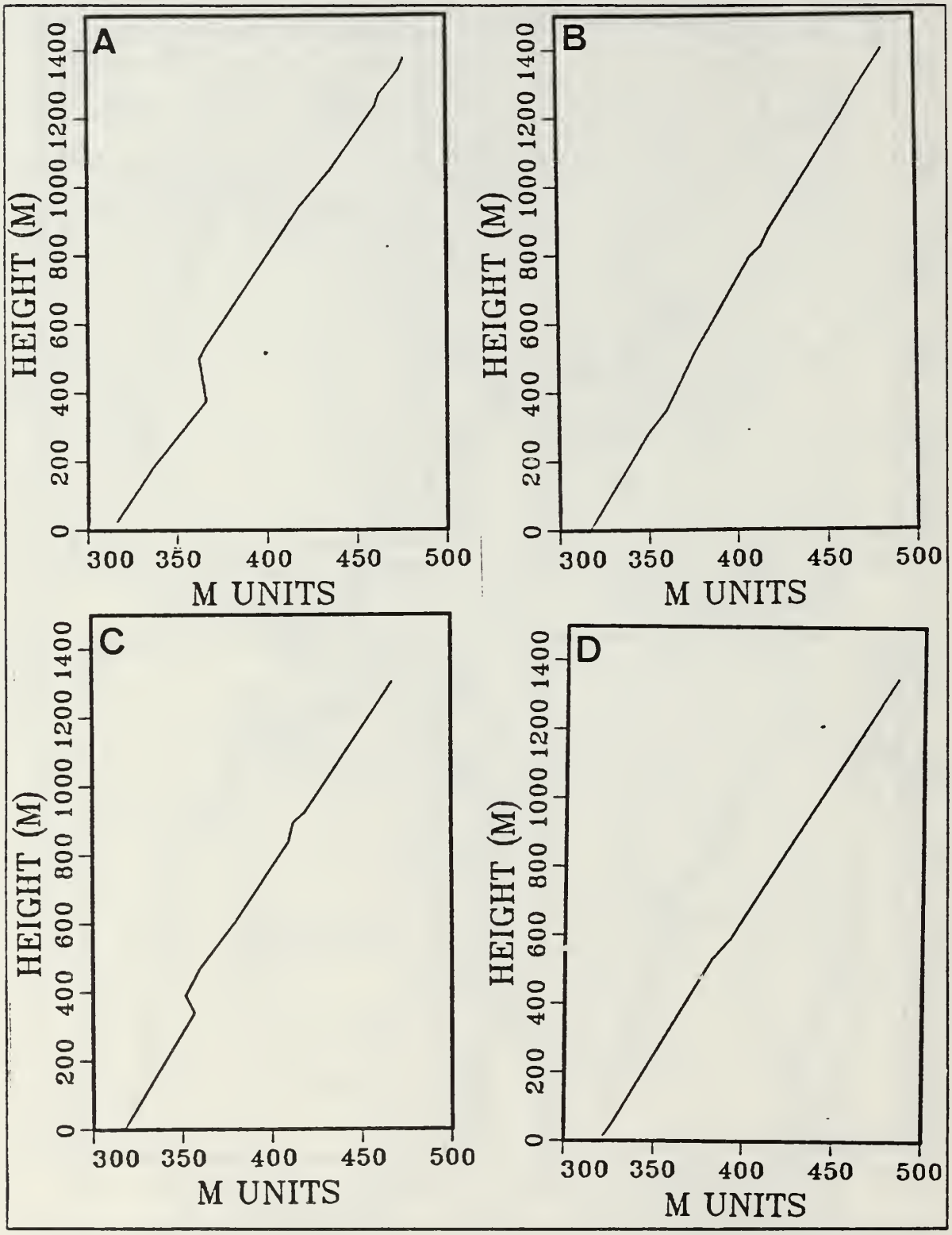

Fig. 5.9 M profiles of each of the ships
(a) Polarstern (b) Polar Queen (c) Hakon Mosby (d) Valdivia.

near the inversion at approximately 200 m. The corrected profile indicated no duct so we were not able to confirm that the duct was actually near the inversion. We suspect this was due to being unable to re-create the sharp decrease in the dewpoint indicated on the sonde launched by Hakon Mosby. The lack of ducting at the MIZ could be explained by the interleaving of the air from the high over Norway and the low to the north of the Polar Queen. The difference in the refractive conditions at the Valdivia may have resulted from the unmodified moist flow from the backside of the High.

b. Case 2

In this case radiosondes were launched at 2300UTC on 2 July by all four ships. The Polarstern and the Valdivia were located at the ice edge. The Polar Queen was located 50 km into the ice and the Hakon Mosby was located at 20 km into the water. The location of the four ships relative to the ice edge is shown in Fig. 5.10. The surface analysis is also shown in Fig. 5.10. A 1026 mb high was centered over Greenland causing parallel to off-ice flow over all four ships.

Fig. 5.11 shows the radiosonde profiles of each of the ships. The temperature curves were nearly identical on the Polarstern and the Valdivia. The dewpoint curves were identical except in the area near the inversion. The profile from the Valdivia showed a sharp decrease in the dewpoint just above the inversion, while the profile from the Polarstern showed saturation above the inversion. The Polar Queen's profile showed a colder temperature structure, and although the inversion was higher, it was weaker. The dewpoint curve from the Polar Queen showed the same saturation as the dewpoint curve taken from the Polarstern. Above the saturated portion of the profile the dewpoint curve was nearly the same as the dewpoint curves from the Polarstern and the Valdivia. The Hakon Mosby's profile shows slightly higher temperatures. The inversion was at nearly the same height as on the profiles from the Polarstern and the Valdivia but was not as well defined. The Hakon Mosby's profile was not saturated below the inversion. However, the dewpoint curve did not indicated as strong a jump as was seen at the inversion from the profiles of Valdivia and Polarstern. All four ships showed a decrease in the dewpoint at 750 mb.

Fig. 5.12 shows the M profiles from each of the ships. Fig. 5.12 shows that ducting occurred at the Polarstern (1987 m) and at the Valdivia (232 m), but not at the other two ships. The Polarstern's was the only profile which the sharp decrease in the dewpoint at 750 mb was sufficient to cause a duct. This could not be explained. When the data were corrected, the Polarstern's profile produced a duct at the inversion

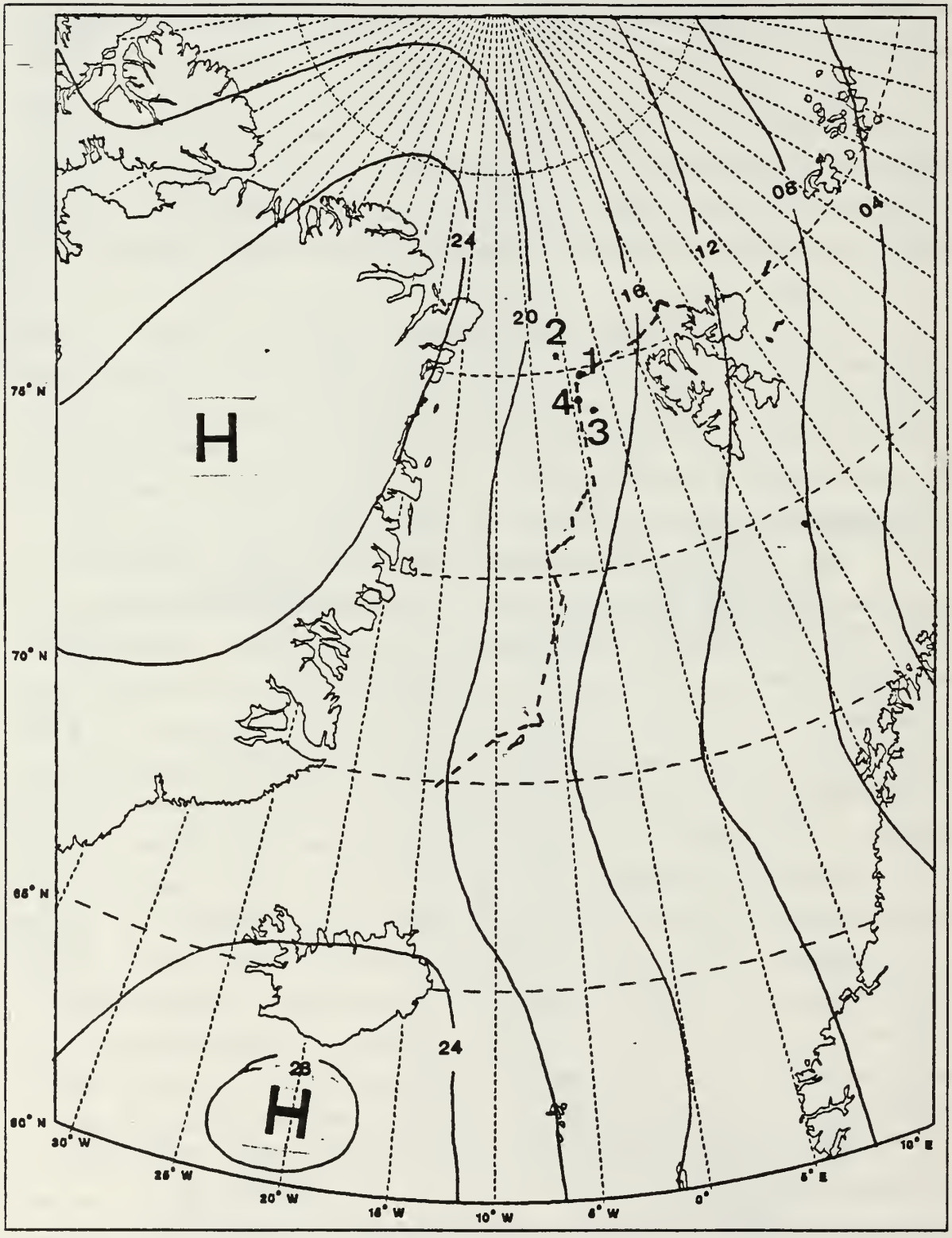

Fig. 5.10 Case 2, Sfc isobars, 2 Jul,1200UTC,and ship's locations at launch,2300UTC, (1) PS, MIZ (2) PQ, 50 km into ice (3) HM, 20 km in water (4) VL, MIZ.

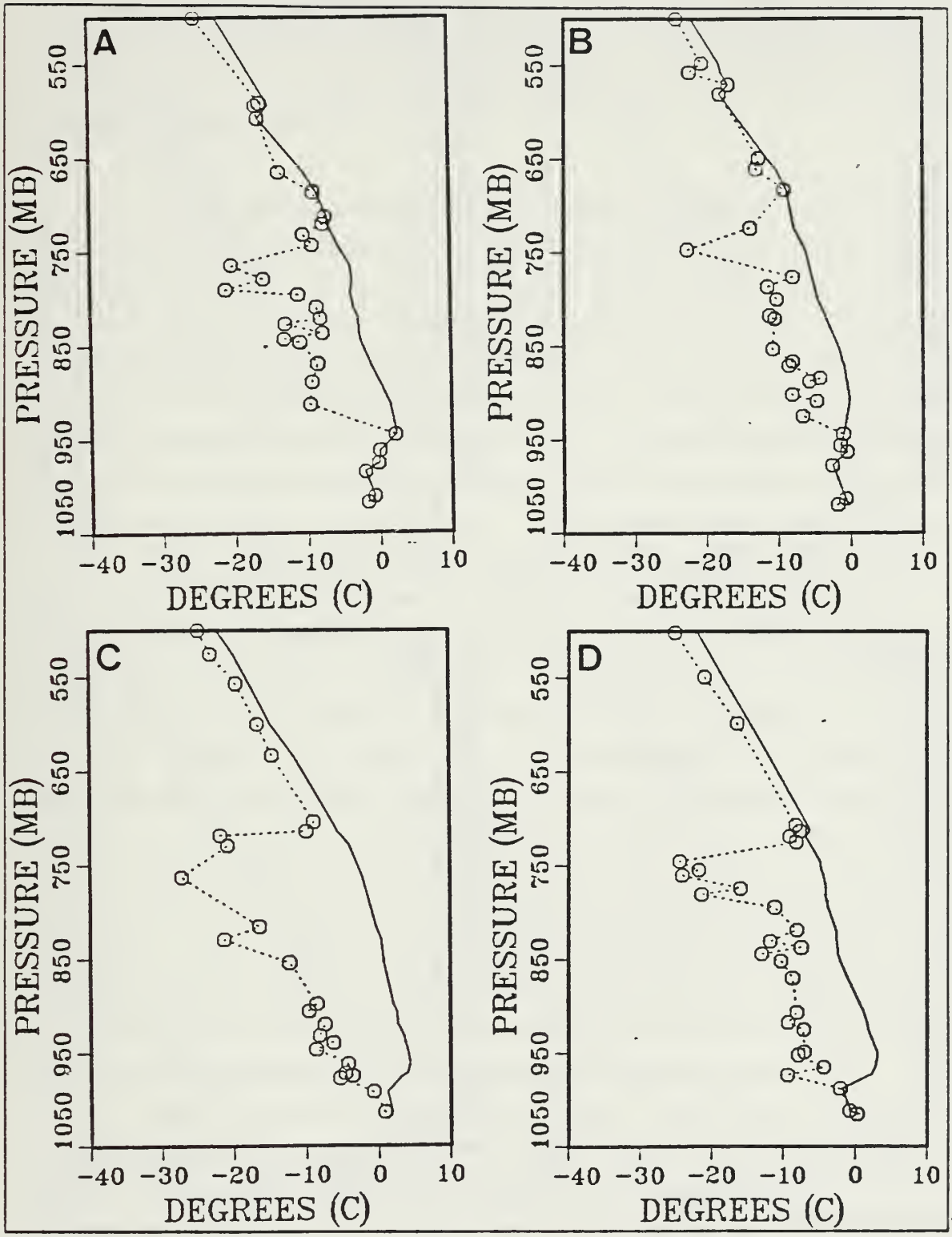

Fig. 5.11 Case 2 radiosonde plots: (a) PS (b) PQ (c) HM (d) VL, temperature is indicated by a and the dewpoint is indicated by a dashed line.

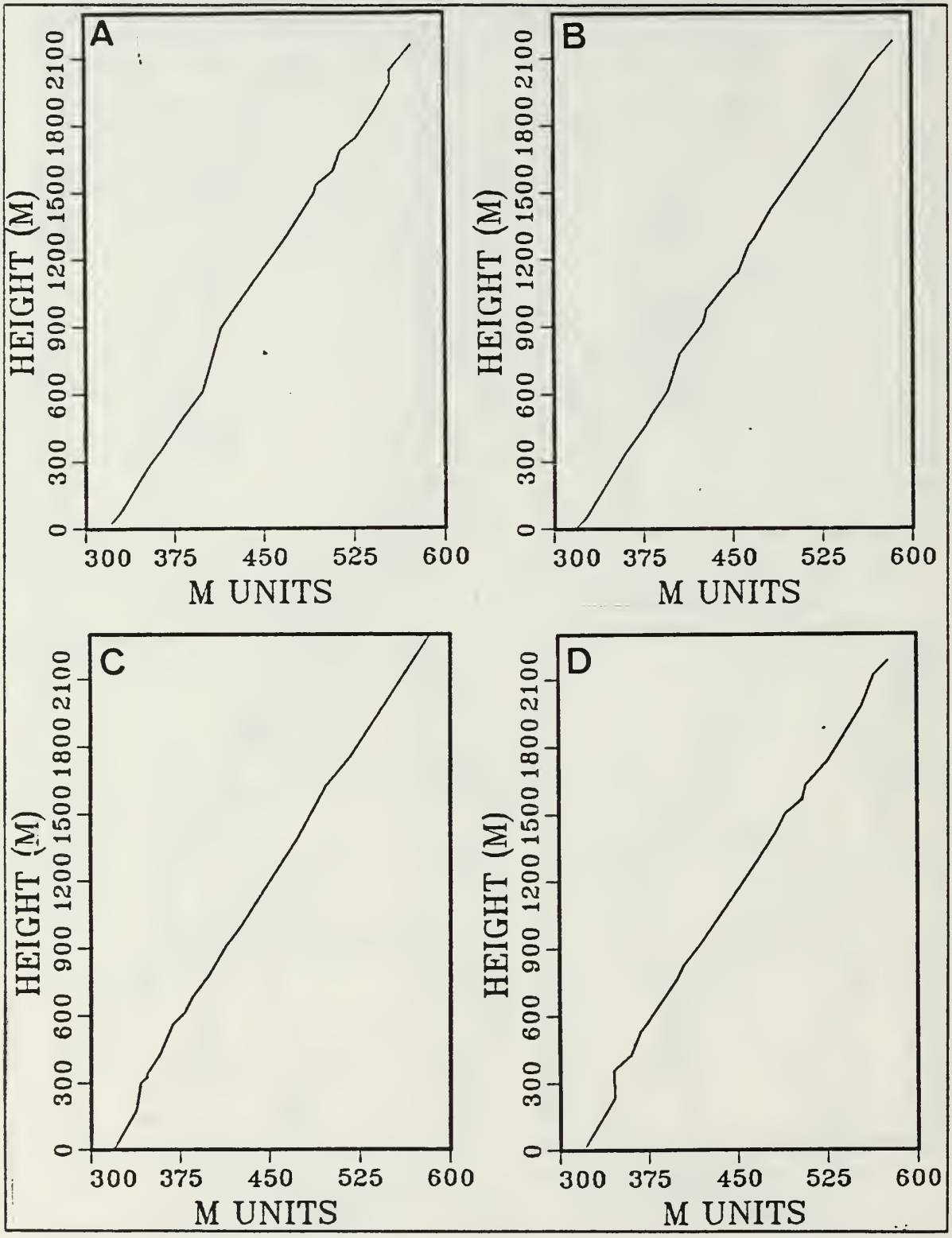

Fig. 5.12 M profiles of each of the ships
(a) Polarstern (b) Polar Queen (c) Hakon Mosby (d) Valdivia.

(285 m) which matched the duct at the Valdivia. Since all four of the ships were within 70 km of one another, and under the influence of strong subsidence from the Greenland high, it was expected that the refractive conditions would be the same. Apparently, this was not true.

c. Case 3

In this case the radiosondes were launched at 1100UTC on 26 June. All four ships launched radiosondes. The Polarstern was located 50 km into the ice, the Polar Queen was located 40 km into the ice, Valdivia was located at the ice edge and the Hakon Mosby was located 40 km into the adjacent water. Fig. 5.13 shows the position of each ship relative to the ice edge. Fig. 5.13 also shows the surface analysis. A weak low was centered north of Greenland with its associated trough extending southeast over Greenland and the Greenland sea. A 1026 mb high was located in the Barents Sea and ridged southwest over Svalbard. On-ice flow persisted over all four of the ships.

Fig. 5.14 shows the radiosondes profiles from each of the ships. The temperature curves on the Polarstern and the Polar Queen were nearly identical. The dewpoint curves were similar above the inversion. The profile from the Polarstern was never saturated and shows a decrease in the dewpoint just above the inversion. The dewpoint curve from the Polar Queen, within 10 km of the Polarstern, was saturated below the inversion and continued to be saturated above the inversion. The temperature curve of the Valdivia was nearly the same as the Polarstern's and the Polar Queen's except the inversion was higher at the Valdivia. The dewpoint curve was saturated below the inversion and continued to be saturated above the inversion. The dewpoint curve above this showed a slightly moister profile than the Polarstern and Polar Queen. The temperature curve from the Hakon Mosby was identical to the Valdivia except the inversion was lower. The inversion was at the same height as at the Polarstern and the Polar Queen. The dewpoint curve did not show saturation below the inversion and showed a slight decrease just above the inversion.

Fig. 5.15 shows the M profiles of the ships. The Polarstern detected a duct at 358 m, the Polar Queen a duct at 441 m and the Valdivia a duct at 704 m. The difference in the ducts between the Polarstern and Polar Queen was due to the saturation seen in the dewpoint curves for the Polar Queen and not for the Polarstern. The duct detected at the Polar Queen more possibly should have been near the inversion at 358 m. This was not confirmed by the corrected profile since the duct did

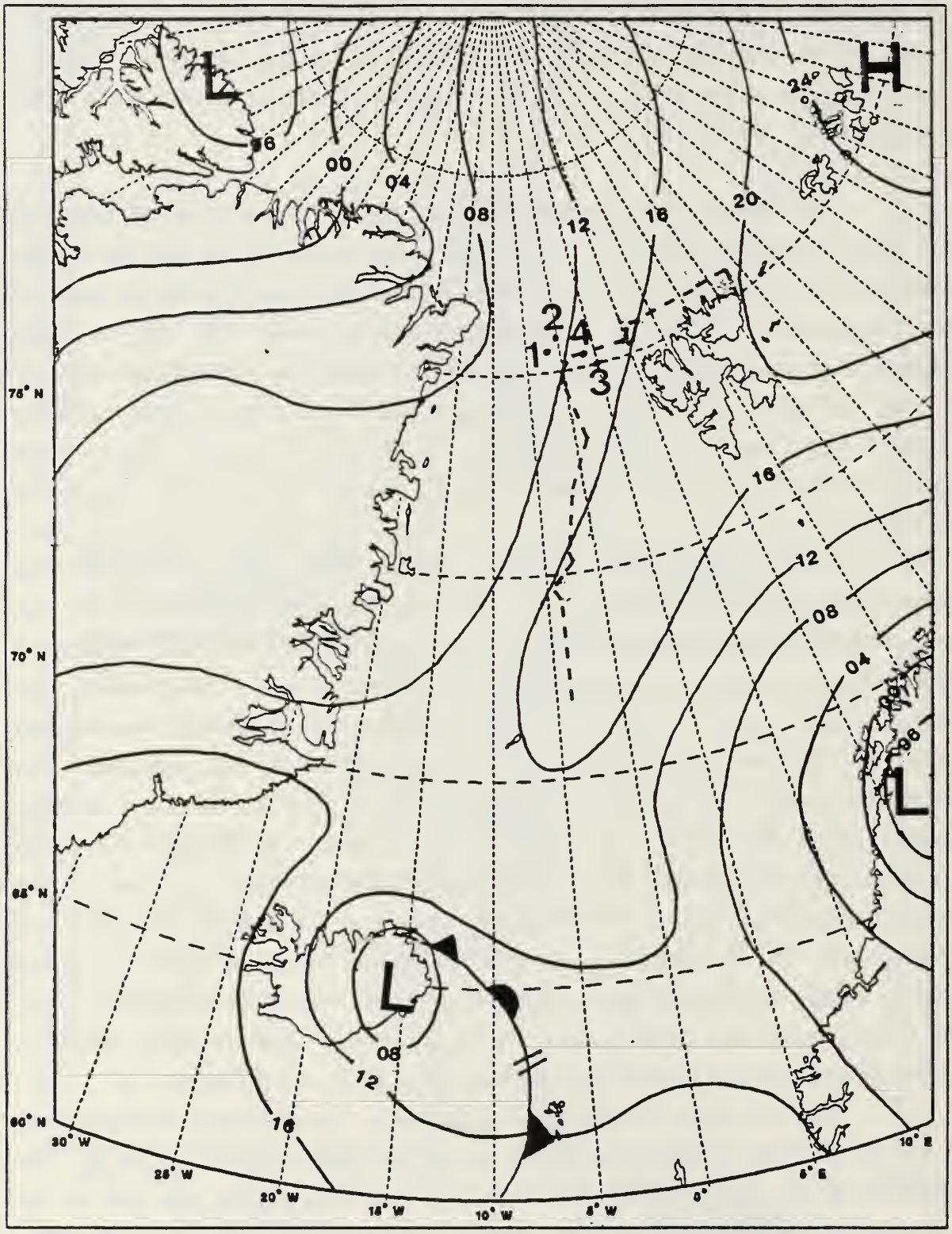

Fig. 5.13 Case 3, Sfc isobars, 26 Jun,1200z,and ship's locations at launch,1100UTC, (1) PS, 50 km in ice (2) PQ, 40 km in ice (3) HM, 40 km in water (4) VL, MIZ.

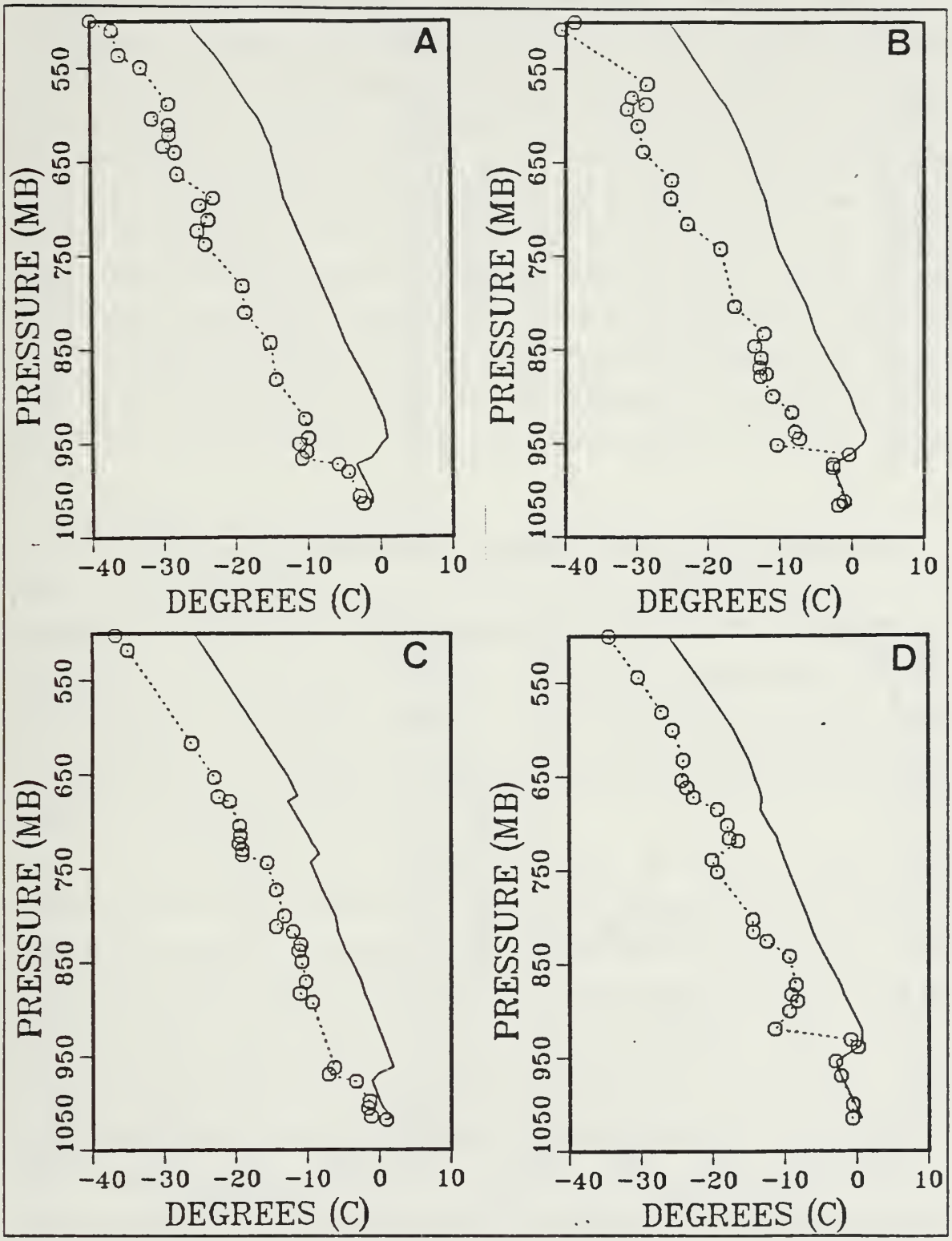

Fig. 5.14 Case 3 radiosonde plots: (a) PS (b) PQ (c) HM (d) VL, temperature is indicated by a solid line, dewpoint is indicated by a dashed line.

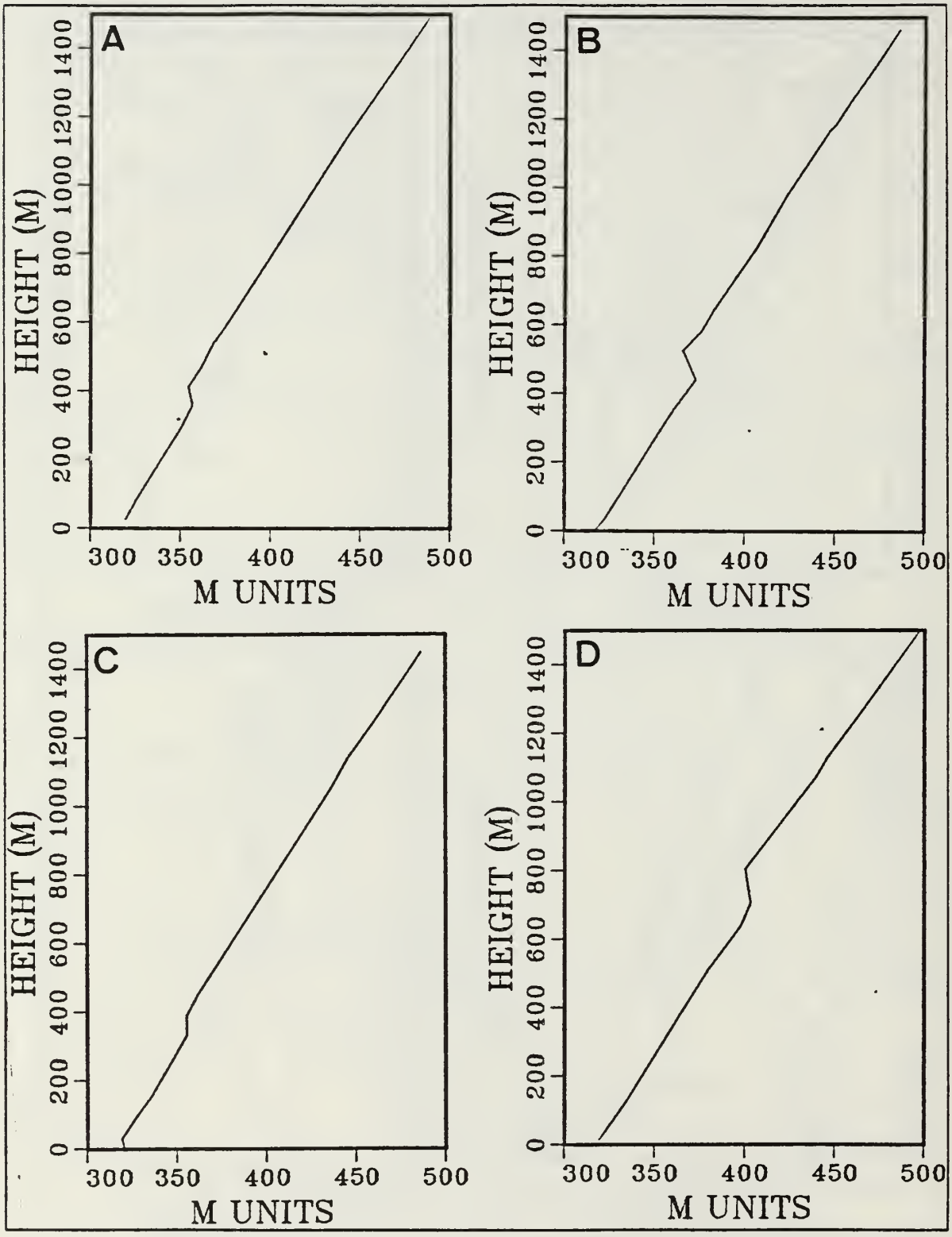

Fig. 5.15 M profiles of each of the ships
(a) Polarstern (b) Polar Queen (c) Hakon Mosby (d) Valdivia.

not exist after the corrected profile was processed. We believe that this is a result of the correction technique. The Valdivia showed a duct at 703 m, when corrected the duct did not exist. Again the height of the duct reflected the gradient at the height above the saturation. The duct, if existed, probably should have been at the inversion level, approximately 500 m. Once again the dry layer could not be re-created. The dewpoint curve from the Hakon Mosby did not show as large a jump at the inversion as in the other profiles. This was the reason why there was no duct at the Hakon Mosby. Overall ducting conditions indicated that, with on-ice flow, ducts did not exist over the ships operating in the water due to a warmer and moister air mass which had not been modified by the ice edge. As the warm, moist air flowed over the ice it cools at the lower layers and the inversion became well defined. The inversion was higher over the MIZ than over the ice. The duct sloped downward from the MIZ to the pack ice.

d. Case 4

In this case the radiosondes were launched six hours after Case three, at 1700UTC on 26 June. Only three of the four ships launched radiosondes. The Polarstern was still located 50 km into the ice, the Hakon Mosby and Valdivia were located at the ice edge. Fig. 5.16 shows the position of the ships relative to the ice edge. Fig. 5.16 shows the surface analysis at 1200UTC. During the next twelve hours the 994 mb low over Norway began to move northwest, and was located off the coast of Norway by 27 June at 0000UTC. A 1026 mb high over the Barents sea remained stationary. Weak on-ice flow persisted.

Fig. 5.17 shows the radiosonde profiles for the three ships. The temperature curve of the two ships at the ice edge were identical. The Hakon Mosby's dewpoint curve showed no saturation below the inversion with a dry layer at the inversion. The dewpoint curve recorded at the Valdivia showed saturation below the inversion which continued above the inversion. The dewpoint curve above the inversion indicated a drier profile at the Hakon Mosby than at the Valdivia. When comparing these profiles to the Polarstern the temperature and dewpoint were very similar. The inversion at the Polarstern was higher than at the MIZ. The dewpoint curve was saturated below the inversion and continued to be saturated above the inversion. In comparing these profiles to those in Case 3 some differences were seen at the Polarstern and the Valdivia. The inversion at the Polarstern increased slightly, responding to the continued advection of the relatively warmer, moister air over the

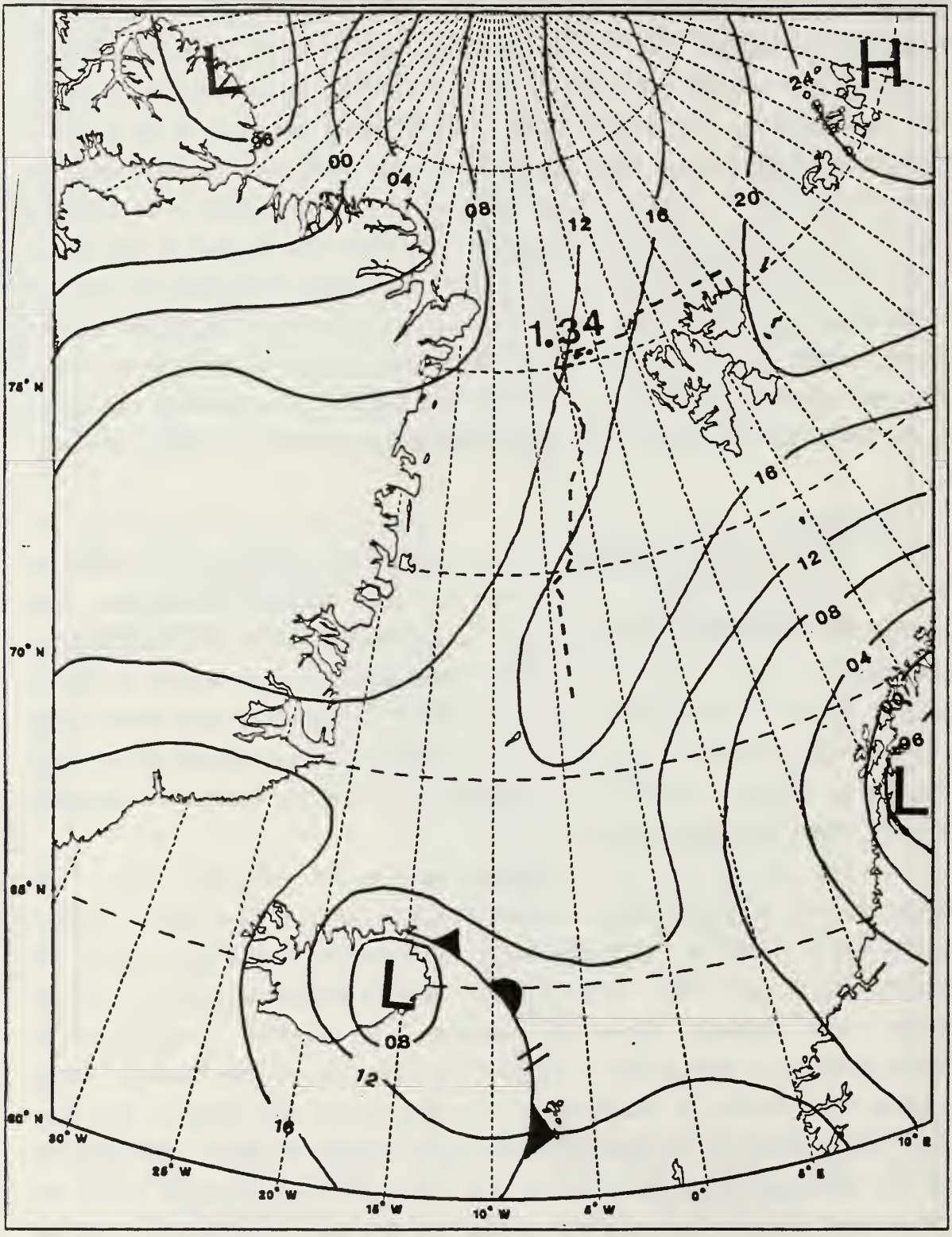

Fig. 5.16 Case 4, Sfc isobars,26 Jun,1200UTC,and ship's locations at launch,1700UTC, (1) PS, 50 km in ice (3) HM, MIZ (4) Valdivia, MIZ.

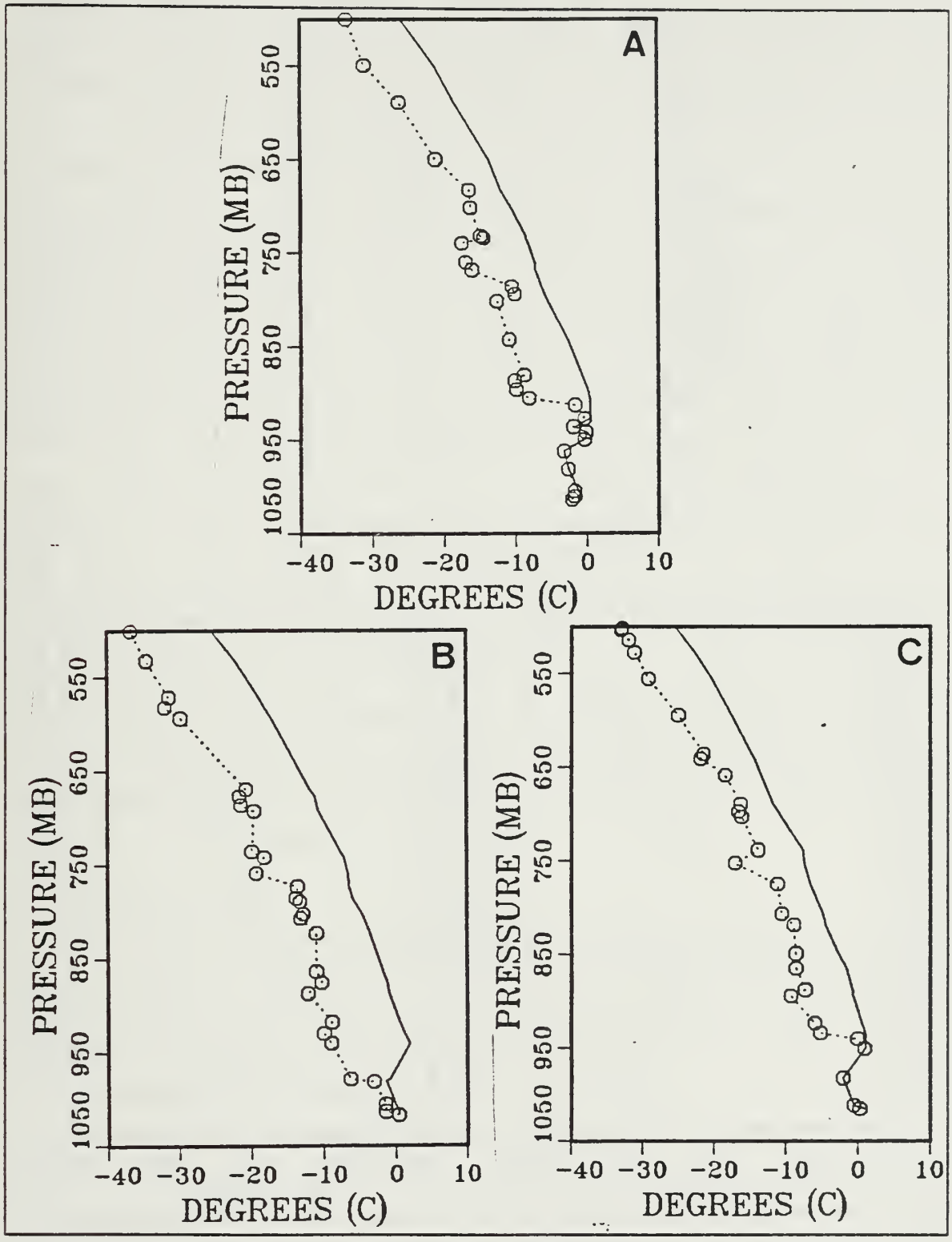

Fig. 5.17 Case 4 radiosonde profiles: (a) PS (b) HM (c) VL, temperature is indicated by a solid line, dewpoint is indicated by a dashed line.

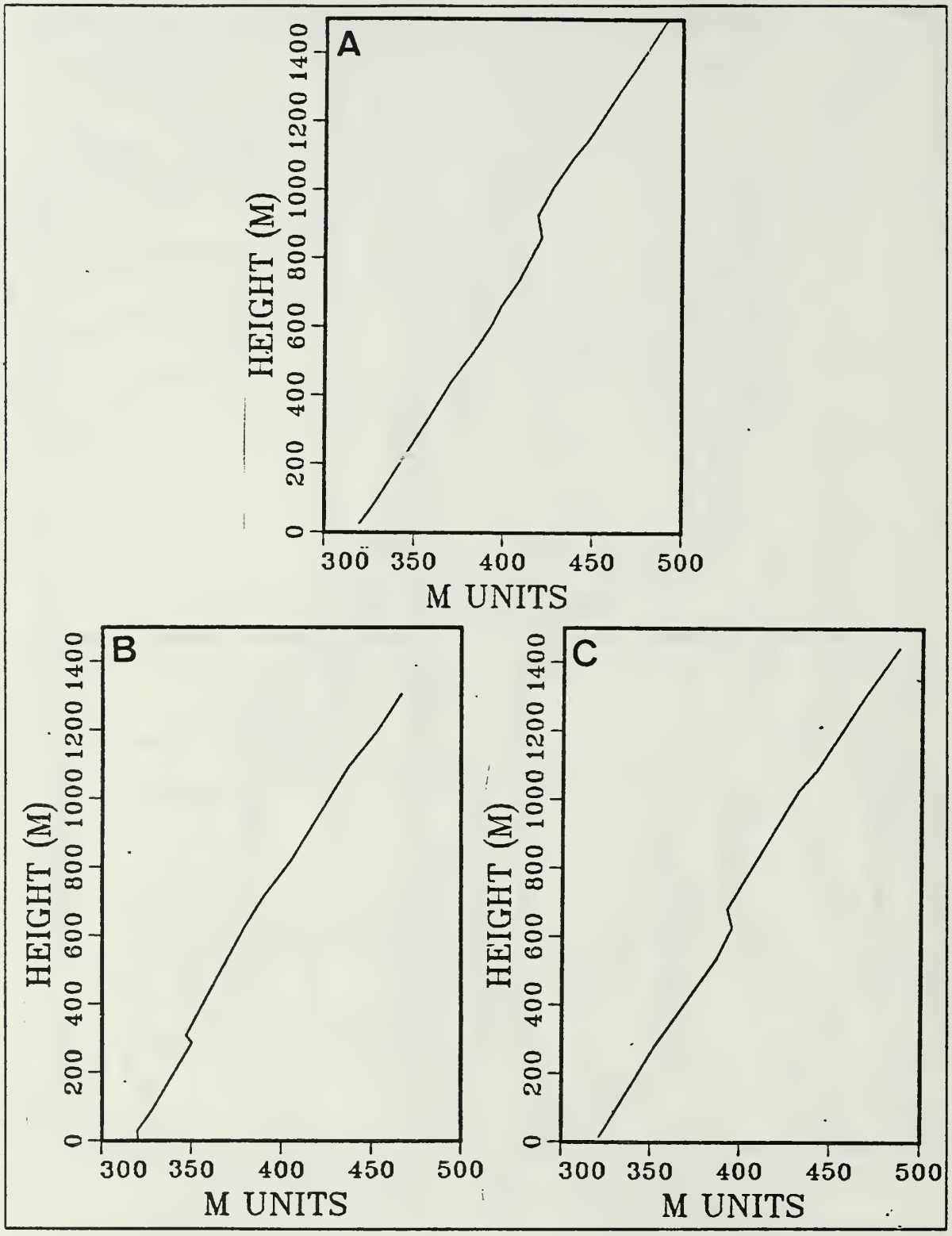

Fig. 5.18 M profiles of each of the ships
(a) Polarstern (b) Hakon Mosby (c) Valdivia.

pack ice. The dewpoint curve supported this by showing a more moist profile at 1700UTC. The only difference in the profiles launched at the Valdivia was a slightly lower inversion at 1700UTC. The profile from the Hakon Mosby remained unchanged.

Fig. 5.18 shows the M profiles of the ships. All three ships detected ducts at 1700UTC. The Polarstern recorded a duct at 861 m, the Hakon Mosby recorded at duct at 288 m and the Valdivia recorded a duct at 626 m. The increase in the duct on the profile from the Polarstern from 357 m at 1100UTC to 861 m at 1700UTC could be explained by the fact that at 1700UTC the sonde was saturated above the inversion. The duct reflected the height at which the profile became unsaturated. We believe that the duct height should have increased in response to the increase in the inversion but should have been located closer to the inversion at approximately 450 m. The decrease in the duct at the Valdivia was reasonable as the inversion decreased over the six hours. In both the 1100UTC and 1700UTC the profile showed saturation above the inversion, so the actual height of the duct would have been lower. We believe that the duct, recorded by the Valdivia, at 1700UTC should have been the same as the duct recorded at the Hakon Mosby at that time, since the profiles were nearly identical. The only exception was the problem of saturation. The true height of the duct of the Valdivia should have been approximately 300 m. The Hakon Mosby picked up a duct at 1700UTC and the only explanation for this would be that as the ship travel closer to the MIZ the temperature inversion became more defined. With the continued on-ice flow the height of the duct at the MIZ and over the ice increased in response to the moist warm air being advected over the area.

B. REGIME STUDY

Six regimes were selected for this study over the period of 19 June to 15 July. Fig. 5.19 shows the breakdown of this period into each of the regimes. The designation of the regions was determined by the synoptic situation as well as by the consistency of the wind direction over all four of the ships.

1. Description of the Regimes

Regime One commenced 19 June at 0000UTC and concluded 22 June at 0000UTC. Flow was generally off-ice. The synoptic situation on the 19th of June showed a weak high centered over northern Greenland. Two cyclones were in the area. A 990 mb low was centered northeast of Svalbard and the second cyclone with a central pressure of 994 mb was located to the southwest of Svalbard. The low southwest of Svalbard moved northeast and deepened to 984 mb by 1200UTC. By 20

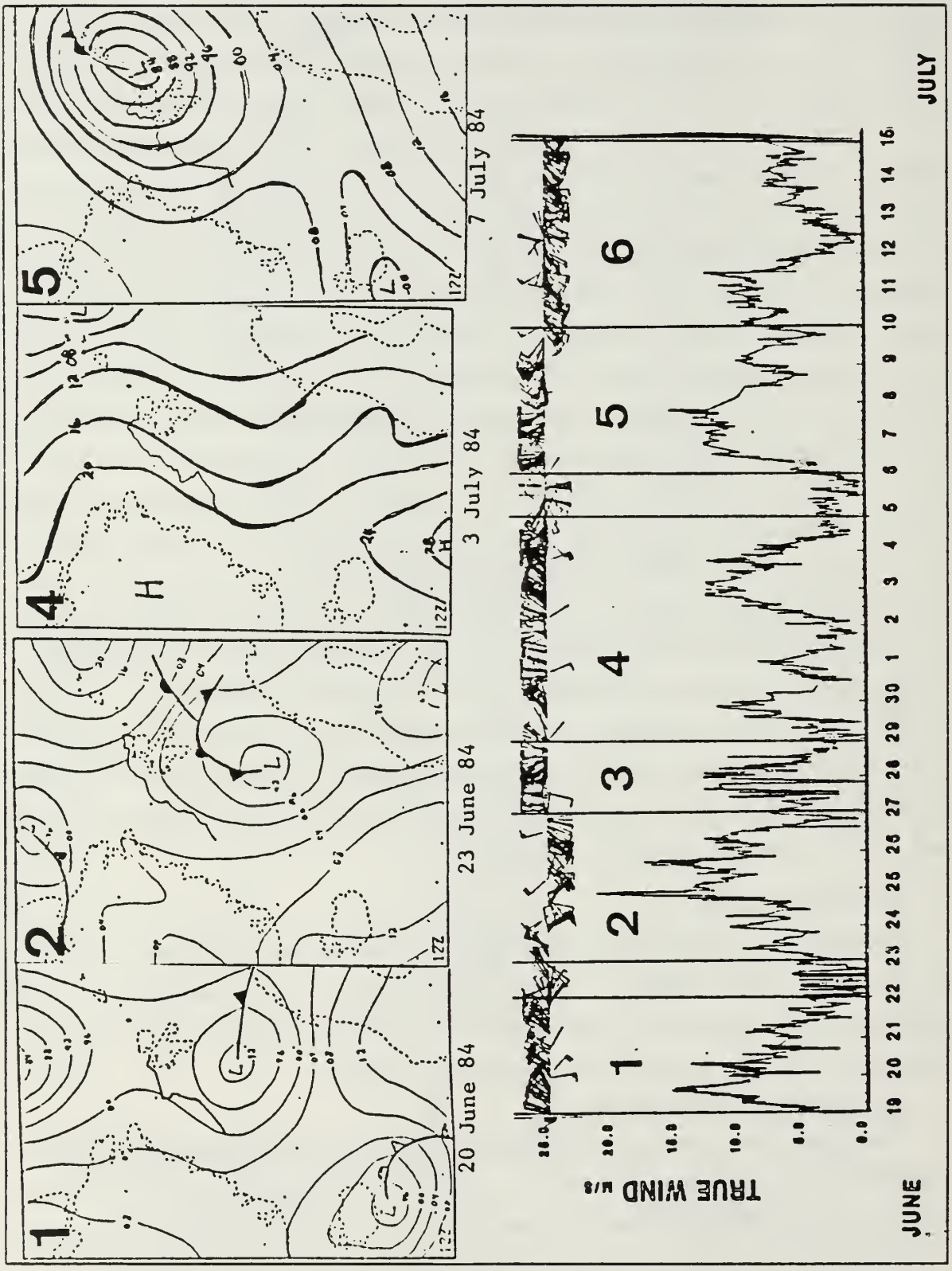

Fig. 5.19 Regimes.

June at 0000UTC, the low began to fill and drift south. The low continued to move southeast toward the coast of Norway and moved out of the area into the Barents Sea by the end of the period. The 990 mb low north of Svalbard remained quasi-stationary weakening through the period. A weak high began to develop over the area on the 21st but the pressure gradient remained weak over the area.

Regime Two commenced on 23 June at 0000UTC and concluded 26 June at 2300UTC. The winds were initially off-ice and became on-ice by the end of the period. A 992 mb low located 60 n mi off the coast of Norway moved northnorthwest into the Fram strait on the 24th. The low slowed down as it crossed the MIZ and filled over the ice pack on the 25th. This low produced the highest winds seen during MIZEX-84. A high pressure centered over the Barents sea began ridging southward over the area at 2300UTC, 25 July and moved southward through the 26th.

Regime Three commenced on 27 June at 0000UTC and concluded on 28 June at 2300UTC. The flow remained off-ice these two days. A low located over Norway moved northwest over Svalbard by 27 June at 1200UTC, maintaining the same intensity. By 28 June at 0000UTC, this low began to weaken and filled by June 28 at 1200UTC. A high pressure ridge from the North Atlantic began to build in over the area from the south during the day on the 28th.

Region Four commenced 29 June at 0000UTC and concluded 4 July at 2300UTC. High pressure and off-ice winds characterized this period. Strong ridging from the North Atlantic was set up by 29 June at 1200UTC. A second weak high developed over central Greenland on the 29th. Ridging from both high pressure centers persisted until the 1st of July. The high over Greenland began to dominate the flow on 1 July and continued through the end of the period.

Region Five commenced 6 July at 0000UTC and concluded 9 July at 2300UTC. A weak low pressure over the Barents sea moved west toward Svalbard, deepening to 990 mbs by 7 July at 0000UTC. The low continued to deepen to its lowest central pressure of 982 mbs at 1200UTC. The low remained stationary until 7 July at 1800UTC when it began to move slowly northeast and fill. The ships were located on the backside of the low and experienced northwest winds throughout this period.

Regime Six commenced 10 July at 0000UTC, and concluded 15 July at 0000UTC. A weak high pressure dominated the area. High pressure centered off the coast of Norway moved over Norway ridging northwest over the area. This system

dominated through 11 July at 0000UTC. A weak high developed over Greenland by 11 July at 0000UTC. By 1200UTC the high over Norway had moved into the Barents seas resulting in a relatively weak gradient over the area. This high continued to move northeast. The weak high over Greenland remained stationary.

Ducting in the Arctic responded to the changing synoptic conditions. High pressure, which produced strong subsidence, caused strong inversions and was most likely to produce necessary conditions for ducting. As the cyclones moved through the area, there was strong vertical mixing associated with these lows. Conditions were not favorable for ducting. Fig. 5.20 shows the percentages of ducts occurring in response to the different synoptic flows. The most ducts were associated with Regimes Four and Six when high pressure dominated the area. Regime Three showed a high percentage of ducts because two of the ships were influenced by a high pressure during the period. The average height, thickness and strength of the duct within each regimes were not significantly different from each other.

2. **Refractive structure during each regime**

Fig. 5.21 shows the OCH of the ducts during ducts Regime One. On three out of nine launch periods ducts were detected. The ducts recorded on 19 June (launch periods one to three) reflected a weak high pressure over Greenland. As the low moved over the area 19 June at 2300UTC to 21 June at 2300UTC, (launch periods four through nine) no ducts were seen. This was due to the increase in the vertical vertical motion which destroyed the inversion. Inspection of of the data from the Polar Queen, operating in the ice, revealed that the Polar Queen detected stronger ducts than the duct recorded by the Hakon Mosby located at the MIZ. This was probably due to the Polar Queen being located closer to the center of the high and experiencing more subsidence. Fig. 5.21 (b) shows that there was no change when the data were corrected.

Fig. 5.22 shows the OCH of the ducts during Regime Two. On five out of 15 launch periods ducts were detected. The Polarstern (at the MIZ), 23 June at 0500UTC, detected a duct (launch period one). The Hakon Mosby, 80 km into the water, did not record a duct on this launch. The Hakon Mosby detected a duct at 1100UTC (launch period two), however, the Polarstern, did not have a successful launch. Fig. 5.22 (b) shows that no changes occurred when the profiles were corrected. No ducts were recorded 23 June at 0500UTC, to 26 June at 0500UTC as the low pressure system was directly over the four ships (launch periods 3-12). Ducts were

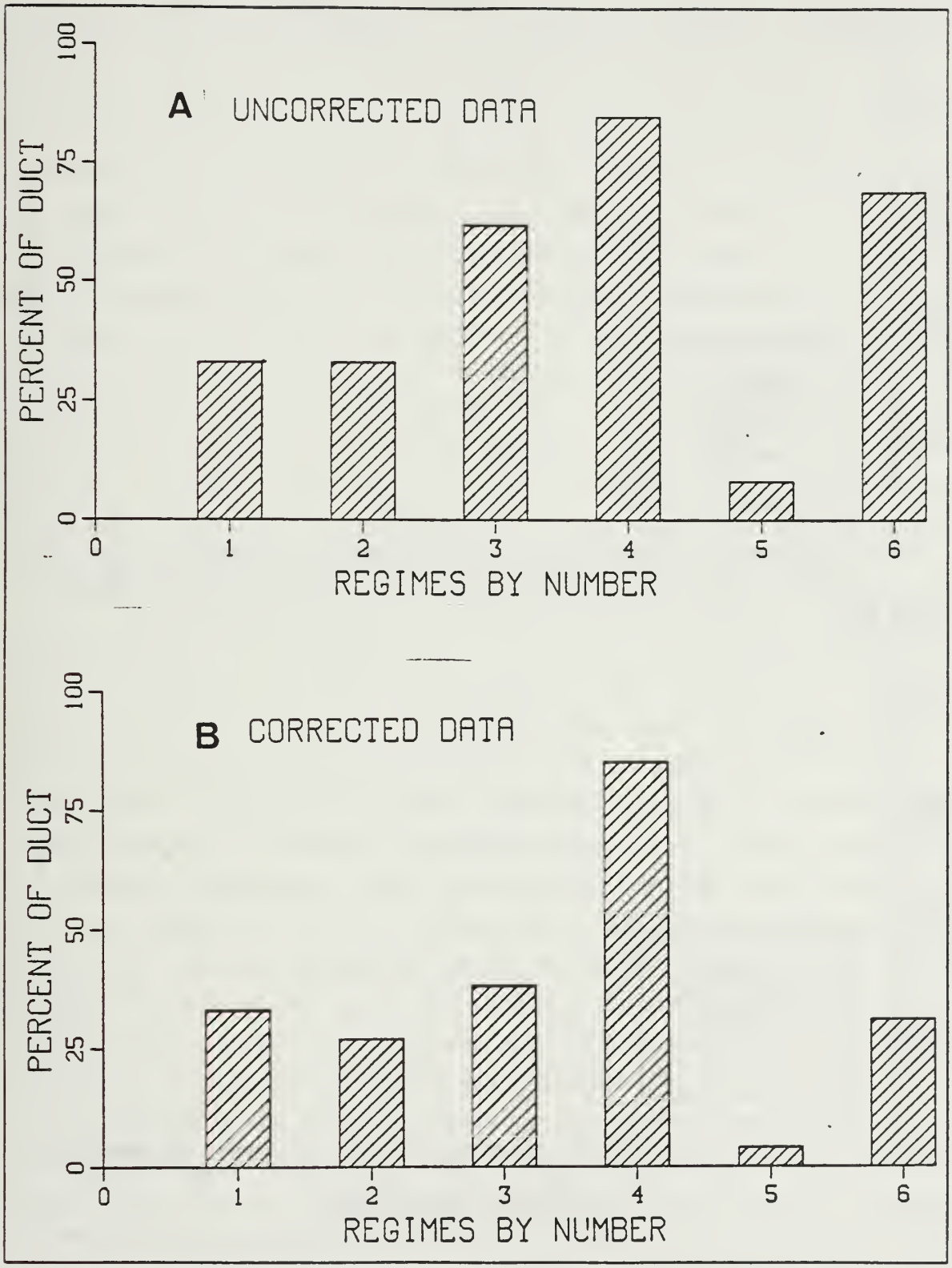

Fig. 5.20 Percent of duct occurrence during each regime, (a) uncorrected, (b) corrected.

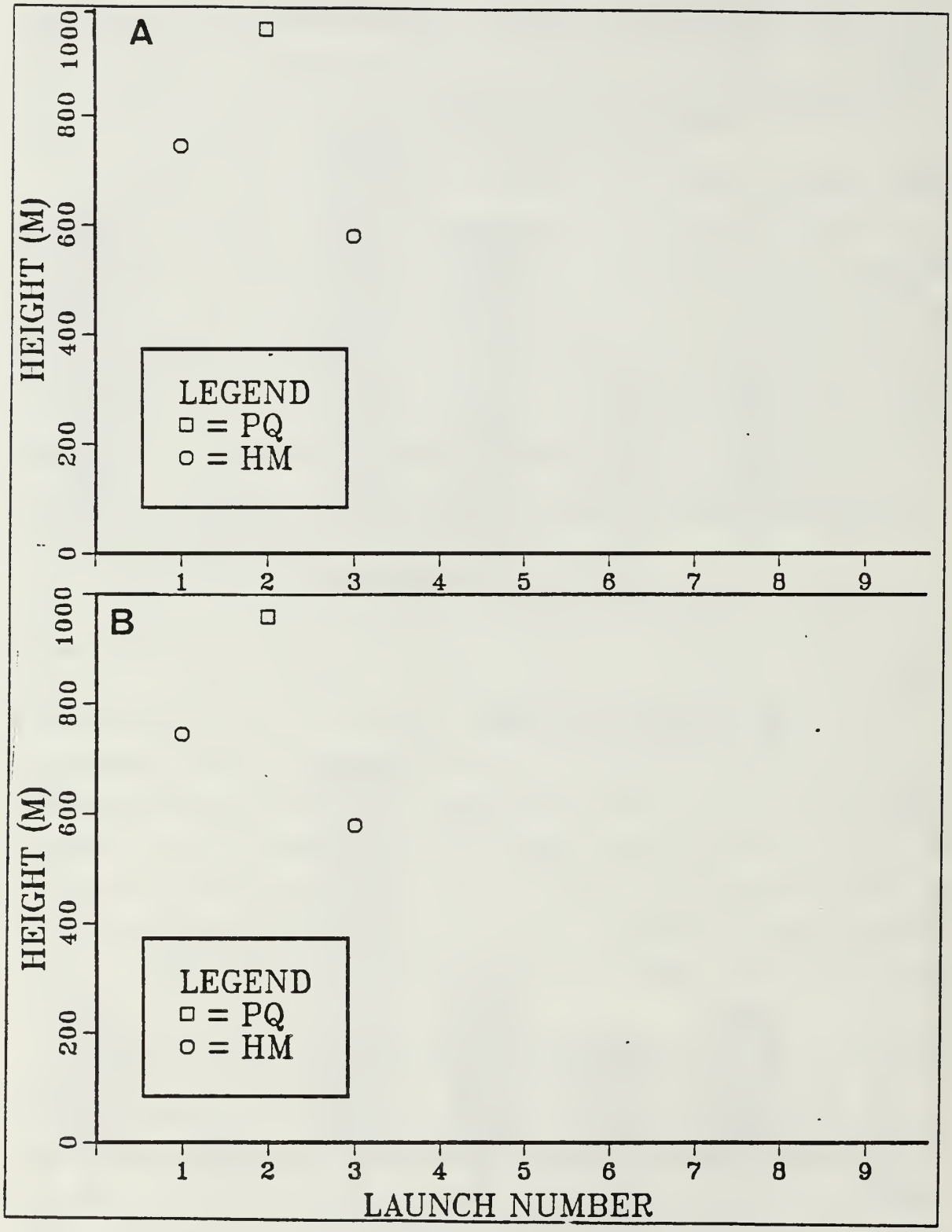

Fig. 5.21 Ducts detected each launch period during Regime 1, Radiosondes were launched every 6 h, 2 symbols on the same launch indicate multiple (vertical) ducts.

detected on 26 June, launch periods 13-15, in response to ridging southward from the high over the Barents Sea. On launch period 13, three out of four ships detected ducts. This case was discussed in detail in Case Three above. The ducts persisted through 1700UTC (launch period 14) over the Polarstern and the Valdivia. The Polar Queen did not have a successful launch at 1700UTC. This launch time was discussed in Case Four above. The Polar Queen recorded a duct at 26 June at 2300UTC, launch period 15. We believe that the duct may have persisted through the day at the Polar Queen and the Polarstern, which were under the influence of the high ridging southwest from the Barents Sea. The Polarstern did not have a successful launch at 2300UTC (launch period 15) to confirm whether the duct persisted or not. The Hakon Mosby and Valdivia, operating in the water, did not detect ducts. They were influenced by the low pressure intensifying over Norway which resulted in less subsidence over these two ships. Fig. 5.22 (b) shows that when the profiles from 26 June were corrected only the Polarstern recorded a duct on launch period 13, and only the Hakon Mosby detected a duct on launch period 14. None of the ships recorded ducts on launch period 15.

Fig. 5.23 shows the OCH of the ducts during Regime Three. In five out of eight launch periods ducts were detected. On 27 June a weak ridge dominated the area. The Polarstern, located the furthest into the ice, recorded a duct on launch period one and two. The height of the duct decreased, which was probably due to the low which moved into the area causing a decrease in the subsidence over the ice. Fig. 5.23 (b) shows that when the data were corrected the Polarstern did not record a duct on launch period two. The Polar Queen also detected a duct on 26 June, launch period two. The Polar Queen did not launch a radiosonde at 1700UTC (launch period three). The Hakon Mosby and Valdivia operating in the water adjacent the ice edge showed no ducts. This could be explained by the fact that the low pressure approached from the southeast. By 1700UTC the low was nearly over the position of the Hakon Mosby and the Valdivia while the Polar Queen and the Polarstern were still under the influence of the North Atlantic ridging over Greenland. The low moved over all the ships by 2300UTC on the 27th and no ducts were recorded by any of the ships. As the low stagnated and filled through 0500UTC on the 28th, no ducts were recorded (launch periods four to five). On the 28th (launch periods six to seven) ducts were recorded by the Polar Queen, operating in the ice near the ice edge, and by the Hakon Mosby, operating at the MIZ. These ducts were in response to the ridging from the North Atlantic which was building over these two ships. The Valdivia, operating 80 km in

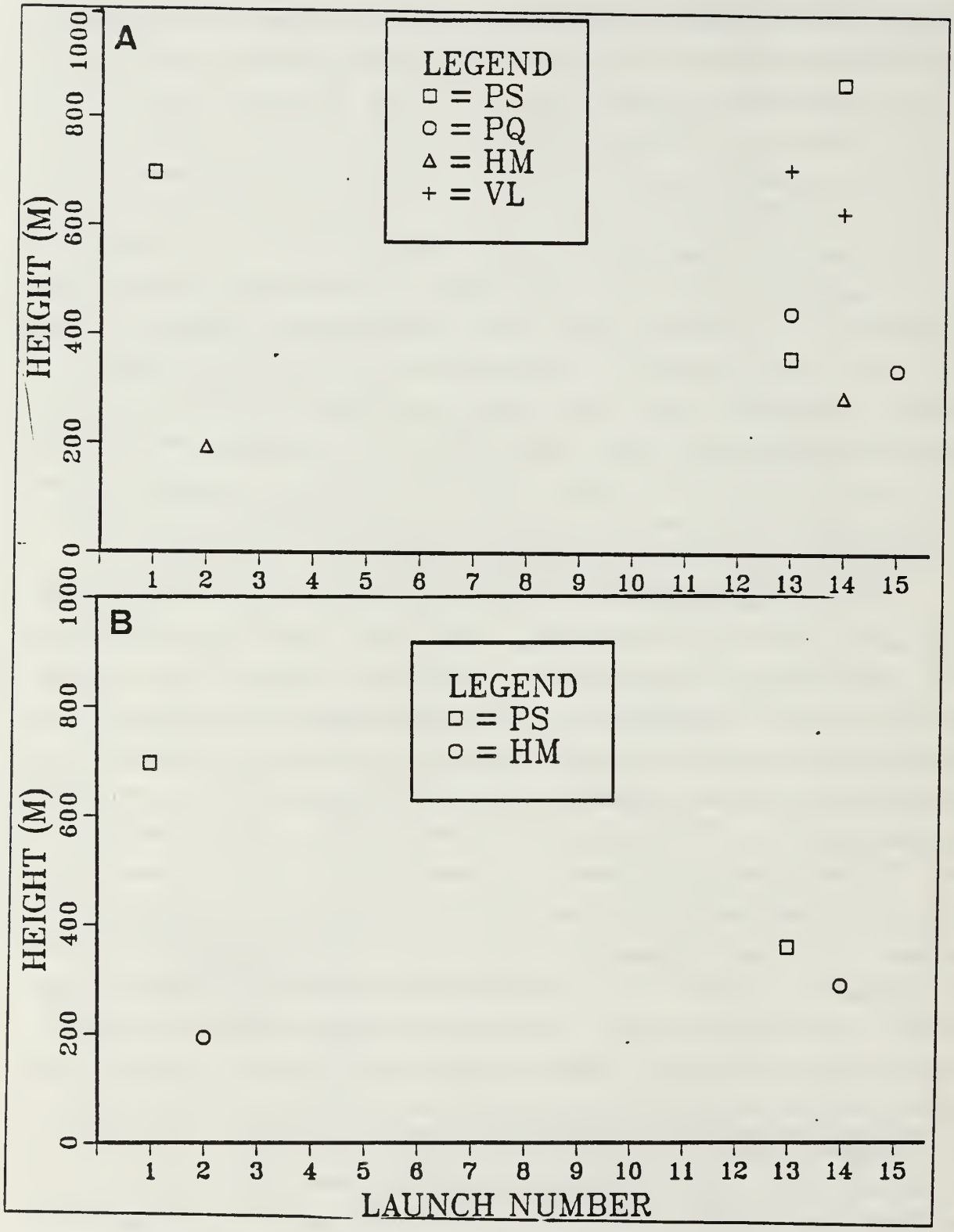

Fig. 5.22 Ducts detected each launch period during Regime 2, Radiosondes were launched every 6 h, 2 symbols on the same launch indicate multiple (vertical) ducts.

the adjacent water, was still under the influence of the weak low over Svalbard and continued to show no ducting. Fig. 5.23 (b) shows that after the data were corrected the duct recorded at the Polar Queen on launch eight was eliminated. The remainder of the ducts remained the same.

Fig. 5.24 shows OCH of the ducts during Regime Four. In 16 out of 19 cases ducts were detected. This was the first time that any persistence was seen in ducting conditions at one ship. The Valdivia, located within 20 km of the ice edge (water side), detected a duct continuously from 30 June at 2300UTC to 1 July at 2300UTC (launch periods seven, nine and eleven). The Valdivia did not launch radiosondes on launch periods eight and ten. The average height of the ducts, which was calculated from the profiles taken from the Valdivia, was 250 m, the average thickness was 103 m, and the average strength was 3.2 M units. The Hakon Mosby, operating at 50 km from the ice edge (water side), recorded a duct continuously from 29 June at 1100UTC to 1 July at 0500UTC (launch periods three through on eight). On all the launches except one, the duct was located near the inversion. On launch period four the duct was detected at 3190 m and no duct was detected at the inversion. No other ship recorded a similar duct at this elevation height. The Hakon Mosby moved to the ice edge on 30 June. The average height of the ducts, calculated from the profiles of the Hakon Mosby, was 225 m, the average thickness was 65 m and the average strength was 2.87 M units. The two ships operating in the ice did not record ducts during this period and we believe that was due to the fact that these ships were located between the weak high pressure cell over Greenland and the ridging from the North Atlantic. Fig. 5.24 (b) shows that the ducting episodes remained unchanged after the data were corrected.

The Polarstern, at the ice edge, on 2 July at 0500UTC detected ducts at the inversion and near 750 mb (launch period 12). The duct at 750 mb persisted through launch period 15. The height of the duct remained the same for two launches and then increased. This duct was associated with the sharp decrease in the humidity recorded by all ships at 750 mb. The Polarstern was the only ship which recorded this elevated duct through the whole period. The Hakon Mosby, at the ice edge, recorded multiple (vertical) ducts on 2 July at 1100UTC (launch period 13). The second duct was associated with the decrease in the dewpoint at 750 mb. The remainder of the ducts recorded, launch periods 16-19, exhibited no pattern. Fig. 5.24 (b) shows that the only change which occurred when the data were corrected was that the Polarstern picked up a duct at the inversion on 2 July at 2300UTC (launch period 15). This duct was at nearly the same height as the duct detected by the Valdivia on this launch.

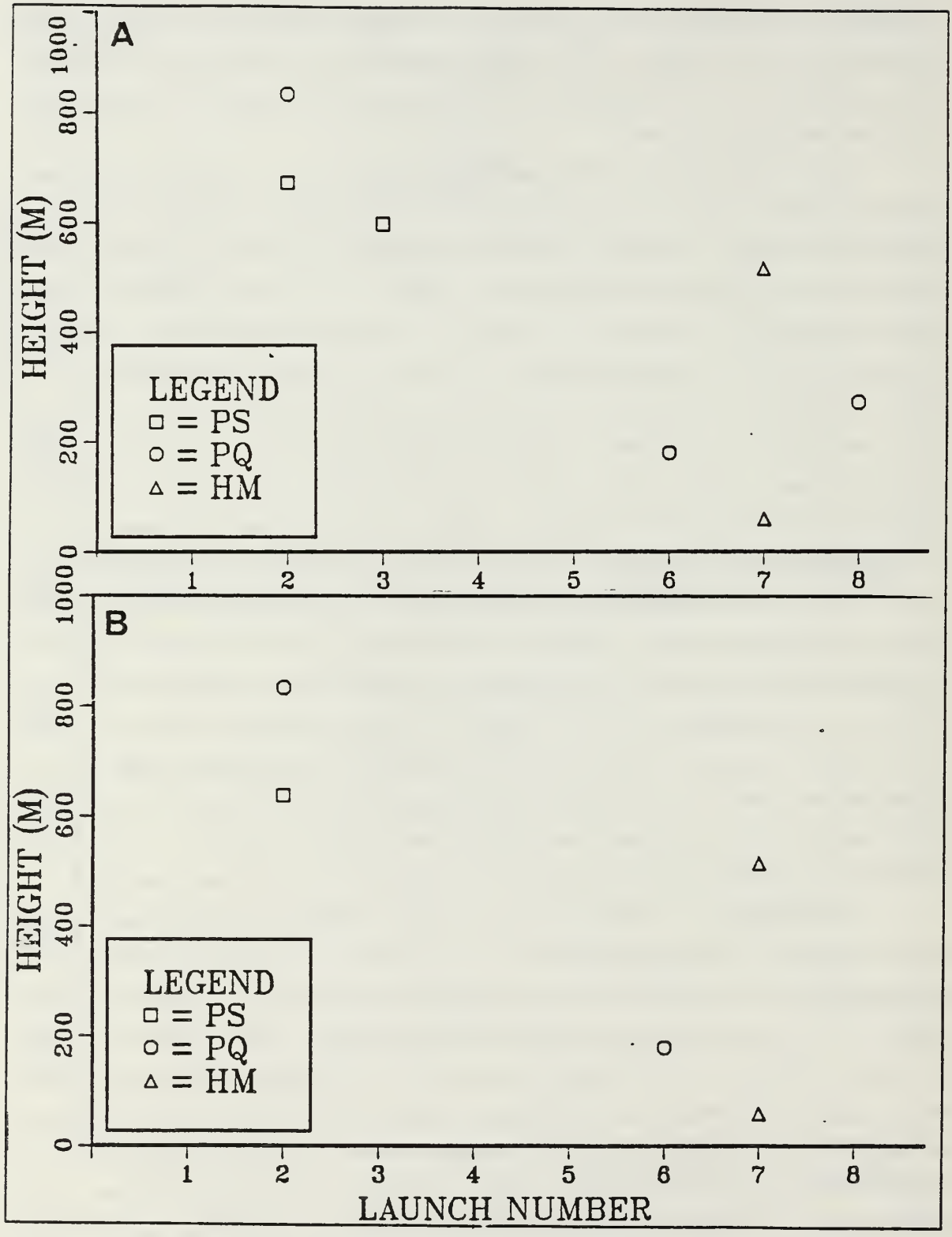

Fig. 5.23 Ducts detected each launch period during Regime 3, Radiosondes were launched every 6 h, 2 symbols on the same launch indicate multiple (vertical) ducts.

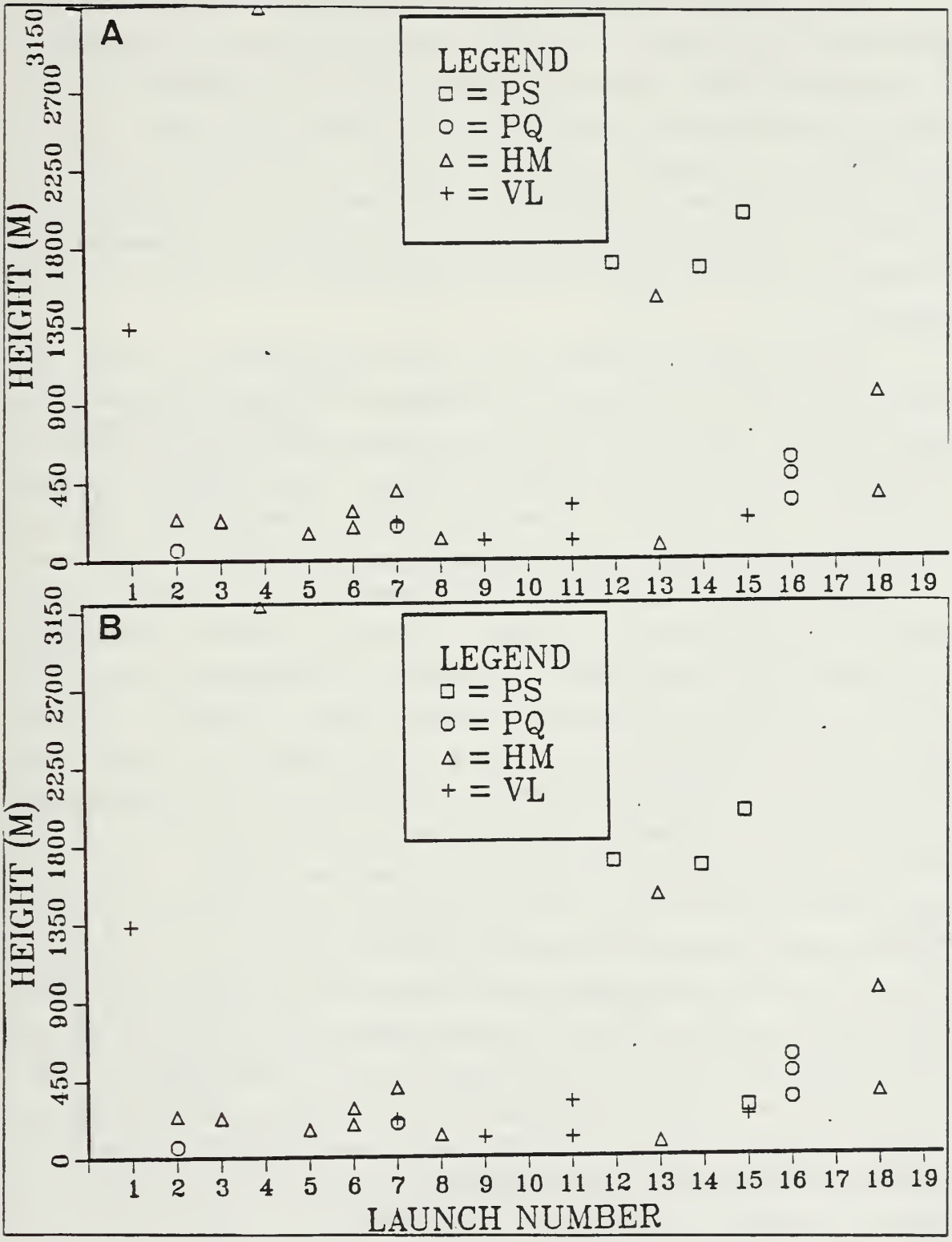

Fig. 5.24 Ducts detected each launch period during Regime 4, Radiosondes were launched every 6 h, 2 symbols on the same launch indicate multiple (vertical) ducts.

Fig. 5.25 shows the OCH of the ducts during Regime Five. On two out of 23 launches ducts were recorded. A low became stationary over the area, accounting for this low number of ducts. The Valdivia detected a duct on 7 July at 1100UTC (launch period 6). The second time a duct was recorded was also by the Valdivia on 9 July. The Valdivia was operating 100 km away from the ice edge and may have been influenced by the high pressure beginning to develop over Norway. Fig. 5.25 (b) shows that when the data were corrected the duct on launch period six was eliminated, and the height of the duct on launch period 18 decreased 500 m and was located near the inversion.

Fig. 5.26 shows the OCH of the ducts during Regime Six. Ducts were recorded on 29 out of 42 launches. The radiosondes were launched every three hours during this period. Fig. 5.26 (b) shows that when the data were corrected the number of ducting episodes was drastically reduced. Again as in Regime Four there was some persistence to the data. The Polar Queen and the Polarstern recorded ducts on launch periods 16-17. At 12 July at 1100UTC (launch period 18) the Polarstern did not record a duct and the Polar Queen did not have a successful launch. At 1400UTC (launch period 19) the Polar Queen again reported a duct but at a significantly lower height. The Polarstern did not record a duct on this launch. The Polarstern, located 140 km into the ice, recorded a duct continuously begining 13 July at 1700UTC on launches 28-41. The duct was near the inversion during the entire period. The average height, calculated from the profiles of the Polarstern, was 358 m, the average thickness was 115 m and, the average strength was 6.2 M. These averages may have been too large since each of these profiles showed saturation above the inversion. The averages should probably have been closer to 270 m because these values reflected the gradients above the saturated portion of the profile and not at the inversion. Fig. 5.26 (b) shows that all of these ducts were eliminated upon correction of the humidity profiles which accounts for the significant difference in the percentage of duct on Fig. 5.19 between the uncorrected and the corrected data. The only other ships which recorded duct with any persistence was the Valdivia, operating 100 km in the adjacent water. The Valdivia recorded a duct on 12 July at 1700UTC (launch period 20). The Valdivia then recorded a duct again 3 launch periods later which persisted to the next launch. A duct was not recorded again until 14 July at 0200UTC (launch period 31) and then not again until launch period 34. After this a duct was continuously recorded until 15 July at 2300UTC (launch periods 34-42). The average height of this duct, calculated from

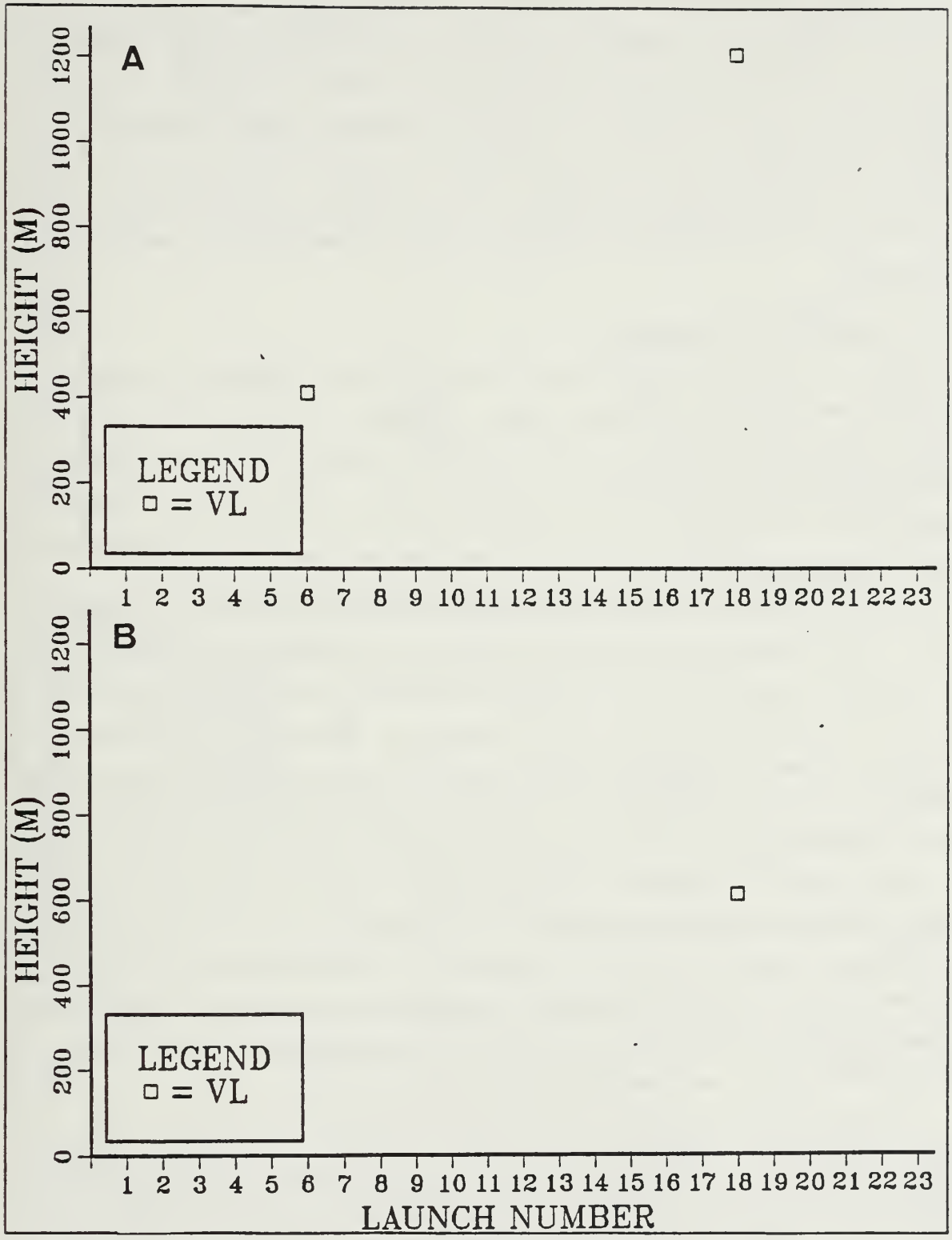

Fig. 5.25 Ducts detected each launch period during Regime 5, Radiosondes were launched every 6 h, 2 symbols on the same launch indicate multiple (vertical) ducts.

the profiles of the Valdivia, was 1286 m, the average thickness was 145 m, the average strength 7.16 M units. Looking at Fig. 5.26 (a) and comparing the ducts recorded by the Polarstern and Valdivia show that the duct was considerably low over the pack ice. Looking at the averages which were calculated the ducts detected by the Valdivia were thicker and stronger. There was no persistence from the other two ships both located between the Polarstern and the Valdivia. This could not be explained since the flow over all four ships was due to the southward ridging from high pressure centered in the Barents sea.

C. PURE TIME VARIATION

Data used in the Regime study did exhibit temporal variation in the refractive structure even though it addressed spatial variation. In order to isolate the pure temporal variation all four of the ships' tracks were plotted to determine whether they operated within a 30 n mi square for a period of time. The only ship which met this criterion was the Polarstern. Fig. 5.27 shows the two areas which were used in this study of time variation.

The first area was a box with boundaries 80.06°N to 80.5°N, and 1.10°E to 7.74°E. The Polarstern was in this box from the 18 to 26 June. Through this period 44 radiosondes were launched, and ducts were detected on three launch periods. The ducts never persisted for more than one launch time. When the data were corrected, no change was seen. During this period a series of lows moved through the area bring unfavorable conditions for ducting. This ship was back in this box from 2300UTC on the 3rd of July through the 5th of July. Ducts occurred on the 2nd, 3rd and 4th when the ship was under the influence of a Greenland high. There was only one time when a duct persisted from one launch period to a second launch period. The height of this duct decreased from 1987 m to 93 m, and we do not believe that this was the same duct persisting over two launch periods. The ship was operating near enough to the ice edge that different air masses could have been the mechanism for the differences in the ducts. No changes were seen after the data were corrected.

The second area's boundaries were 79.4°N to 79.82°N, and 0.5°W to 6.6°W. The Polarstern operated 140 km into the ice and was in this area from 9-15 July. The only persistence of ducts was from the 13-15 July. Seventeen consecutive launch periods product a duct. The heights of ducts were between 250 m and 550 m. The thickness varied from 77-115 m and the strength from 1.2-11.5 M units. When the data were corrected, all these ducts were eliminated. If this was an accurate assessment of the

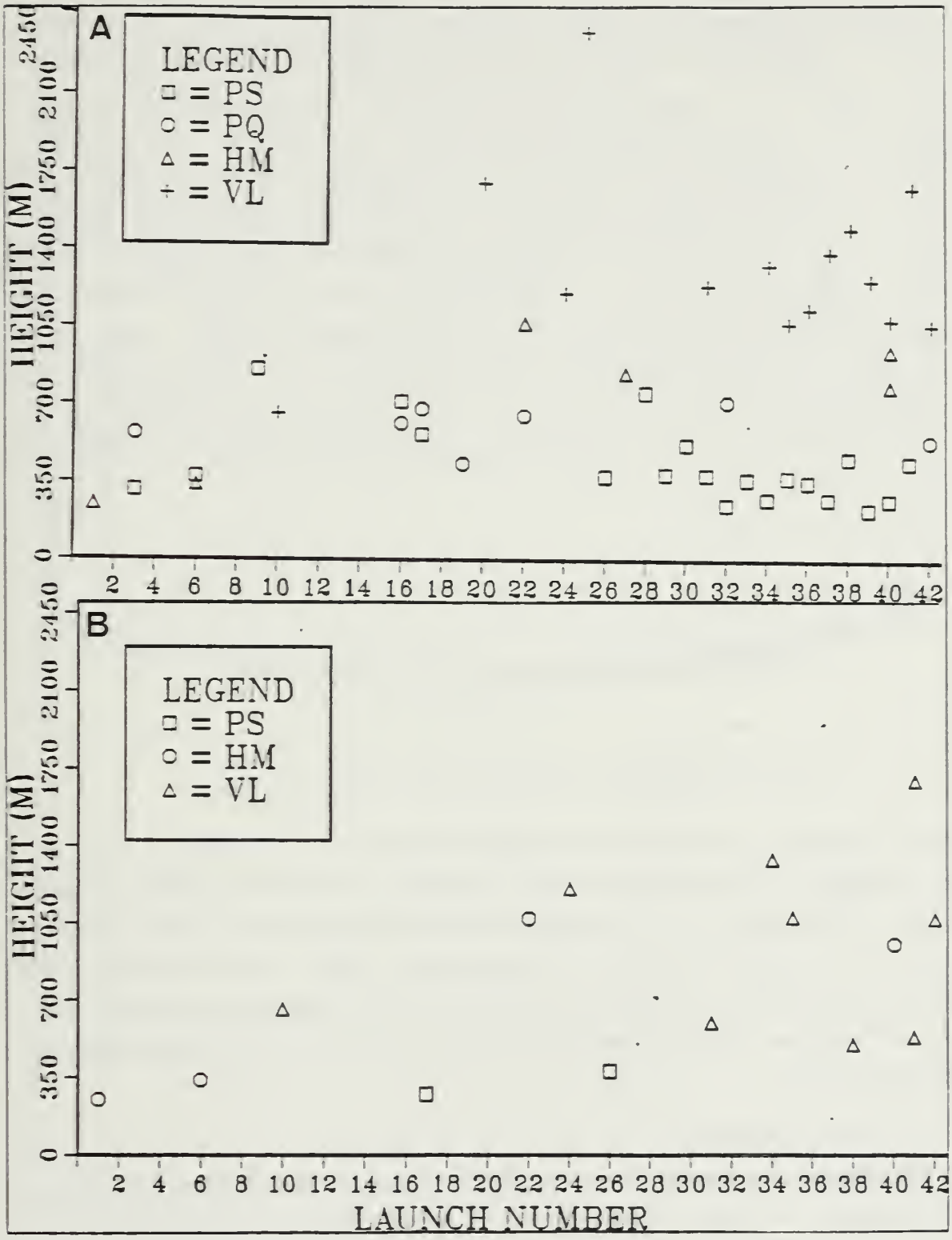

Fig. 5.26 Ducts detected each launch period during Regime 6, Radiosondes were launched every 3 h, 2 symbols on the same launch indicate multiple (vertical) ducts.

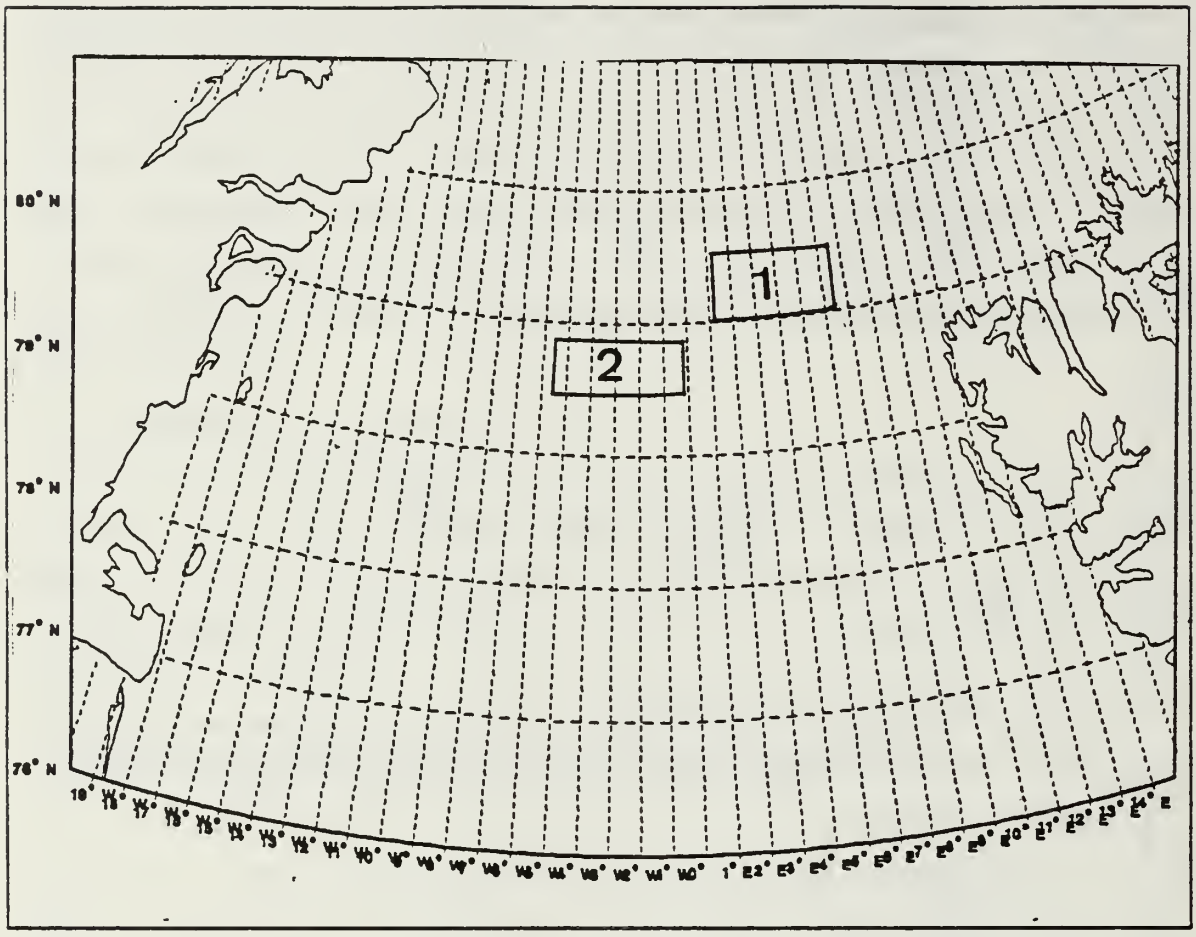

Fig. 5.27 Two areas chosen for the Pure Temporal Study.

refractive conditions, we would have expected the ducts to be somewhat lower to reflect the height of the inversion and not the height to which the profile remained saturated. We looked to see if the ducts which were eliminated as a result of being corrected would appear instead as super-refractive layers. We found that the occurrence and height of the super-refractive layers were generally not affected. In three cases there was a super-refractive layer lower and closer to the inversion than in the uncorrected data.

D. EVAPORATIVE DUCT

Evaporative duct heights were calculated by using the surface relative humidity, air temperature, sea-surface temperature and wind values as well the height of observation. IREPS first uses the air/sea temperature differences and the surface wind speed to compute the Richardson number. The Richardson number is defined as a

stability index. The vapor pressure at observation height and at the air-sea interface is then calculated using air temperature, sea-surface temperature and relative humidity. With these values the refractivity of the air at observation height and the refractivity of the air-sea surface is computed. The lapse rate, dependent upon the Richardson number, is then computed. The evaporative duct is then calculated based on the value of the Richardson number, the lapse rate, the difference in the refractivity of the air at observation height and the refractivity of the air-sea surface and the height of the observation. In the 427 radiosondes processed, an evaporative duct was seen in almost all the profiles. With the exception of seven cases the evaporative duct was less than five meters and was of little tactical importance. The shallowness of the evaporative duct was due to the low saturation specific humidity at the cold sea surface, which prevented a large specific humidity gradient from forming.

VI. CONCLUSIONS

This thesis examined the spatial and temporal variability of the refractive structure of the lower atmosphere in the vicinity of the Marginal Ice Zone. The data used in this thesis were collected by four ships during MIZEX-84. The ships operated in the pack ice, at the MIZ and in the water adjacent the ice edge. The upper-air data were collected by the Vaisala RS-80 radiosonde. The data set comprised 427 radiosonde profiles collected from 19 June to 15 July.

The results of a spatial study showed that the refractive structure leading to ducting was different over the pack ice and the MIZ from over the open water adjacent the ice edge. The ducts were generally lower, weaker and thinner over the pack ice with the averages of height, strength and thickness dramatically increasing over the water as one travel away from the ice edge. Scatter diagrams showed that the duct height, strength and thickness exhibited a linearly increasing relationship with respect to distance from the ice. The average height, strength and thickness values increased slightly from the pack ice to the MIZ and then dramatically increased from the MIZ to 210 km from the ice edge. This linearly increasing relationship from the pack ice to the open water was strongest with the height data. These differences in the refractive structure over this relatively narrow region are tactically important. An EM wave transmitted from a source located over the ice would be affected differently from a EM wave transmitted from a source over the water. Multiple (vertical) ducts were seen only at the ice edge and may have reflected the multiple inversions which were seen on sodar traces. Geernaert *et al.* (1987) have explained these multiple (vertical) ducts by a theory of convergence of different air masses along the ice edge.

Although the IREPS version 2.2 user's manual implies horizontal inhomogeneity of the atmosphere should not be a serious refractivity consideration 85% of the time, the results from this study showed that only 40% of the time a duct recorded by more than one ship. This dropped to 13% when the data had been corrected. There was never a case when all four ships detected ducts on the same launch, even when operating within 20 km of each other.

A temporal study was done by selecting six regimes to assess the effect of the difference in synoptic flow on the refractive structure. In four of six regimes a cyclone

passed over the area. When the low passed directly over all four of the ships no ducts were recorded. The greatest number of ducts was associated with the two regimes in which high pressure dominated the period. This was the only situation in which persistence of the ducts was seen. On two separate occasions two ships reported ducts which persisted for 24 hours. However, at both these times only two out of the four ships reported ducts, so once again it was seen that considerably spatial inhomogeneity existed. The longest case in which a duct persisted was for 36 hours.

Super-refractive layers were not significantly changed when the data were corrected. In a few cases the super-refractive layer were lowered to near the inversion. The evaporative duct, although always present, was less than 5 meters 97% of the time.

A disturbing feature of the dewpoint curve lead to a dilemma on how to treat the data. In 37% of the radiosondes the dewpoint curve followed the temperature curve above the inversion. Since this was not expected, and ducting was found to be controlled by the humidity gradient, this feature could not be ignored. In view of this a review of the literature was done to determine whether this problem was a sensor problem or a real meteorological phenomenon. Conclusive evidence was not found to support either theory, so the data were presented in an uncorrected and corrected format. Although most of the trends in the spatial and temporal studies were nearly the same, the number of ducting episodes was drastically reduced after correction. The corrected data probably represent the minimum ducting conditions in the MIZ, since the correction applied to these profiles could not re-create the expected decrease in dewpoint just above the inversion. Because of this problem with the data, one must carefully evaluate the data collected before implementing this into a predictive model such as IREPS

The method in which the data were collected for this thesis was exceptional. The distribution of the ships between the pack ice, the MIZ, and the adjacent waters, as well as the high percentage of radiosondes launched within 15 minutes of each launch period, provided ample data to evaluate the differences of the refractive structure over the area. However, due to the discrepancy in the profiles, further investigation needs to be done to determine the cause. If airplane data are used to compare with the profiles of the lower atmosphere, care must be taken to use data collected by the aircraft on a descent through the clouds. If this is a sensor problem then the aircraft's sensors could also be affected by moisture, frost or icing when ascending through the

clouds. Until the cause is determined complete guidelines for determining the ducting in this region is not possible.

LIST OF REFERENCES

Andreas, E.L. and W.A. Richter, 1982: An Evaluation of the Vaisala's MicroCORA Automatic Sounding System, CREL Report 82-28, 24 pp.

Augstein, E., 1984: Overview on "Polarstern" Activities. *MIZEX Bulletin.*, V, 12-13.

Battan, L.J., 1973: *Radar Observation of the Atmosphere.* University of Chicago Press, 323 pp.

Bean, B.R., and E.J. Dutton, 1966: *Radio Meteorology.* NBS Monagr 92. U.S. Department of Commerce, Nation Bureau of Standards, Washington. Dover, New York, 435 pp.

Brost, R.A., D.H. Lenschow and J.C. Wyngaard, 1982: Marine Stratocumulus Layers. Part I: Mean Conditions. *J. Atmos. Sci.*, 39,800-817.

Businger, J.A., 1985: The Marine Boundary Layer, from Air-Sea Interface to Inversion. NCAR Technical Note 252+STR, 84 pp.

Davidson K.L., and G.L. Geernaert, 1984: R/V Hakon Mosby Meteorological Measurements/Conditions. *MIZEX Bulletin*, V, 93-95.

Dotson, M.E., 1987: An Evaluation of the Impact of Variable Temporal and Spatial Data Resolution upon IREPS, Master Thesis, Naval Postgraduate School, Monterey, California, 62 pp.

Fairall C.W. and R. Markson, 1987: Mesoscale Variations in Surface Stress, Heat Fluxes, and Drag Coefficient in the Marginal Ice Zone During the 1983 Marginal Ice Zone Experiment, *J. of Geophysical Research.*, **92**, 6921-6932.

Fleagle, R.G., and J.A. Businger, 1980: *An Introduction to Atmospheric Physics.* Second Ed., New York, Academic Press, 432 pp.

Gathman, S.G., 1986: Sensitivity of Refractive Index Profile Models to Relative Humidity Sensor Errors. Naval Research Laboratory Memorandum Report 5758, 36 pp.

Geernaert G.L., K.L. Davidson, and P.S. Guest, 1987: Observed Short-Term Characteristics of the Marginal Ice Zone Planetary Boundary Layer and its impact on Elevated Ducts., *Radio Science*, (submitted), 14pp.

Guest P.S., and K.L. Davidson, 1984: R/V Polar Queen Atmospheric Boundary Layer Measurements. *MIZEX Bulletin*, V, 98-100.

------ and ------, 1987: Factors Affecting the Atmospheric Boundary Layer over a Summertime Marginal Ice Zone - An Observational Study. *Abstracts, 19th IUGG General Assembly*, Vancouver, Canada, **2,** 143.

------ and ------, 1987: The Effect of Observed Ice Conditions on the Drag Coefficient in the Summer East Greenland Sea Marginal Ice Zone., *J. of Geophysical Research.*, **92,** 6921-6923.

Helvey, R.A., 1982: Guidelines for Correction of Radiosonde-Derived Refractive Profiles and Climatologies. Pacific Missile Test Center Technical Publication TP0000005, 36 pp.

Holton, J.R., 1979: *An Introduction to Dynamic Meteorology*. second Ed., New York, Academic Press, 391 pp.

Johannessen, O.M. and D.A. Horn, 1984: MIZEX 84: A Brief Overview. *MIZEX Bulletin.*, V, 1-5.

Johannessen, O.M., D.A. Horn, E. Augstein, A.B. Baggeroer, B.A. Burns, W.J. Campbell, K.L. Davidson, G.G. Duckworth, I. Dyer, B.A. Farrelly, T. Grenfell, A. Heiberg, W.D. Hibler III, J.A. Johannessen, 1986: MIZEX East 83/84: The Summer Marginal Ice Zone Program in the Fram Strait/Greenland Sea. *EOS.*, **67,** 513-517.

Kellner, G., C. Wamser, and R.A. Brown, 1987: An Observation of the Planetary Boundary Layer in the Marginal Ice Zone., *J. of Geophysical Research.*, **92,** 6955-6965.

Lindsay, R.W, K.L. Davidson, M. Gube-Lenhardt, P.S. Guest. R. Picard, C. Wamser, 1986: *Synoptic Weather Events of MIZEX 84.*, unpublished manuscript, 46 pp.

McNitt, J.A., 1984: Mesoscale Features and Atmospheric Refraction conditions of the Arctic Marginal Ice Zone, Master Thesis, Naval Postgraduate School, Monterey, California, 128 pp.

Mooney B., 1985: Executive Summary of Rear Admiral John B. Mooney, Jr to the U.S. Navy Symposium on Arctic/Cold Weather Operations of Surface Ships., *Proceedings, US Navy Symposium on Arctic/Cold Weather Operations of Surface Ships.* 23-41.

Muench, R.D., 1983: Marginal Ice Zone Experiment. *Oceanus.*, **26,** 55-60.

Naval Ocean Systems Center, 1981: *IREPS Revision 2.2 User's Manual*, TD 659, San Diego, California.

Overland, J.E., 1985: Atmospheric Boundary Layer Structure and Drag Coefficients Over Sea Ice. *J. Atmos. Sci.*, **42**, 9029-9049

Ohtake, T., K. Jayaweera and K.I. Sakurai, 1982: Observation of Icé Crystal Formation in Lower Arctic Atmosphere. *J. Atmos. Sci.*, **39**, 2898-2904.

Quadfasel D., H. Baudner, P. Damm and K Schulze, 1984: Hydrographic and Current Observations in the Eastern Fram Strait, R/ V Valdivia. *MIZEX Bulletin*, V, 47-48.

Sater, J.E., A.G. Ronhovde, and L.C. Van Allen, 1971: *Arctic Environment and Resources*. The Arctic Institute of North America, Washington D.C., 309 pp.

Stewart, R.W., 1979: *The Atmospheric Boundary Layer*. World Meteorological Organization No. 523, 44 pp.

Tsay S.C., K. Jayaweera, 1984: Physical Characteristics Of Arctic Stratus Clouds. *Journal of Climate and Applied Meteorology*, **23**, 584-596.

Wyngaard, J.C., 1973: On Surface Layer Turbulence, Amer. Meteor. Soc., *Workshop on Micrometeorology*, D.A. Haugen, Ed., Boston, 101-148.

INITIAL DISTRIBUTION LIST

		No. Copies
1.	Defense Technical Information Center Cameron Station Alexandria, VA 22304-6145	2
2.	Library, Code 0142 Naval Postgraduate School Monterey, CA 93943-5002	2
3.	Chairman Code 63Rd Department of Meteorology Naval Postgraduate School Monterey, CA 93943-5000	1
4.	Chairman Code 68Co Department of Oceanography Naval Postgraduate School Monterey, CA 93943-5000	1
5.	Professor W.J. Shaw Code 63Sn Department of Meteorology Naval Postgraduate School Monterey, CA 93943-5000	4
6.	Professor K.L. Davidson Code 63Ds Department of Meteorology Naval Postgraduate School Monterey, CA 93943-5000	5
7.	LT Zdenka S. Willis, USN 717 Carlin Court Carmel, IN 46032	2
8.	Director Naval Oceanography Division Naval Observatory 34th and Massachusetts Avenue NW Washington, DC 20390	1
9.	Commander Naval Oceanography Command NSTL Station Bay St. Louis, MS 39522	1
10.	Commanding Officer Naval Oceanographic Office NSTL Station Bay St. Louis, MS 39522	1

11.	Commanding Officer Fleet Numerical Oceanography Center Monterey, CA 93943-5000	1
12.	Commanding Officer Naval Ocean Research and Development Activity NSTL Station Bay St. Louis, MS 39522	1
13.	Commanding Officer Naval Environmental Prediction Research Facility Monterey, CA 93943	1
14.	Chairman, Oceanography Department U. S. Naval Academy Annapolis, MD 21402	1
15.	Chief of Naval Research 800 North Quincy Street Arlington, VA 22217	1
16.	Office of Naval Research (Code 420) Naval Ocean Research and Development Activity 800 North Quincy Street Arlington, VA 22217	1
17.	Scientific Liaison Office Office of Naval Research Scripps Institution of Oceanography La Jolla, CA 92037	1
18.	Dr. Paul Twitchell Code 1244 Office of Naval Research 800 North Quincy Street Arlington, VA 22217-5000	1
19.	Mr.Vladimir V. Saba 717 Carlin Court Carmel, IN 46032	1
20.	Commander Naval Ocean Systems Command San Diego, CA 92152	1
21.	Officer in Charge Naval Oceanography Command Detachment Monterey, CA 93943-5000	1
22.	Commanding Officer Space and Naval Warfare Systems Command NC #1 Code 3211K Washington,D.C. 20363-5100	1

23. John Cook — 1
Naval Environmental Prediction Research Facility
Monterey, CA 93943-5000

24. Commander — 1
Naval Sea Systems Command
Washington D.C. 20362

25. Mr. Wayne Patterson — 1
Attn code 532
Naval Ocean Systems Command
271 Catalina Blvd.
San Diego, CA 92152

26. Commanding Officer — 1
Naval Polar Oceanography Center
4301 Suitland Road
Washington, D.C. 20390-5180

27. Dr. Juergen Richter — 1
Attn code 54
271 Catalina Blvd.
San Diego, CA 92152

28. COMPATWING 5 — 1
Attn code N3
NAS Brunswick, ME 04011

29. Professor R. Bourke, Code 68Pa — 1
Department of Oceanography
Naval Postgraduate school
Monterey, CA 93943-5002

30. Mr R. Fett — 1
Head, Analysis and Forecasting
Department
Naval Environmental Prediction Facility
Monterey, CA 93943-5000

31. Mr. Peter Guest — 1
Department of Meteorology
Naval Postgraduate school
Monterey, CA 93943-5000

32. Mr. D.A. Horn — 1
Arctic Sciences,Code 1125AR
Office of Naval Research
800 No. Quincy Street
Arlington, VA 22217

33. Mr. R. Helvey — 1
Code 3252
Pacific Missile Test Center
Point Mugu, CA 93042

34. Detlef Quadfasel — 1
Institute for Meereskunde
Heimhuder Str. 71
2000 Hamburg 13
Federal Republic of West Germany

35. Dr. Richard Armstrong — 1
CIRES, Campus Box 449
University of Colorado
Boulder, CO 80309

36. Dr. Ernst Augstein — 1
Alfred Wegener Institute for Polar Research
Burgermeister Strasse 20
2850 Bremerhaven
West Germany

37. Professor Authur Baggeroer — 1
MIT Room 5-204
Ocean Engineering Department
77 Massachusetts Ave
Cambridge, MA 02139

38. Dr. T. Curtin — 1
Arctic Sciences, Code 1125AR
Office of Naval Research
800 No. Quincy Street
Arlington, VA 22217

39. Professor Ira Dyer — 1
Department of Ocean Engineering
MIT Room 5-212
77 Massachusetts Ave
Cambridge, MA 02139

40. Dr. Heinrick Hoeber — 1
Max-Planck Inst for Meteorology
Budesstrasse 55
D-2000 Hamburg 13
West Germany

41. Dr. J.A. Johannessen — 1
Nansen Remote Sensing Center
Edvard Griegsv. 3a
5037 Solheimsviken

42. Dr. Ola M. Johannessen — 1
Nansen Remote Sensing Center
Edvard Griegsv. 3a
5037 Solheimsviken

43. Dr. James E. Overland — 1
MPAA/PMEL
7600 Sandpoint Way N.E.
Seattle, WA 98115

44. Dr. Steve Stage — 1
Department of Meteorology
Florida State University
Tallahassee, FL 32306-3034

45. Stuart G. Gathman — 1
Code 8350
Naval Research Laboratory
Washington, D.C. 20375

46. Vaisala INC — 1
Attn. K. Goss
2 Tower Office Park
Woburn, MA 01801

316 - 891

Thesis
W62797 Willis
c.1 The spatial and temporal variability of the Arctic atmospheric boundary layer and its effect on electromagnetic (EM) propagation.

Thesis
W62797 Willis
c.1 The spatial and temporal variability of the Arctic atmospheric boundary layer and its effect on electromagnetic (EM) propagation.

thesW62797
The spatial and temporal variability of
3 2768 000 78750 1
DUDLEY KNOX LIBRARY